2015

SENTINEL LYMPH NODE ASSESSMENT IN OESOPHAGEAL CANCER: CREATION OF A MULTIMODALITY TRACER

GEORGE L BALALIS

MBBS   BOND UNIVERSITY   2009

A Thesis presented for the degree of Masters of Philosophy (Surgery) from the Discipline of Surgery, University of Adelaide, South Australia, Australia

TABLE OF CONTENTS

CHAPTER 5:   A MULTIMODALITY ^{99m}Tc-LABELLED IRON OXIDE NANOTRACER TO IMPROVE SENTINEL NODE IDENTIFICATION IN EARLY OESOPHAGEAL CANCER   89

iv

LIST OF FIGURES

LIST OF TABLES

GLOSSARY

AJCC	American Joint Committee on Cancer
ATC	antimony trisulphide colloid
CT	computed tomography
DT	dye technique
EMR	endoscopic mucosal resection
ESD	endoscopic submucosal dissection
ESR	erythrocyte sedimentation rate
EUS	Endoscopic ultrasound
FDA	Food and Drug Administration
FNA	fine needle aspiration
FOV	field-of-view
FWHM	full width half maximum
Gd	gadolinium
GOJ	gastroesophageal junction
GORD	gastro-oesophageal reflux disease
H&E	haematoxylin and eosin
HCl	hydrogen chloride
ICG	indocyanine green
ID	injected dose
IHC	immunohistochemistry
ITC	isolated tumour cells
ITLC-SG	instant thin layer chromatography silica-gel
MRI	magnetic resonance imaging
MTJ	magnetic tunnelling junction
NIR	near infrared
NPS	nonpoint-source
PCB	printed circuit board
PET	Positron emission tomography
PS	point-source

QC	quality control
RCT	radiocolloid technique
RF	random forest
RT-PCR	reverse-transcriptase polymerase chain reaction
SLN	sentinel lymph node
SNR	signal to noise ratio
SPIONs	superparamagnetic iron oxide nanoparticles
TC	technetium
TNM	tumour node metastasis
UICC	Union for International Cancer Control
WECC	worldwide esophageal cancer collaboration

x

ABSTRACT

Introduction

Early oesophageal cancer can now be treated endoscopically; however, more accurate lymph node assessment is required. The sentinel lymph node (SLN) is defined as the first lymph node to which the primary tumour drains. This node should reflect the status (i.e. benign or malignant) of the entire lymph node basin. Our aims were to identify current difficulties that limit the acceptance of the SLN concept in oesophageal cancer, as well as to create a multimodal (magnetic resonance imaging [MRI] and gamma) tracer, to enable more detailed perioperative SLN assessment.

Methods

A literature review was undertaken, targeting studies assessing oesophageal cancer and SLN. MEDLINE, the Cochrane Database of Systematic Review, as well as PUBMED, were consulted. The keywords and medical subject headings (MeSH) used were '(o)esophageal cancer', '(o)esophageal adenocarcinoma', '(o)esophageal squamous cell carcinoma' and 'SLN' used in combination with AND or OR. Only studies in English were considered. ^{99m}Tc-labelled magnetic nanoparticle formulations were then investigated for further use as a multimodality SLN contrast agent. Radiolabelling of the dextran-coated magnetic nanoparticles was undertaken, and instant thin layer chromatography developed to assess efficiency. Bio-

distribution was determined after intravenous and subdermal injection in the tails of Sprague-Dawley rats. Lymphoscintigraphy was performed on the subdermally injected rats to assess lymphatic mapping.

Following this, the multimodality SLN tracer was injected into the oesophagus of four swine. MRI images were then acquired, and then sentinel nodes were further assessed intraoperatively with a gamma probe. Bio-distribution was then assessed, comparing ^{99m}Tc-antimony trisulphide colloid (ATC) and ^{99m}Tc-superparamagnetic iron oxide nanoparticles (SPIONs). Lymph nodes and reticuloendothelial organs were then harvested and counted to determine the percentage of injected dose (%ID).

Results

The literature review demonstrated at least four issues limiting the use of the SLN concept in oesophageal cancer. These included: timing of tracer – different radiocolloids overseas, with different rates of flow; the chest cavity – difficulty of access post-injection; blue dye – not useful, with proven false-negative rate; and shine-through effect.

The multimodality tracer formulation was optimised, with labelling efficiency confirmed at >99%. In the Sprague-Dawley rats, the tracer was injected subdermally, with lymphoscintigraphy demonstrating excellent delineation of the sentinel nodes. The reticuloendothelial organs were then removed and activity measured, with the liver showing 3.2% highest mean activity, followed by the kidneys with 2%, the spleen at 0.3% and the lungs at 0.1%.

The gamma probe detected all nodes identified on MRI imaging of the four swine injected with ^{99m}Tc-SPIONs. Radiolabelling efficiency was >98%. ^{99m}Tc-ATC and ^{99m}Tc-SPIONs were taken up by swine liver and lungs with similar percentage ID values, and there was 7% ID of ^{99m}Tc-SPIONs by the kidneys, compared to <1% ID of ^{99m}Tc-ATC in the same organs.

Conclusion

There are numerous issues that require evaluation and agreement in the international community to ensure greater use of the SLN concept in oesophageal cancer.

A multimodality, ^{99m}Tc-SPIONs, tracer was validated using both MRI imaging and a gamma probe. This tracer requires further assessment, as it could allow pre-operative assessment of sentinel lymph nodes in early oesophageal cancer.

THESIS DECLARATION

This work contains no material which has been accepted for the award of any other degree or diploma in any university or other tertiary institution to *George L Balalis* and, to the best of my knowledge and belief, contains no material previously published or written by another person, except where due reference has been made in the text. In addition, I certify that no part of this work will, in the future, be used in a submission in my name, for any other degree or diploma in any university or other tertiary institution without prior approval of the University of Adelaide.

I give consent to this copy of my thesis when deposited in the University Library, being made available for loan and photocopying, subject to the provisions of the Copyright Act 1968.

The author acknowledges that copyright of published works contained within this thesis (as listed below) resides with the copyright holders of those works.

I also give permission for the digital version of my thesis to be made available on the web, via the University's digital research repository, the Library catalogue and also through web search engines, unless permission has been granted by the University to restrict access for a period of time.

Signed

PUBLISHED WORKS AND PRESENTATIONS

Publications

Balalis GL, Thompson SK. Sentinel lymph node biopsy in esophageal cancer: an essential step towards individualized care. *Annals of Surgical Innovation and Research* 2014, 8:2. Published by Biomed Central Ltd. The original publication, http://www.asir-journal.com/content/8/1/2 doi:10.1186/1750-1164-8-2

Balalis GL, Cousins A, Tsopelas C, Devitt P, Madigan D, Bartholomeusz D, Thierry B, Thompson SK. A multimodality ^{99m}Tc-labelled iron oxide nanotracer to improve sentinel node identification in early oesophageal cancer. *Currently in review*

Publications related to this thesis

Cousins A, Balalis GL, Thompson SK, Forero Morales D, Mohtar A, Wedding AB, Thierry B. Novel Handheld Magnetometer Probe Based on Magnetic Tunnelling Junction Sensors for Intraoperative Sentinel Lymph Node Identification. *Sci. Rep. 5, 10842; doi: 10.1038/srep10842 (2015)*

Cousins A, Balalis GL, Tsopelas C, Thompson SK, Bartholomeusz D, Wedding BA, Thierry B. Radiolabelling of ^{99m}Tc-labelled iron oxide for use in sentinel node detection. *Currently in review*

Oral presentations

Balalis GL. A novel multimodality nanotracer to improve sentinel node identification in early oesophageal cancer. *Australian and New Zealand Gastric and Oesophageal Surgeons Association (ANZGSOA) Annual Meeting 2014, Queenstown, New Zealand.*

Balalis GL. MRI imaging with nanoparticles to assess lymphatic drainage of the distal oesophagus in a swine model. *Royal Australasian College of Surgeons Annual Scientific Congress, 2014, Singapore.*

Balalis GL. Multimodality Nanotracer For Assessment Of Sentinel Lymph Nodes In Oesophageal Cancer. *Board in General Surgery (South Australia) Registrar's Paper Day, 2015, Adelaide, South Australia.*

Oral presentations related to this thesis

Cousins A, Balalis GL, Wedding BA, Thompson SK, Thierry B. Oesophageal Sentinel Lymph Node Identification in a Swine Model using Magnetic Lymphotropic Contrast Agents. 2014 *International Conference on Nanoscience and Nanotechnology (ICONN), Adelaide, South Australia.*

Poster presentations

Balalis GL. Reproducibility of sentinel lymph node drainage pathways in the lower oesophagus using a novel multimodality tracer. *5th Asia Pacific Gastroesophageal Cancer Congress (APGCC), Brisbane, Australia, 2015.*

Balalis GL. MRI imaging with nanoparticles to assess lymphatic drainage of the distal oesophagus. 2014 Florey International Postgraduate Research Conference, *Adelaide, Australia.*

ACKNOWLEDGEMENTS

CHAPTER 1: INTRODUCTION

George Balalis MBBS

Discipline of Surgery, University of Adelaide, Adelaide, South Australia

1.1 STAGING IN CANCER

1.1.1 Purpose and principle of cancer staging

Staging of cancer plays an important role in determining appropriate treatment decisions, and is at the cornerstone of individual patient management.

Staging can be clinical or pathological. Clinical staging, identified with the prefix 'c', is performed using physical examination, imaging and laboratory tests. This includes surgical exploration without resection.

Pathological staging, identified with the prefix 'p', is performed following resection of the specimen, and provides in-depth information regarding the size, type of cells, invasion, proximity to margins and relationship to native tissue.

It is critical to ensure appropriate and accurate staging for any type of cancer. Staging provides both a framework upon which to optimise treatment and also a general guideline of prognosis to discuss with the patient. Stratification of cancer also provides an international platform upon which it is possible to compare clinical outcomes for similar patients between clinicians and cancer institutions, irrespective of the country of origin. It is an objective assessment of disease that can be compared to historical staging criteria, and provides clarity to treatment regimens.

1.1.2 Tumour node metastasis staging

Staging of the cancer, as well as appropriate treatment(s), continues to be a topic of debate and literature review. The tumour node metastasis (TNM) system is maintained

collaboratively by the American Joint Committee on Cancer (AJCC) and the Union for International Cancer Control (UICC). Historically, cancer staging has been purely anatomical, and this remains the most significant factor. However, more recent advances in cancer staging have allowed the introduction of non-anatomical factors.

There have been several updates to the *AJCC cancer staging manual*, sometimes with significant changes in classification (Table 1-1). For the purpose of this thesis, the 7th edition of the *AJCC cancer staging manual* will be used. The 8th edition will be released in mid-2016, with an effect date of 2017.

Table 1-1   Year and edition of AJCC staging

Edition	Year
Edition 1	Published 1977, into effect 1978
Edition 2	Published 1983, into effect 1984
Edition 3	Published 1988, into effect 1989
Edition 4	Published 1992, into effect 1993
Edition 5	Published 1997, into effect 1998
Edition 6	Published 2002, into effect 2003
Edition 7	Published 2009, into effect 2010

1.2   SENTINEL LYMPH NODE CONCEPT

The sentinel lymph node (SLN) is defined as the first lymph node to which the primary tumour drains. This node should reflect the status (i.e. benign or malignant) of the entire lymph node basin.

It is important to realise the beginnings of the SLN surgical concept. *Cabanas* (1) first described this approach in 1977, in his article, 'An approach for the treatment of penile carcinoma', where he used 'lymphangiograms' that demonstrated 'the existence of

specific lymph node centres, the so-called sentinel lymph nodes'. *Cabanas* was able to demonstrate that if the SLN was negative, survival was significantly higher.

Morton (2) was the first to describe the technique of localisation of SLNs in patients with a melanoma in 1992, using an intradermal isosulfan blue dye injection. He successfully identified the SLN in 194 of 237 patients, with a false-negative rate of less than 1%. The blue dye mapping technique was then applied to the nodal assessment of breast cancer by *Giuliano et al.* in 1994.(3) The continuing success of SLN mapping, extraction, and histologic examination has led to this approach becoming the gold standard for patients with breast cancer and malignant melanoma.

There are two main techniques for SLN biopsy: the dye technique (DT) and the radiocolloid technique (RCT). Main steps of each include the injection of a tracer (either dye or radiocolloid), identification of the SLN, excision of the SLN, and examination via a histopathological protocol.
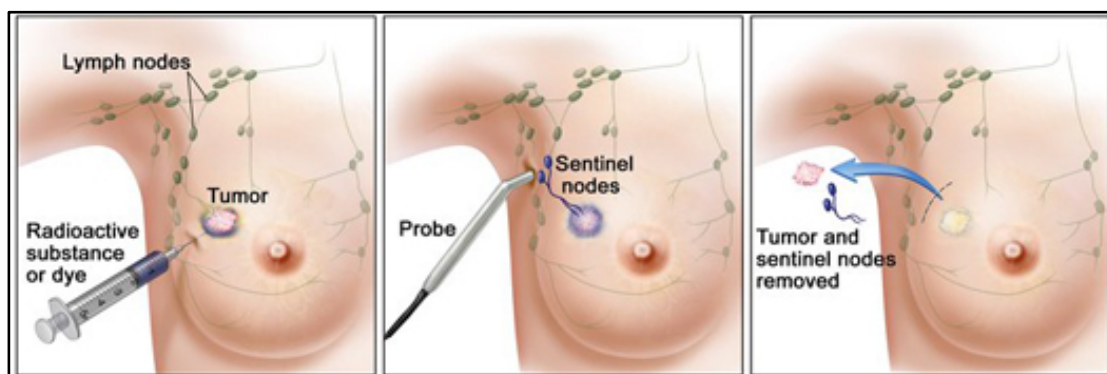
Figure 1-1 Demonstration of sentinel lymph node technique in breast cancer
Source: www.cancer.gov/about-cancer/diagnosis-staging/staging/sentinel-node-biopsy-fact-sheet

1.2.2   Blue dye technique

In early breast cancer and melanoma, the blue DT is the standard of care for sentinel node assessment.(4, 5)

In breast cancer, blue DT has been demonstrated to be a reliable and minimally invasive method of determining nodal status.(6) The majority of studies in breast cancer, as well as melanoma, have used blue dye, in conjunction with a radiocolloid, for assessment of nodal status.(7, 8) This is because dual assessment demonstrates a higher rate of lymph node detection.(9) In a study of breast cancer patients by *Radovanovic et al.* (7), the accuracy of detection was found to be 68% (34/50) with blue dye alone, compared with 83% (83/100) with combined radiotracer and blue dye.

There is an issue regarding allergic and anaphylactic reaction to blue dye. The Australian Medical Services Advisory Committee reports the risk of an allergic reaction to blue dye to be between zero and 1.6%. Blue dye should not be used if there is prior evidence of an allergic reaction to this type of agent, or in a patient with severe renal impairment. The other disadvantage of blue dye is a permanent blue tattoo of the skin following injection, which occurs in some patients.

1.2.3   Radiocolloid technique

The type of radiocolloid in use differs in most countries, due to the particular country's legislation. This means that different results are achieved depending on the time the colloid takes to migrate into the lymphatic system; this prevents the development of a universal protocol for SLN biopsy in cancer. *Gretschel et al.*(10) in their work (in Europe), injected the commonly used 100 μm radiocolloid one day prior to surgery, whereas in

Australia, *Thompson et al.* (11) injected a 10 ± 3 µm antimony radiocolloid prior to operation.

In breast cancer and melanoma, the RT is encouraged, with blue dye used only as a complementary assessment tool. In a meta-analysis by *Valsecchi et al.* (8), all studies used radiocolloid whilst 89% used blue dye as well. As discussed previously, the radiocolloid used varied in the studies, with at least 5 different sized colloids described.

The potential for improvement to current radiocolloid options will be discussed later in this proposal, and is the basis of this thesis. If future radiocolloid tracers were to be multimodal, with a combination of magnetic resonance imaging (MRI) and gamma camera capabilities, then this may require a larger radiocolloid with an extended transit time to facilitate additional imaging.

1.2.4 Other experimental techniques

There are further techniques for SLN assessment, which are currently being investigated. The aim of these modalities is to improve on potential limitations of radiocolloid and blue dye methods.

One technique being trialled is near-infrared (NIR) fluorescent light (700–900 nm). This has the potential to improve cancer surgery outcomes, and potentially decrease operative time. NIR light can travel up to around a centimetre in depth, compared with micrometres for visible light, improving identification of tissue below the surface. Due to tissue demonstrating near zero autofluorescence in the NIR spectrum, the signal-to-noise

contrast can be maximised by using fluorescent contrast agents activated by NIR light.

There are numerous contrast agents that have been prepared to target different tissues.

SLN contrast agents include indocyanine green (ICG), which is currently Food and Drug

Administration (FDA) approved for other uses (including determining cardiac output). ICG

NIR fluorescence has been demonstrated in a few studies (12, 13) to locate sentinel

nodes in colorectal and breast cancers.(14, 15) However, some of these studies are

limited by the depth of field with ICG. Current imaging platforms only demonstrate

visualisation of SLNs to around ≤10 mm. Current research is being sought to demonstrate

ICG efficacy compared with a radioactive tracer.

A further technique that is being investigated is the use of quantum dots. These are very

bright fluorescent nanoparticles that overcome some of the depth limitations of

traditional fluorophores. Quantum dots are excited over a broad spectrum of light, but

only emit a narrow spectrum. This allows quantum dots to be distinguished with the

naked eye, without the need for cameras, as well as providing a potential depth of up to 2

cm.(16) The benefit of quantum dots has been overshadowed by their toxicity concerns.

They have been shown to cause cell death *in vitro* through production of reactive oxygen

species.(17) The safety profile of quantum dots requires significant investigation prior to

use in a human population.

1.3   OESOPHAGEAL CANCER

1.3.1   Epidemiology

Oesophageal cancer is the 6th leading cause of cancer death worldwide, and is

characterised by its overall poor prognosis. An estimated 482,300 new oesophageal

cancer cases with 406,800 deaths occurred worldwide in 2008.(18) In 2011, Australia had 1427 new oesophageal cancers, with an age-standardised incidence in males of 9.0.(19, 20)

Incidence rates vary significantly with location, as Southern and Eastern Africa and Eastern Asia have the highest incidence, and Western and Middle Africa and Central America have the lowest (Fig. 1-2). The incidence of oesophageal cancer in Australia is approximately 5.1 per 100,000. Oesophageal cancer is also 3 to 4 times more likely to occur in males than females.

When discussing oesophageal cancer, it is important to appreciate that there are two different disease processes. There is squamous cell carcinoma, generally of the middle or upper one-third of the oesophagus, and adenocarcinoma, usually of the lower one-third of the oesophagus or oesophagogastric junction. In Australia, the majority of oesophageal cancer is adenocarcinoma, accounting for over 60% of all cases, and this number is increasing every year.(21)
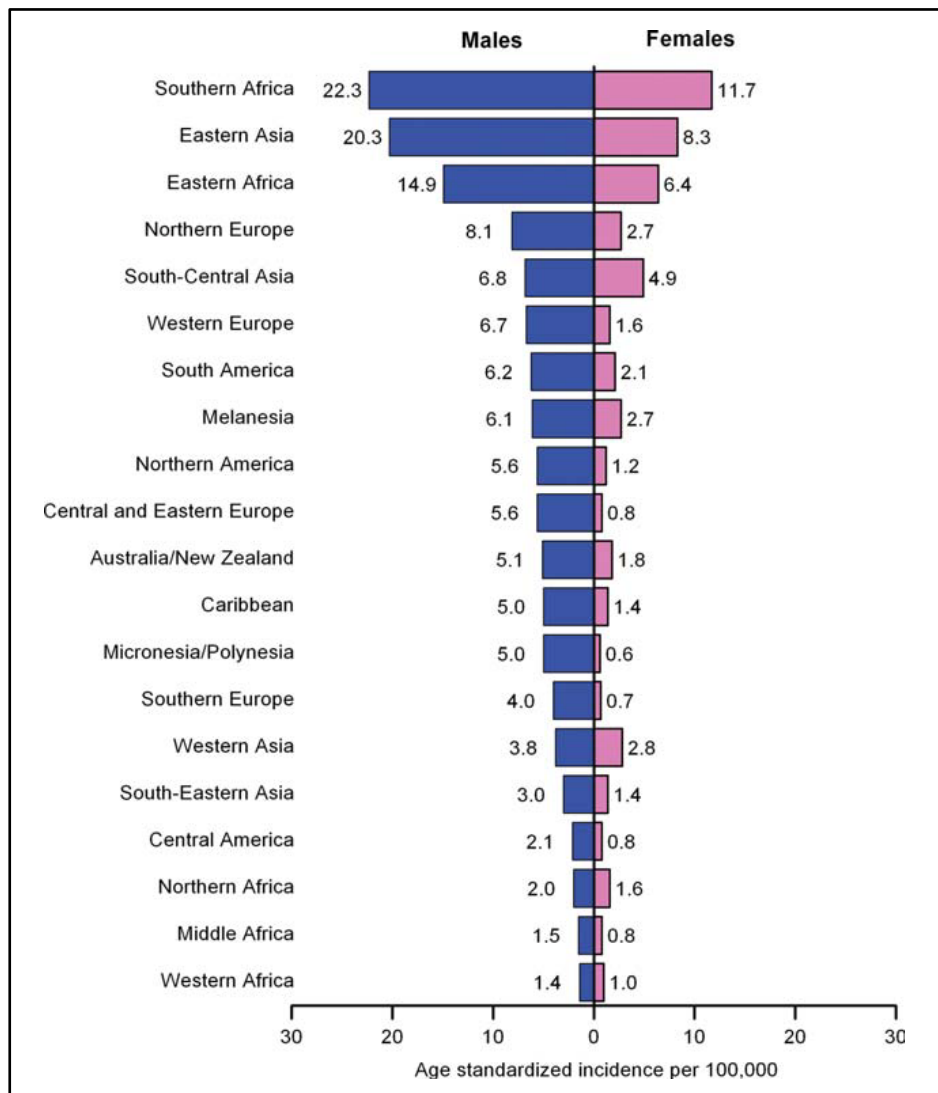
Figure 1-2   Age standardised oesophageal cancer incidence rates by sex and world area
Source: GLOBOCAN 2008

1.3.2   Aetiology

Squamous cell carcinoma of the oesophagus remains the most prevalent type of

oesophageal cancer in the world, and its incidence has been stable over the last 20–30

years. This is in contrast to oesophageal adenocarcinoma, which has dramatically

increased in incidence in Australia, Europe and the Unites States. This increase is

especially true in men, and it is likely that gastro-oesophageal reflux and the prevalence

of obesity are important contributing factors.

Squamous cell carcinoma of the oesophagus is a cancer that begins in the squamous cells of the epithelium of the oesophagus. It is mainly found in the middle to upper third of the oesophagus. It is a cancer that occurs after repeated injury and damage to the lining of the oesophagus, often associated with tobacco, alcohol and hot drinks; it occurs more frequently in those of poor socioeconomic status.

Adenocarcinoma is a cancer that begins in the gland cells of the oesophagus, which produce mucus. These cancers are mainly found in the distal oesophagus, or gastro-oesophageal junction.

Oesophageal adenocarcinoma is traditionally a disease that affects white males from higher socioeconomic groups. The strongest risk factor is symptomatic gastro-oesophageal reflux disease (GORD). It is not surprising then, that adenocarcinoma is associated with obesity, as obesity is a strong risk factor for GORD.[22] Obesity is of itself a risk factor for oesophageal adenocarcinoma, and this may be due to physiological effects via modulation of polypeptides, such as insulin-like growth factors and ghrelin.

Another predisposing factor is hiatal hernia, with a risk of 2–6 fold, likely due to increasing GORD.[23] A hiatus hernia is present when part of an organ (usually stomach) protrudes above the oesophageal opening in the diaphragm. The laxity of the oesophageal hiatus can cause reflux and Barrett's oesophagus. Hiatus hernias are typically classified anatomically (Fig. 1-3). Type I is a sliding hernia, with the gastroesophageal junction (GOJ) above the diaphragm, compared with Type II where the GOJ is below the diaphragm but a portion of stomach is above. Type III is a mixed picture,

with the GOJ above the diaphragm along with a part of the stomach, and Type IV is a

giant hernia with other contents above the diaphragm.
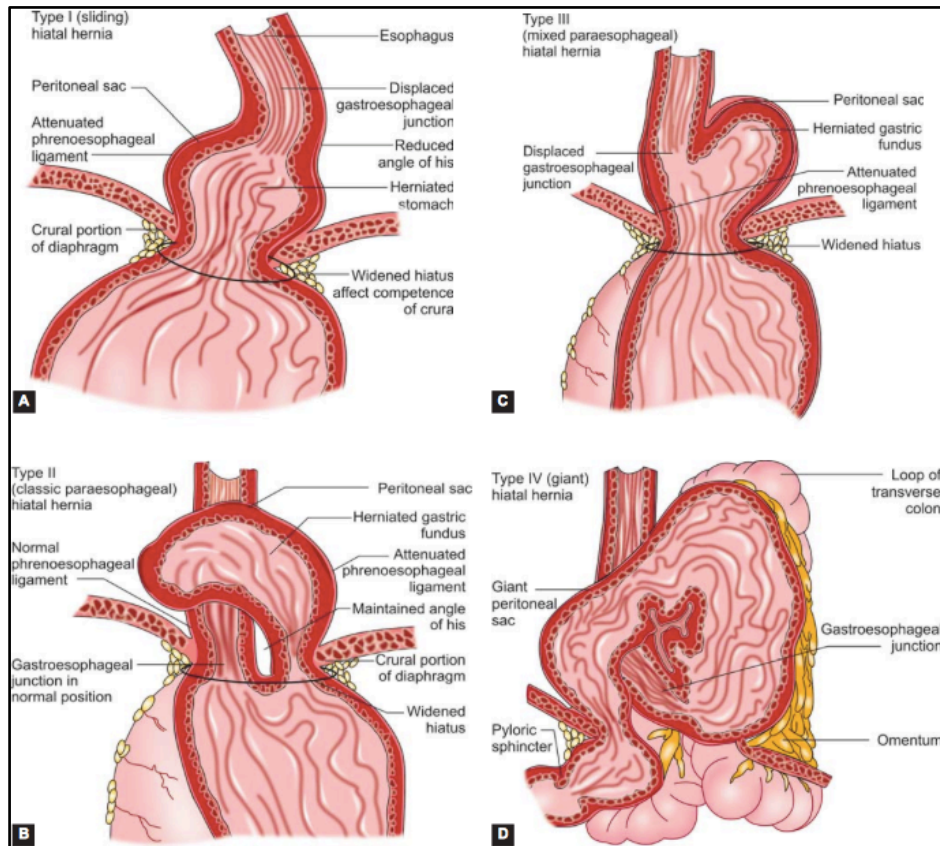
Figure 1-3   Classification of hiatus hernias
Source: World Journal of Laparoscopic Surgery, May-August 2010; 2 (2): 85–90

Achalasia is also a risk factor for oesophageal carcinoma, with a 10-fold increased risk of

either histological type when compared with the general population.(24) Achalasia is

'characterised by the absence of oesophageal peristalsis and impaired relaxation of the

lower oesophageal sphincter, in response to swallowing.'(25)

1.3.2.2   *Gastro-oesophageal reflux disease*

Chronic GORD may lead to oesophagitis, which may then lead to Barrett's metaplasia.

Oesophagitis is defined as inflammation of the oesophagus. There is a classification system for describing endoscopic findings of reflux oesophagitis, which ensures uniform reporting; The Los Angeles Classification.(26, 27) This is defined as shown in Figure 1-4.
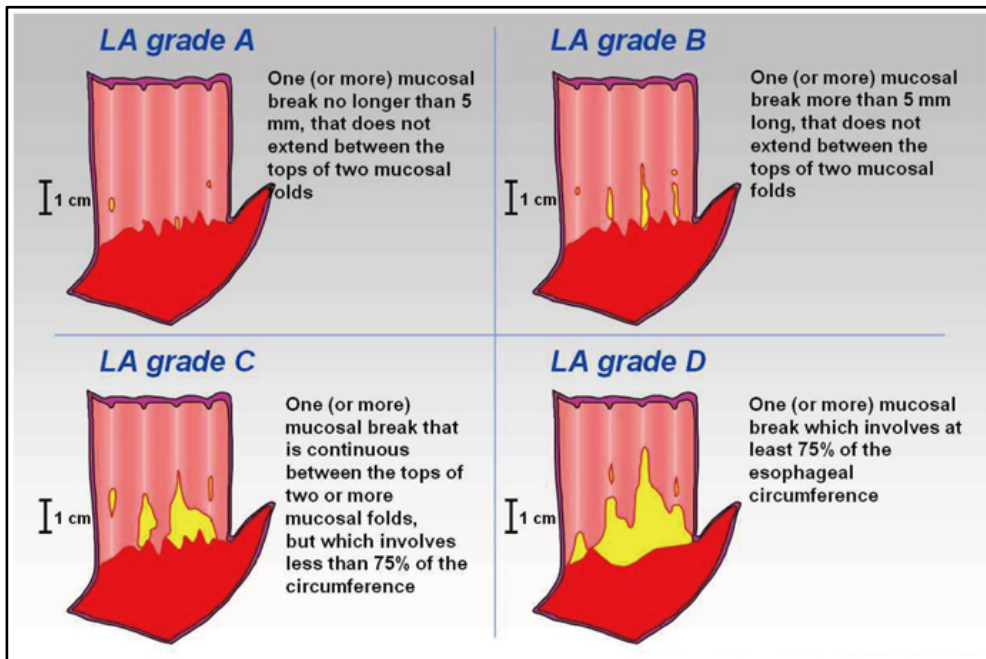
Figure 1-4   Los Angeles Classification of Oesophagitis
Source: Korean J Otorhinolaryngol-Head Neck Surg. 2012 Jun; 55:334-345

1.3.2.3   Barrett's oesophagus

Oesophagitis may lead to Barrett's disease, which in turn may transform into oesophageal adenocarcinoma. Barrett's oesophagus, or Barrett's mucosa, is defined as a condition 'in which a metaplastic columnar mucosa that confers a predisposition to cancer replaces an oesophageal squamous mucosa damaged by gastro-oesophageal reflux disease (GORD).'(28)

Barrett's oesophagus is an acquired condition, secondary to GORD damage. There are differing opinions; however, it is suggested that GORD may alter the expression of

important transcription factors, causing mature oesophageal squamous cells to mutate into columnar cells, or causing immature oesophageal progenitor cells to become columnar instead of squamous.(29)

Figure 1-5   Endoscopic picture of Barrett's oesophagus, classified as C2M4
Notes: C: extent of circumferential metaplasia; M: maximal extent of the metaplasia (C plus a distal 'tongue' of 2 cm
Source: Whiteman DC et al: Australian clinical practice guidelines for the diagnosis and management of Barrett's esophagus and early esophageal adenocarcinoma. J Gastroenterol Hepatol 2015, 30:804-820

Barrett's oesophagus describes a metaplastic change of the lining of the oesophagus, with replacement of normal squamous epithelium by columnar intestinal type epithelium. The Cancer Council Australia Barrett's Oesophagus and Early Oesophageal Adenocarcinoma Working Party have taken the American Gastroenterology Association view that intestinal metaplasia is required for a diagnosis.(30) This is because intestinal metaplasia is the only type of oesophageal columnar epithelium that predisposes patients to adenocarcinoma.(31) This is different from the British Gastroenterology Society, which

does not deem intestinal metaplasia necessary for a diagnosis of Barrett's oesophagus.(32)

In a study by *Wani et al.* (33) in 2011, 3.6% and 0.48% of patients with Barrett's oesophagus progressed to low-grade and high-grade dysplasia per year, with 0.27% progressing to adenocarcinoma.

It has been demonstrated that some adenocarcinomas of the oesophagus develop in an area of Barrett's oesophagus.(34) It is difficult to ascertain the exact prevalence of Barrett's oesophagus in the population; however, it has been estimated at around 3–7% in patients with frequent reflux symptoms undergoing endoscopic examination. This is compared with approximately 1% for patients undertaking an endoscopy for another indication. It is important to note, however, that reflux symptoms are a poor predictor of Barrett's oesophagus.(35)

The precise risk of patients with Barrett's oesophagus developing adenocarcinoma remains unclear; however, it has been estimated that it is approximately 0.5% per year.(36) A recent paper by Pohl *et al* has confirmed that the risk increases with length of Barrett's oesophagus.(37) Patients who have been shown to have Barrett's oesophagus with high grade dysplasia are at a risk of approximately 6 per 100 patient-years, in the first few years of follow up, as described in a meta-analysis; however, this included only 4 articles and 236 patients for 1241 patient-years.(38)

1.3.2.4 *Lifestyle*

Tobacco use and alcohol consumption increase the risk of oesophageal carcinoma.

Tobacco consumption is more strongly associated with squamous cell carcinoma with a 3- to 7-fold increase; however, it has also been associated with a 2-fold increase in the incidence of adenocarcinoma.(23)

Alcohol intake is strongly associated with squamous cell carcinoma; however, there is no confirmed link to adenocarcinoma of the oesophagus.

1.4 STAGING IN OESOPHAGEAL CANCER

1.4.1 Siewert classification

In the literature there is some confusion with regard to the classification of GOJ carcinomas. The topographic-anatomic classification from Siewert and Holscher is often referenced to help describe the location of a particular tumour of cancer of the GOJ (Fig. 1-6).
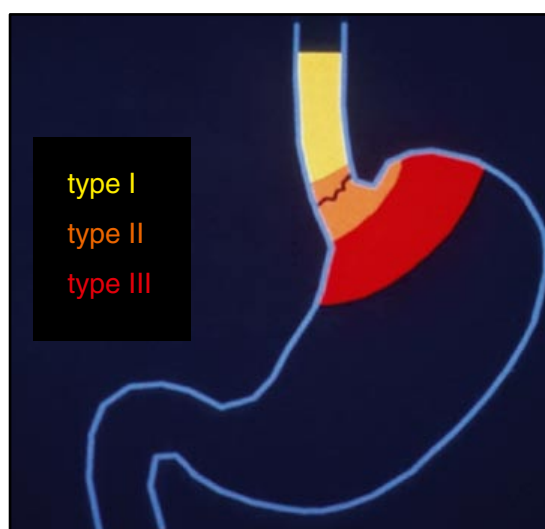
Figure 1-6   Classification of adenocarcinoma of the gastroesophageal junction
Note: Type I: centre of tumour >1 cm above the cardia
Type II: centre of tumour within 1 cm above and 2 cm below the cardia
Type III: centre >2 cm below the cardia

The authors described all tumours with an epicentre of 5 cm of the anatomical cardia as GOJ lesions. Type I is considered an oesophageal adenocarcinoma, Type III is considered gastric cancer, and Type II still continues to cause some debate between clinicians.

A recent article has described a pragmatic solution, in which the procedure performed dictates the staging system used. In other words, if a gastrectomy is performed, then gastric cancer staging should be used, and if an oesophago-gastrectomy is performed, then oesophageal cancer staging should be used.(39)

The 7th edition of the *AJCC cancer staging manual* unifies this issue, by deeming all GOJ tumours amenable to classification via the oesophageal cancer staging system (and this includes Siewert Type III tumours).

1.4.2   Tumour node metastasis staging

The 7th edition of the *AJCC cancer staging manual* (published in 2009, and to be used for staging any patient from 2010 onwards) documented several significant changes to the oesophageal and oesophagogastric junction cancer staging. It used data from an international database (worldwide esophageal cancer collaboration [WECC] data) and developed random forest (RF) analysis, to create homogeneous survival groups and, from this, identify important anatomical and non-anatomical characteristics.

T classification was changed, for Tis (in situ) and T4 cancers. Tis was redefined as high-grade dysplasia and includes all non-invasive neoplastic epithelium, previously known as carcinoma-in-situ. T4 cancers have been broken up into T4a and T4b tumours. T4a

tumours are defined as resectable cancers, which invade adjacent structures, including

the pleura or diaphragm. This is in contrast to T4b tumours, which are defined as un-

resectable cancers invading adjacent structures, such as the aorta and trachea.

Table 1-2   Classification of primary tumour

Classification	Tumour
Tis	High-grade dysplasia
T1	Tumor invades lamina propria, muscularis mucosae, or submucosa
T1a	Tumor invades lamina propria or muscularis mucosae
T1b	Tumor invades submucosa
T2	Tumor invades muscularis propria
T3	Tumor invades adventitia
T4	Tumor invades adjacent structures
T4a	Resectable tumor invading pleura, pericardium, or diaphragm
T4b	Unresectable tumor invading other adjacent structures, such as aorta, vertebral body, trachea, etc.
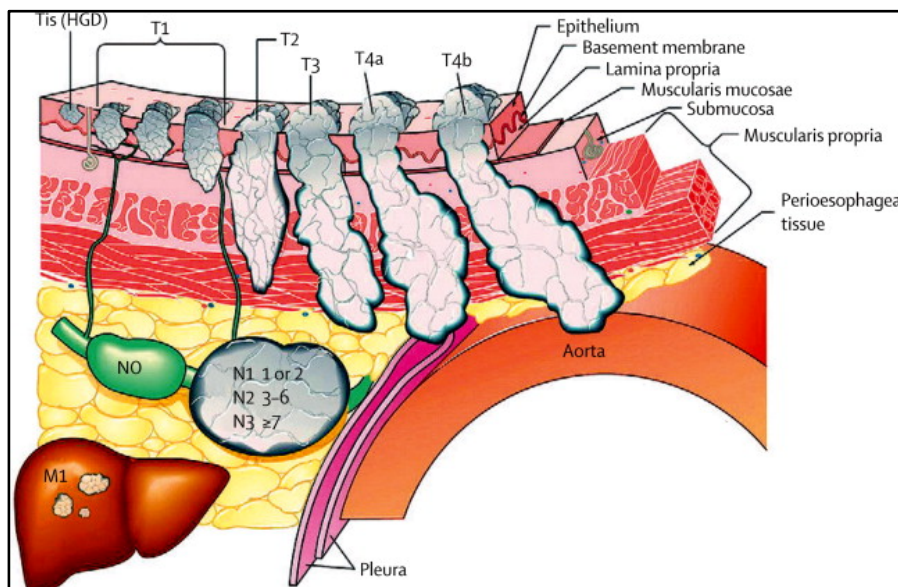
Figure 1-7   Illustrative classification of primary tumour
Source: 7th Edition *AJCC cancer staging manual*

N classification has also been updated. Regional lymph nodes have been updated to include any paraoesophageal node from the cervical chain to the coeliac axis, irrespective of the site of the primary tumour, and excluding supraclavicular nodes. The grouping of regional lymph nodes has been changed to parallel groupings in gastric cancer patients, with N1 (1–2 metastatic lymph nodes), N2 (3–6 positive nodes) and N3 (≥7 metastatic lymph nodes) (Table 1-2). M classification has also been simplified with patients classified as M0 (no distant spread of cancer) and M1 (distant metastasis).

Table 1-3   Classification of regional lymph nodes

Classification	Nodes
N1	1–2 metastatic lymph nodes
N2	3–6 metastatic lymph nodes
N3	≥7 metastatic lymph nodes

The 7th edition also includes non-anatomical classifications. These include histopathologic cell type, histologic grade and tumour location. For Stages I and II, adenocarcinoma and squamous cell carcinoma have now been separated due to the disparity in survival between the two tumour types; Stage I adenocarcinoma risk-adjusted survival being superior to squamous cell carcinoma, and Stage II squamous cell carcinoma being superior to adenocarcinoma.

In Stage I and Stage IIA adenocarcinoma, the statistics showed that it was important to distinguish between tumours that were G1 (well differentiated) or G2 (moderately differentiated) compared with G3 (poorly differentiated) (Fig. 1-8).

Stage	T	N	M	G
0	is (HGD)	0	0	1
IA	1	0	0	1–2
IB	1	0	0	3
	2	0	0	1–2
IIA	2	0	0	3
IIB	3	0	0	Any
	1–2	1	0	Any
IIIA	1–2	2	0	Any
	3	1	0	Any
	4a	0	0	Any
IIIB	3	2	0	Any
IIIC	4a	1–2	0	Any
	4b	Any	0	Any
	Any	N3	0	Any
IV	Any	Any	1	Any

Figure 1-8   Adenocarcinoma stage groupings
Source: 7th Edition *AJCC cancer staging manual*

1.4.3   Lymphatic spread

Lymph node metastasis has been consistently found to be one of the most important independent prognostic factors, and this is once again reflected in the revised 7th edition AJCC classification. The data supported 'convenient coarse groupings' of positive lymph nodes; however, it is a continuous dataset, with worsening results for patients with more positive lymph nodes.

When dealing with lymphatic spread, it is important to realise the disparity that exists with adenocarcinoma, compared to squamous cell carcinoma. *Kakeji et al.* demonstrated this in 2012.(40) They showed that adenocarcinoma metastasised less frequently to the mediastinal lymph nodes, and more frequently to the abdominal lymph nodes.

In their study, 129 patients had oesophageal adenocarcinoma (6 patients with Type I tumours, 60 patients with Type II tumours and 63 patients with Type III tumours). Within this cohort, limited metastasis was observed in the mediastinal lymph node stations, with a much higher rate of metastasis to the abdominal lymph node stations.

Kakeji et al. concluded that due to the difference in lymph node metastases between oesophageal adenocarcinoma and squamous cell carcinoma, they should be treated with different operations. They suggest a transhiatally extended gastrectomy with lower mediastinal and abdominal lymph node dissection for oesophageal adenocarcinoma. In contrast, they suggest an oesophagectomy with mediastinal and abdominal lymph node dissection for squamous cell carcinoma.

This is compared with the previous work of *Schröder et al*.(41) Their study in 2002 included 51 Type I adenocarcinomas, all resected with a transthoracic *en-bloc* oesophagectomy and radical two-field lymph node dissection. Schroder's group resected a mean of 33 lymph nodes per patients, with 28 of the 51 patients classified as pN1. The majority of metastatic lymph nodes were located in the abdominal compartment (73% compared with 27% in the mediastinal compartment). In all 28 patients, the abdominal compartment was involved; in 9 patients (32%) only the abdominal compartment was involved, and in 19 patients (68%) the abdominal and mediastinal compartments were both involved. In the 19 patients with mediastinal involvement, 15 showed lower mediastinal involvement, 3 at the level of the tracheal bifurcation and 5 in the upper

mediastinum. In summary, 7 of the 28 patients had lymph node metastasis proximal to the primary tumour; 6 of the 7 had locally advanced pT3 tumours.

Schröder et al.(40) concluded that there was increasing evidence to advocate for a transthoracic resection in patients with a lower oesophageal adenocarcinoma. With this type of resection, a more radical two-field lymphadenectomy can be completed, including the lymph node stations at the level of the tracheal bifurcation and upper mediastinum. These nodes were positive in 7 of the 28 patients (25%).

This was also supported by *Rudiger Siewert et al.* (42), who demonstrated that in 271 Type II patients, the main locations for lymphatic spread were in the abdominal lymph node stations: left (68%) and right (57%) paracardial stations, lesser curvature (68%), and the left gastric artery, splenic artery and coeliac axis (27%). Lymph node stations in the lower mediastinum were positive in only 16% of patients. *Siewert et al.* also demonstrated that in patients with Type III tumours, the lymphatic spread clearly followed a path within the abdomen from the left (49%) and right (52%) paracardial region to the lesser curvature (85%), towards the coeliac axis (39%), and finally, the greater curvature of the stomach (33%).(43) So-called 'skip lesions' occurred in less than 5% of the patients.(42)

The remaining unanswered question is whether an extended lymphadenectomy is associated with a prognostic benefit; either in terms of decreased loco-regional recurrence or increased survival.

It has been demonstrated by *Akiyama et al.*(44) that in squamous cell carcinoma, a radical 3-field lymph node dissection resulted in an increased 5-year survival, compared with 2-

field lymphadenectomy. This has historically been used to base the management of patients with adenocarcinoma; however, the above studies suggest that the two tumour types are different entities. There are currently no robust randomised control trials comparing the two methods.

Omloo et al.(45) compared an extended transthoracic oesophagectomy (Fig. 1-9) with a transhiatal oesophagectomy (Fig. 1-10) for mid/distal oesophageal adenocarcinoma. They demonstrated no 5-year survival difference. However in subgroup analysis, there was a 14% survival difference for the transthoracic approach in 90 patients with a Type I tumour. A 5-year loco-regional disease-free survival advantage was demonstrated with a transthoracic approach, for the 104 patients with 1–8 positive lymph nodes only. This is likely due to the improved surgical view within the thorax, and a better ability to resect mediastinal lymph node stations.
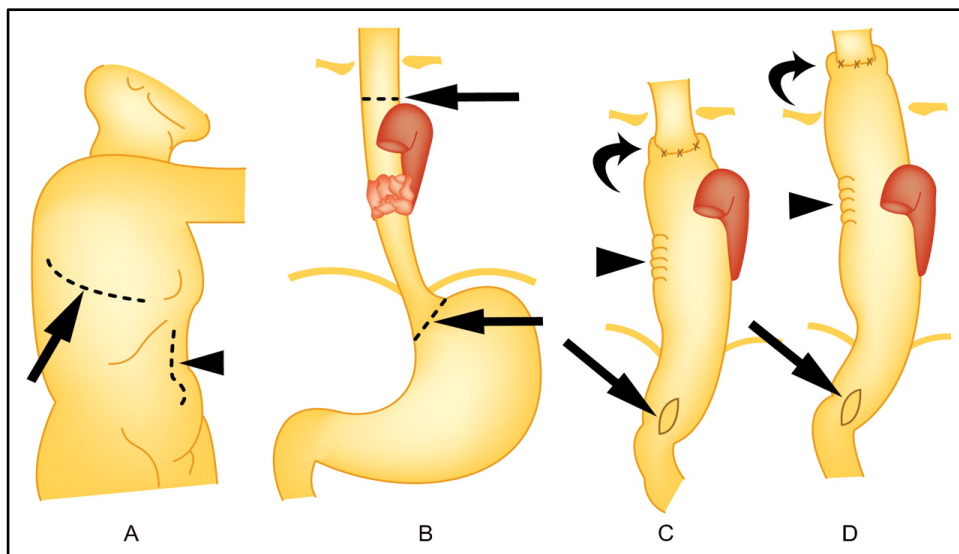
Figure 1-9   Transthoracic oesophagectomy through right thoracotomy and laparotomy
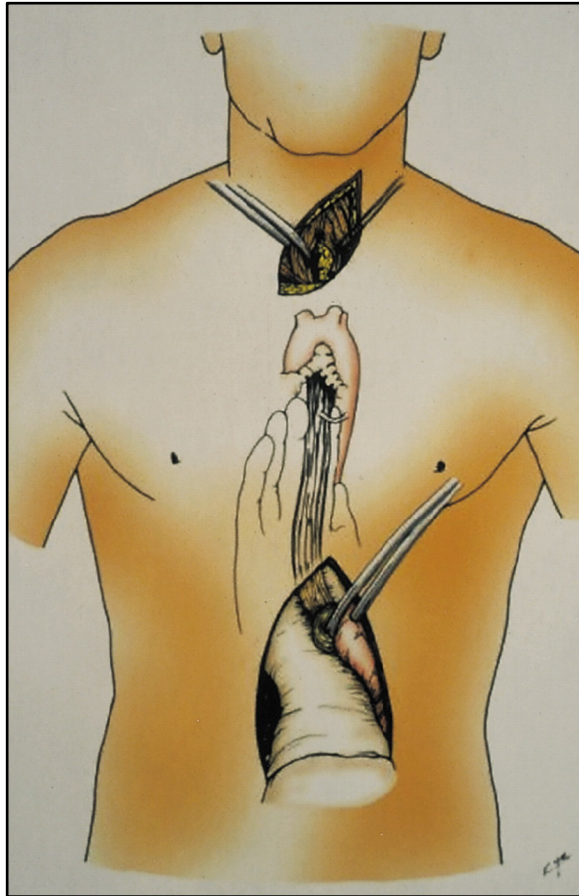
Table 1-4   Transhiatal oesophagectomy through laparotomy and cervical incision

1.4.4   Challenges of sentinel lymph node assessment in oesophageal cancer

In oesophageal adenocarcinoma, it is important to appreciate that significant portions of the relevant lymph nodes are within 3 cm of the primary tumour, as demonstrated by *van de Ven et al*.(46) This complicates the detection of lymph nodes preoperatively, because Positron emission tomography (PET)/ computed tomography (CT) scanners are unable to distinguish positive nodes close to the primary tumour, due to the shine-through effect, described by *Gretschel et al.* (10): 'where a strong radioactive signal from the primary tumour hinders the SLN detection with radiocolloid.'

The issue regarding micrometastatic disease is also important, as continuing information tends to suggest that micrometastases and isolated tumour cells (ITC) are associated with decreased survival.(47) These are not readily identifiable preoperatively with the current PET/CT scanners; which cannot distinguish positive lymph nodes less than 7 to 8 mm in size. SLN acquisition and fine slice immunohistochemistry is required, and to do this effectively, there is a need to improve the detection ability of SLNs. The potential for multimodal tracers, with increased sensitivity, along with a unified assessment intraoperatively from surgeons and pathologists, may be able to improve the detection rates of micrometastases in adenocarcinoma.

Work completed in 2011 by *Thompson et al.*(11) at the University of Adelaide, demonstrated that SLN biopsy was successful in 94% (29/31) of 31 consecutive patients with oesophageal cancer. The unsuccessful identifications occurred in one patient with extensive previous gastrointestinal surgeries, and in another with a BMI of 42. In this study there was a median of 3 SLNs removed per patient (92 total), with a median of 14 lymph nodes removed per patient (438 total). Of the successful 29, 30% had the SLNs identified once the tumour and adjacent nodes had been removed. The sensitivity of the SLN biopsy was 90% (9/10), as there was one false negative, in a patient with overt metastases in four non-SLNs, but no metastatic deposits in two identified sentinel nodes. In the published results, there was an upstaging of 14% of the patients, consistent with other published results. Another patient was found to have micrometastases in an SLN, and underwent adjuvant chemotherapy based on these findings.

The above work demonstrated that the SLN concept in oesophageal cancer is feasible with an acceptable sensitivity rate. It is through studies such as these that more tailored patient lymphadenectomy and more accurate treatment decisions can be achieved with better staging.(48)

1.4.4.1   Blue dye technique

The blue DT has its own limitations in oesophageal cancer. It cannot be injected superficially under the skin as it is in breast or melanoma surgery. It has also been shown by *Gretschel et al.* that using a DT as well as an RCT does not improve sensitivity, when identifying SLN biopsies in gastric cancer.(10) A further problem identified by *Grotenhuis et al.* was an unacceptably high false negative rate of 15%.(49) This meant that 6 of the 39 patients in whom the SLN was negative for metastasis were later found to have metastatic cancer in the non-SLNs positive for tumour cells.

1.4.4.2   Radiocolloid technique

The RCT has been investigated in oesophageal cancer previously. In 2002, a Japanese study demonstrated that the technique was feasible and applicable.(50) There were still relevant issues regarding the concept of sentinel lymph biopsy. One problem encountered was the finding that in 3 of the 18 patients in the study, all the hot nodes resected were negative for metastases. Two of these patients had pT3 tumours, with tumour beyond the muscle layer. The authors also discussed the type of ^{99m}Tc (technetium) tracer used. In their study, ^{99m}Tc-tin colloid was used, however albumin and antimony were also mentioned as possibilities. The different colloids impact on the tracer's lymph node uptake and time interval, and it is important to try and find a universal colloid with the most useful properties, for the technique to be applied in

oesophageal cancer. An ideal radiocolloid size is suspected to be between 10 and 100 nm.(51) This is a balance between a small tracer (<5 nm) that is not retained in lymph nodes, and a large tracer (>500 nm) that does not migrate through lymphatic vessels. In Australia, a ^{99m}Tc-antimony colloid with an approximate size of 10 nm is used.

In a study by *Kato et al.* (51) a similar problem was encountered to that of *Yasuda et al.*(48) There were two patients (2/25) who had false-negative results, and both of these patients had advanced tumours (T3 or T4). This suggests that advanced tumours might disrupt lymphatic drainage, diminishing the accuracy of sentinel node biopsy. It may also be due to the submucosal injection of the radiocolloid, and the tumour comprising deeper layers of the oesophagus. On further analysis, however, with cytokeratin immunohistochemistry staining, those two patients had occult metastases. This finding was part of the reason that the authors concluded that SLN mapping can be used, and is a feasible technique; however, it may be more useful in patients with early oesophageal squamous cell carcinoma. This sentiment is also expressed in the paper by *Takeuchi et al.*(52) where two of the four false-negatives were in pT3 oesophageal cancers. A similar result was achieved by *Kim et al.*(53), who identified SLNs in 100% of patients with cT1 or T2N0M0 disease; however, in two patients with cT3N1M0 and cT4N1M0 disease the SLNs were unable to be identified.

Figure 1-11 summarises the issues of using SLN biopsies in oesophageal cancer.

1. Timing of tracer – different radiocolloids overseas, with different rates of flow

2. Chest cavity – difficulty in accessing post-injection

3. Blue dye – not useful, with proven false-negative rate

4. Shine through – PET/CT not as useful for assessing nodes as they are close to primary tumour

Figure 1-10   Issues with SLN biopsy in oesophageal cancer

1.5   ADVANCING THE SENTINEL LYMPH NODE CONCEPT IN OESOPHAGEAL CANCER

1.5.1   Future options

Through the previous discussion on SLN biopsy and the lymphatic drainage of patients with oesophageal cancer, it is evident that current methods of staging require further investigation and modification, or new methods may be required.

Patients with oesophageal cancer provide a challenge to clinicians, as there is no preoperative modality that can accurately predict lymph node involvement.

Improved lymphatic mapping could accurately identify drainage pathways that would enable surgeons to tailor their lymphadenectomy. In turn this might reduce the number of lymph nodes requiring histological section and allow a more detailed analysis of those lymph nodes, subsequently improving the yield of micrometastases and ITC.

Another option, which would be available if SLN assessment was accurate in oesophageal cancer, is thoracoscopic preoperative staging. If patients with early cancers (i.e. cT1a or cT1b N0M0) could have SLN sampling thoracoscopically, then a more conservative

endoscopic therapy could be used. The caveat to this would be that the sentinel node assessment is accurate, and able to distinguish effectively which patients have positive lymph nodes, and would therefore benefit from operative management.

Techniques such as ICG fluorescence (HyperEye Medical System) are available to assess the blood flow of oesophageal conduits.(54) Using standard operating room lights, this system allows the surgeon to assess tissue viability and it might be feasible to apply this principle in the detection of SLNs.

Endoscopic ultrasound (EUS) has a diagnostic accuracy of between 65 and 75% in the detection of nodal disease in oesophageal cancer.(39) This was improved to 83% with fine needle aspiration (FNA) of suspicious lymph nodes at the time of EUS. EUS cannot detect micrometastases, which, when present, are associated with decreased survival rates, compared with patients who remain node-negative.(47)

PET with [18]FDG has limited spatial resolution, in the region of 5–8 mm for modern machines, which creates difficulties when dealing with lymph nodes that are frequently located close to the primary tumour.

Identification of SLN with radiolabelled colloids, coupled with nuclear imaging has been shown to be beneficial in patients with oesophageal cancer. As previously discussed, the work conducted at the University of Adelaide has provided a framework upon which to improve the accuracy of lymph node acquisition.

1.5.2   Nanotechnology

Nanotechnology is defined as all objects that are man-made and contain nano-scale dimensions, which possess distinctive properties due to their dimension.(55)

Nanotechnology was first used in contrast agents, to compete with gadolinium (Gd)-based agents for MRI. MRI is a modality with potential in improving nodal accuracy. The increased spatial resolution of MRI, coupled with the advent of improved novel lymphotrophic agents, such as ferumoxitran-10, could provide the basis upon which to improve lymph node staging in oesophageal cancer.

Current nanovectors are now based on SPIONs, the first nanoparticle to be approved for *in vivo* imaging, with a ferumoxides injectable solution in 1996 (Fig. 1-12). Currently, there is interest in an ultra-small (20 nm diameter) SPIO; ferumoxtran-10. This is coated with low-molecular weight dextrans for use in lymph node imaging.
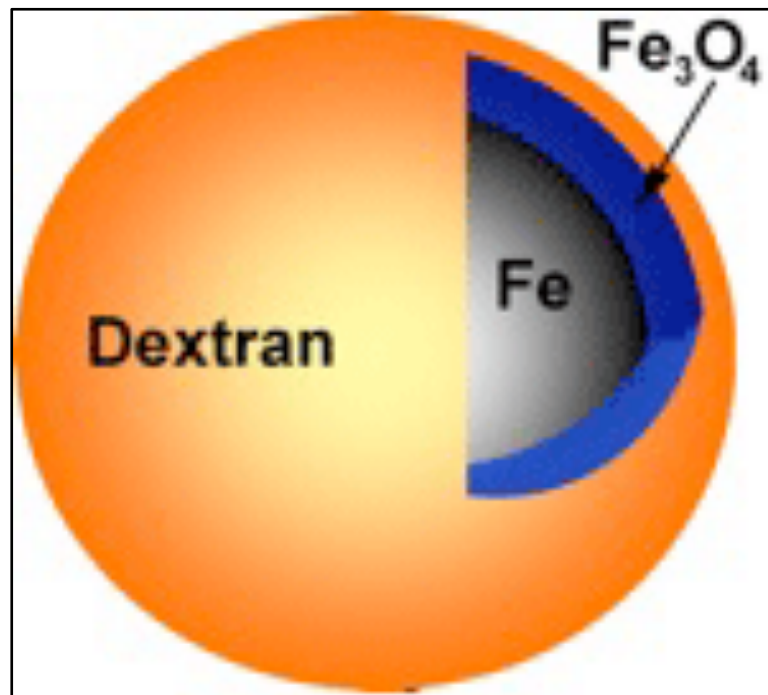
Figure 1-11 Schematic of iron-oxide nanoparticle with iron oxide layer and dextran coating
Source: Property of Dartmouth

SPIONs are termed 'negative' contrast agents, because their iron content produces strong local disruptions in the magnetic field, creating decreased signal intensity in areas of accumulation. Macrophages in lymph nodes can incorporate ferumoxtran-10, creating a dark image, compared with malignant cells that remain bright, therefore enabling identification even in normal sized nodes.(56) This property could also be detrimental, if the tracers are used in low signal body regions. Gd is another potential alternative that is currently being investigated, as it is a positive enhancement compound that provides good MRI images. It will need to be tailored to improve its lymphotropic ability.

A study by *Nishimura et al.* demonstrated that in 16 patients with oesophageal cancer, using the ferumoxtran-10 provided a combined accuracy of 96%, with 100% sensitivity

and 95% specificity for SLN detection. There was a negative predictive value of 100%; 104/104 nodes.(56)

The ability to combine tracers, and to create a dual or multimodality tracer appears to be an enticing possibility. This may lead to improved accuracy in detecting lymph nodes, staging of patients, and tailored lymphadenectomy. The tracer could also have further applications in the treatment of other solid organ tumours.

1.6   AIMS

The aims of this research are:

1. To critically evaluate current literature of the SLN concept in less superficial cancers (i.e. oesophageal cancer).

2. To create a multimodal ^{99m}Tc labelled SPION tracer, and to assess its stability in a small-animal model.

3.   To use the ^{99m}Tc labelled SPION tracer in a large animal model to assess its accuracy and bio-distribution.

1.6.1   Clinical significance

To improve the clinical staging of patients with oesophageal cancer, which may lead to more appropriate treatment(s).

1.6.2   Summary

The overall objective of the research is to develop a multimodality sentinel node tracer that is able to improve the efficacy of SLN assessment in patients with oesophageal cancer.

CHAPTER 2:   SENTINEL LYMPH NODE BIOPSY IN OESOPHAGEAL CANCER: AN ESSENTIAL STEP TOWARDS INDIVIDUALISED CARE

Balalis GL*, Thompson SK

*Discipline of Surgery, University of Adelaide, Adelaide, South Australia

Statement of Authorship

Title of Paper	Seninel Lymph Node Biopsy in Esophageal Cancer: An Essential Step Towards Individualised Care
Publication Status	☑ Published ☐ Accepted for Publication ☐ Submitted for Publication ☐ Publication Style
Publication Details	Balalis GL, Thompson SK. Sentinel lymph node biopsy in esophageal cancer: an essential step towards individualized care. *Annals of Surgical Innovation and Research* 2014, 8:2.

Principal Author

Name of Principal Author (Candidate)	George Balalis		
Contribution to the Paper	Assessment and interpretation of literature, development of manuscript		
Overall percentage (%)	80%		
Signature		Date	1/9/15

Co-Author Contributions

By signing the Statement of Authorship, each author certifies that:

i.   the candidate's stated contribution to the publication is accurate (as detailed above);

ii.   permission is granted for the candidate in include the publication in the thesis; and

iii.   the sum of all co-author contributions is equal to 100% less the candidate's stated contribution.

Name of Co-Author	Sarah Thompson		
Contribution to the Paper	Supervised development of work and assisted in editing manuscript		
Signature		Date	1/9/15

2.1   INTRODUCTION

In the United Kingdom, the rate of death from oesophageal cancer in men has increased by more than 65% since the 1970's.(57) Over the years, there has been some improvement in treatment outcomes, with neoadjuvant therapies and better patient selection.(58, 59) There is still, however, much room for improvement, as current survival rates for resectable disease remain less than 50% at 5 years.

Regional lymph node status is the single most important prognostic factor for patients with oesophageal cancer.(60) It is this prognostic factor that has spawned considerable interest in the SLN concept, as a method for decreasing the extent of surgery, as well as improving staging of patients, by concentrating the pathologist's attention on 1 or 2 important lymph nodes.

The SLN concept, first described by Morton in the early 1990s, depicts the preferential lymphatic metastasis of a tumour to one or more regional nodes. It is the gold standard for patients with breast cancer and malignant melanoma.(61-65) The ALMANAC trial, demonstrated a marked reduction in morbidity and mortality associated with SLN biopsy compared to routine axillary lymphadenectomy, in patients with breast cancer.(66, 67) Through SLN biopsy, patients can be accurately staged, comparable to axillary node dissection, with less morbidity and cost.(67) This has been further demonstrated in several meta-analyses and randomised control trials.

In melanoma patients, SLN allows approximately 80% of patients to be spared a formal lymph node dissection, avoiding the complications of lymphadenectomy; post-operative infection and seroma, long-term stiffness and sensory changes in a peripheral limb

dissection, and most importantly lymphoedema.(68, 69) Due to its low false-negative

rate, quoted at around 1%, SLN biopsy negative patients can be assumed to have no

microscopic disease in the remainder of the lymphatic basin.(68, 70)

So why has the SLN biopsy not become standard of care in other solid organ tumours?

2.2   REVIEW

2.2.1   Benefits

There are two main ways in which routine SLN biopsy in patients with oesophageal cancer

could dramatically influence current treatment options.

2.2.1.1   Endoscopic mucosal resection

Similar to breast cancer and melanoma patients, more accurate preoperative SLN

detection could improve the ability to tailor resection of a more superficial oesophageal

cancer, and potentially avoid the need for an oesophagectomy.

The risk of nodal disease in pT1a (intra-mucosal) lesions has been shown in most studies

to be 5%, compared to 12 to 37% in pT1b (submucosal) lesions.(71-74). A recent study by

Manner et al. describes successful endoscopic submucosal resection (ESR) of oesophageal

cancers restricted to the upper third of the submucosal (pT1b sm1 lesions) in 66 patients

over a 15-year time period.(75) They achieved an 87% complete endoluminal remission

rate and, in patients with small focal lesions less than 2cm in size, a 97% complete

resection rate. It this study they started with double the number or patients, but excluded

those with high risk features for lymph node metastasis. If we could preoperatively assess

lymph node involvement with precision, up to 88% of pT1b sm1 patients could avoid a highly morbid oesophagectomy, and instead undergo a much less invasive ESR. At present however, *Sepesi et al*, have concluded that superficial submucosal oesophageal adenocarcinoma should not be treated by endoscopic resection alone, until more accurate predictors of nodal spread are found.(76)

Currently, there is no randomised controlled trial to compare endoscopic mucosal resection (EMR) and oesophagectomy for early oesophageal cancer (pT1). Various retrospective analyses show that EMR/ESR is comparable to oesophagectomy, with similar complete remission rates and 5 year overall survival. EMR/ESR has also been shown to result in less morbidity and mortality.(77-79) These studies however, suffer from their retrospective nature, heterogeneity in patient groups, and heterogeneity in treatment modalities. It appears that at present, pT1a oesophageal cancer can be treated quite safely with EMR alone, however pT1b cancers warrant a more invasive oesophagectomy and lymphadenectomy until we can improve on current preoperatively investigations.(80)

2.2.1.2   Histopathological assessment

Selective identification of the most important lymph nodes allows the pathologist to 'ultra stage' these nodes with serial sectioning, immunohistochemistry (IHC), and/or reverse-transcriptase polymerase chain reaction (RT-PCR). In an ideal world, all resected lymph nodes would undergo this rigorous assessment. However routine serial sectioning and IHC is prohibitively expensive and time consuming, and therefore a more selective approach is required to ensure that only the most important nodes are selected for the pathologist.

Why is such a detailed pathological assessment necessary?

The 7th Edition of AJCC *cancer staging manual* upstages patients with a breast cancer ≤ 20mm with nodal micrometastases only from Stage 1A to Stage 1B, to reflect a poorer outcome.(81) Accordingly, nodal micrometastases are classified pN1mi, and not pN0mi. At the current time however, isolated tumour cells (ITC), are still considered pN0 disease even though a *New England journal of medicine* paper, published in 2009, found that patients with favourable early-stage breast cancer and either micrometastases or ITCs in regional lymph nodes had a reduced 5-year rate of disease-free survival.(82)

In oesophageal cancer, even in patients with pT1 N0 M0 disease, micrometastases are associated with a significant negative impact on survival.(83-87) These occult deposits, either micrometastases or ITC, are not visible using conventional pathology and require both serial sectioning and IHC.

Further to this, *Thompson et al.* identified that ITC are as important as micro-metastases in determining the overall survival of patients with oesophageal cancer.(47, 88) *Yonemura et al.* also found that a larger proportion of patients died from recurrent disease, if found to have ITC (5 of 37 with ITC compared to 1 of 271 patients without).(89) This clearly has important implications for staging and in the provision of individualised treatment plans, in patients with oesophageal cancer.

2.3   CURRENT LIMITATIONS

First, and probably most important, the type of radiocolloid available for clinical use to detect sentinel nodes is strongly dependent on that particular country's legislation, which hinders the development of uniform protocols. A radiocolloid should 'show rapid transit towards sentinel nodes with persistent retention in the nodes.'[90] The balance of these two properties lies in the size of the particle.[91] Smaller particles allow faster visualisation of SLN and better uptake in metastatic nodes, whilst larger particles have the advantage of a longer retention time and slower transit that minimises detection of nodes downstream to the SLN.

Throughout Europe, ^{99m}Tc-albumin is used, compared to ^{99m}Tc-tin fluoride colloid in Japan, ^{99m}Tc-sulfur colloid in North America, and ^{99m}Tc-antimony colloid here in Australia. The size of the colloid ranges from a 100–220 nm sulfur that can be injected one day prior to surgery, to a 10 ± 3 nm antimony that is injected just prior to the operation.[92, 93] Smaller sized colloids were found to have greater success in preoperative visualisation and intraoperative identification of axillary sentinel nodes in breast cancer patients, compared to larger sized colloids.[94] No similar studies exist for upper gastrointestinal cancer patients.

A second limitation, alluded to earlier, is the logistical issue of injecting the colloid. This is a simple superficial injection in melanoma and breast cancer patients. In contrast, the tracer must be injected via endoscopy/colonoscopy or laparoscopy/thoracoscopy in patients with a cancer of the gastrointestinal tract. This is much more invasive than a skin

injection and the timing differs depending on the radiotracer legislated for use in the country of origin.

Third, in oesophageal adenocarcinoma, greater than 95% of lymph nodes are within 3 cm of the primary tumour, as demonstrated by *van de Ven et al.*(46) This complicates the detection of lymph nodes preoperatively by lymphoscintigraphy, with PET/CT scanners unable to distinguish positive nodes close to the primary tumour due to the shine-through effect (10): 'where a strong radioactive signal from the primary tumour hinders the SLN detection with radiocolloid.' The inability to have a clear anatomical pathway preoperatively, to guide the intraoperative dissection, is a deterrent towards routine clinical application of the SLN concept. The incorporation of more spatially accurate imaging modalities, and better minimally invasive gamma probes (i.e with orthogonal 90-degree probes) may avoid interference from injected tracer in the primary tumour.

2.4 NEXT STEPS

As stated above oesophageal cancer should adopt the SLN concept. It is the only practical method in today's economic climate to identify the most important nodes for detailed histopathological analysis. As well, widespread adoption of this technique will promote the development of novel sentinel node tracers, which may even be capable of non-invasive lymph node staging, and delivery of therapeutic agents to disseminated tumour cells within the nodes. However, as an initial step, we need to improve upon detection of the SLN in non-superficial cancers.

Second, a universally appropriate tracer is required. This will provide consensus on methodology, timing of migration, and results of SLN detection. The timing of endoscopic injection will therefore be able to be standardised. Probably, a tracer with a longer half-life between injection and migration to sentinel nodes will be more appropriate, to enable preoperative imaging.

Third, improved contrast agents are needed, especially for oesophageal cancer. An ideal tracer is one that can enter the initial lymphatic capillary with ease, and move freely to the SLN where it is retained. The tracer should be chemically stable, inexpensive, easily produced and reproducible, and concentrate in the node without spillage. It should also have a short transit time, but remain in the sentinel nodes to allow detection prior to moving on second-tier nodes. Nanotechnology, the use of man-made objects, which contain nano-scale dimensions, may provide the answer.(55) These particles have many of the properties listed above, and some, such as SPIONs, have already been approved for *in vivo* imaging. For example, in 16 patients with oesophageal cancer, Nishimura et al. found that ferumoxtran-10 (an ultra-small 20 nm SPION) provided a combined accuracy of 96%, with 100% sensitivity and 95% specificity in locating the SLN (56) Taking this application one step further, *Weissleder et al.* have shown that lymphotropic SPIONs, injected systemically as exogenous contrast, can discriminate healthy versus tumor-burdened nodes by the degree of accumulation of particles in the nodes.(95)

Dual-modality tracers using blue dye and radioisotope tracer have proven very reliable in many solid organ tumours, including breast cancer, melanoma, and gastric cancer (96-98) This technique facilitates non-invasive preoperative imaging, coupled with subsequent

intraoperative assessment, for SLN detection. Blue dye however is of limited use in oesophageal cancer, due to its short transit time (too short when considering the amount of time needed to enter the chest cavity), and discoloration of adjacent tissues, which may obscure the surgical field. Different dual-modality tracers are needed; perhaps those using MRI with nanoparticles. MRI has advantages over CT lymphography as it provides higher spatial and temporal resolution, and avoids ionising radiation. We are currently trialing a dual-modality tracer with both MRI capability (using iron oxide) and radioactive properties (using 99mTc-antimony colloid) in a pig model.

2.5   CONCLUSION

There are two principal ways in which the SLN concept could improve staging and thereby individualised care in patients with oesophageal cancer. First, adoption of the sentinel node biopsy as a staging investigation (i.e. preoperative lymph node assessment) could tailor resection of a more superficial oesophageal cancer, and potentially avoid the need for an oesophagectomy. Second, identification of the most important lymph nodes allows the pathologist to 'ultra stage' these nodes with serial sectioning, immunohistochemistry, and/or reverse transcriptase polymerase chain reaction. This enables detection of micrometastatic disease, and identifies a patient subset that may benefit from adjuvant therapy.

Three limitations to widespread acceptance of the SLN concept in all solid organ tumors include the lack of a universally legislated radiocolloid for clinical use, the need for an invasive procedure to inject the colloid in many non-superficial cancers, and the inability

to have a clear anatomical pathway preoperatively (due to the "shine through effect"), to guide intraoperative dissection.

We believe that oesophageal cancer management should adopt the SLN concept. This will promote intense research in this field, and lead to improved tracers capable of not only non-invasive lymph node staging, but delivery of therapeutic agents to disseminated tumor cells within the nodes. A universally appropriate tracer is also required to provide consensus and standardisation on methodology, timing of migration, and results of SLN detection. Finally, improved contrast agents are needed, especially those with novel dual-modality 'visibility'.

CHAPTER 3:   RADIOLABELLED ^{99m}Tc-Dx-Fe$_3$O$_4$ NANOPARTICLES FOR DUAL MODALITY SENTINEL LYMPH NODE MAPPING

Cousins A*, Balalis G, Tsopelas C, Thompson SK, Bartholomeusz D, Wedding BA, Thierry B

*Ian Wark Institute, University of South Australia, Australia

(In submission)

Statement of Authorship

Title of Paper	Radiolabelled ^{99m}Tc-magnetite nanoparticles for dual modality sentinel lymph node mapping
Publication Status	☐ Published ☐ Accepted for Publication ☑ Submitted for Publication ☐ Publication Style
Publication Details	Cousins A, Balalis GL, Tsopelas C, Thompson SK, Bartholomeusz D, Wedding BA, Thierry B. Radiolabelled ^{99m}Tc-magnetite nanoparticles for dual modality sentinel lymph node mapping. *Currently in review.*

Co-Author

Name of Candidate (Second author)	George Balalis			
Contribution to the Paper	Assisted with all experiments on animals. Assisted with data collection and editing of paper.			
Overall percentage (%)	30%			
Signature			Date	1/9/15

Principal Author

Name of Co-Author	Aidan Cousins			
Contribution to the Paper	Was main author responsible for project, whose PhD project was the development and validation of the magnetoprobe. Assisted with development of experiments, the execution of experiments and writing of manuscript.			
Signature			Date	1/9/15

Co-Author Contributions

By signing the Statement of Authorship, each author certifies that:

    i.   the candidate's stated contribution to the publication is accurate (as detailed above);

    ii.   permission is granted for the candidate in include the publication in the thesis; and

    iii.   the sum of all co-author contributions is equal to 100% less the candidate's stated contribution.

Name of Co-Author	Chris Tsopelas			
Contribution to the Paper	Assisted with development of experiments, including assisting with performing of all experiments. Also assisted with writing and editing of manuscript.			
Signature			Date	1/9/15

Name of Co-Author	Sarah Thompson		
Contribution to the Paper	Assisted with editing of manuscript.		
Signature		Date	1/9/15

Name of Co-Author	Dylan Bartholomeusz		
Contribution to the Paper	Supervised development of work and assisted in editing manuscript.		
Signature		Date	1/9/15

Name of Co-Author	Bruce Wedding		
Contribution to the Paper	Supervised development of work and assisted in editing manuscript.		
Signature		Date	1/9/15

Name of Co-Author	Benjamin Thierry		
Contribution to the Paper	Supervised development of work and assisted in editing manuscript		
Signature		Date	1/9/15

3.1 INTRODUCTION

Extensive application of ^{99m}Tc-based tracers for sentinel node mapping in breast cancer and melanoma has shown lymphoscintigraphy to be a powerful prognostic tool in the early stages of disease.(99, 100) Whilst the gamma ray energy, half-life, and photon yield of ^{99m}Tc-tracers couple well with highly sensitive pre- and intraoperative scintillation detectors, the technique is not without its limitations, most notably, the poor spatial resolution of gamma cameras and gamma probes. As discussed, detection of sentinel nodes in these cancers can be improved with the addition of organic dyes to stain the lymphatic vessels and nodes to providing additional confirmation.(101-103) However, with co-injection single-mode tracers, small differences in physicochemical properties of each tracer type can lead to widely varied migration speed, lymphatic uptake, and nodal retention. As such, in these superficial cancers, accuracy of the radiocolloid + DT can be further advanced with the use of novel dual tracers (such as ^{99m}Tc-Evans blue).(104) Hence, through the use of single particle, dual modality tracers, one can ideally control the lymphatic migration of both signals compared to co-injection of single mode-tracers. As a result, dual tracers can be useful for studies aimed at comparing techniques for identifying sentinel nodes that rely on different forms of tracer signal (e.g. visual identification of blue dyes vs. gamma probe detection).

From initial preclinical animal experiments using magnetic tracers, the magnetic tunnelling junction (MTJ) magnetometer probe has demonstrated excellent spatial resolution, and an ability to differentiate nodes in a close-packed array. Importantly, it

has demonstrated the ability to intraoperatively detect accumulations of magnetic tracer

in primary draining nodes in swine. Of interest now is to compare the performance of the

magnetometer probe with the conventional gamma probe; that is, using a dual magnetic

/ radioactive tracer in breast cancer or melanoma models. As these tracers are currently

not commercially available, this chapter details the production and characterisation of a

dual magnetic / radioactive tracer formulation based on the techniques of *Henze et*

al.(105)

Whilst dual magnetic / radioactive tracers have been described previously,(106-111) the

methodology, quality, bio-distribution, and logistics of producing such tracers varies

greatly between reports. As a result, one of the objectives of this study was to optimise

the production of a logistically simple formulation made from long shelf-life constituents,

with excellent reproducibility and labelling efficiencies.

3.2   MATERIALS AND METHODS

3.2.1   Magnetic tracer

An aqueous magnetic tracer solution consisting of single crystal magnetite cores with

dextran coating (Dx-Fe_3O_4) was purchased from Chemicell (*FluidMag-DX*, Berlin,

Germany). Magnetic tracer particles were washed via centrifugation and redispersed in

0.9% saline solution (35 mg (Fe) /mL) to remove any excess dextran. Washed magnetic

tracer was deoxygenated by bubbling with dry N_2 gas for 60 minutes, before storing at

5˚C in sterile nitrogen filled vials until required.

3.2.2 Stannous reductant

A primary stock of concentrated stannous solution (33 mg/mL) was prepared by

dissolving $SnCl_2$ powder in a diluted hydrogen chloride (HCl) solution (5 µL of 36% HCl per

1.0 mL of deoxygenated 0.9% saline). Primary stock was stored in a freezer at −15 °C in

sterile nitrogen filled vials for up to 9 months. Stannous solutions for $^{99m}TcO_4^-$ reduction

were prepared by diluting the primary stock with deoxygenated 0.9% saline to a 2.0

mg/mL concentration in sterile nitrogen filled vials. Hydrogenation of stannous solutions

was minimised by storing the vials at −15 °C, and only thawing when required.

3.2.3 Radiolabelled formulation

Sodium ^{99m}Tc-pertechnetate elution in 0.9% saline was obtained daily from a ^{99}Mo / ^{99m}Tc

generator (Gentech: Australian Radioisotopes, Sydney, Australia). In a sealed N_2 vial,

deoxygenated and washed magnetic tracer was mixed with dilute stannous solution and

sodium ^{99m}Tc-pertechnetate. The formulation was briefly agitated, and incubated at room

temperature for 10 minutes before quality control (QC) tests were performed. QC tests

were performed using instant thin layer chromatography paper embedded with instant

thin layer chromatography silica-gel (ITLC-SG). ITLC-SG sheets were cut into 10 x 200 mm

strips, and marked every 10 mm for 100 mm to define the retention factors. Activity

along the strips was measured using an automated gamma counter (WIZARD^2, Perkin

Elmer, Massachusetts, USA). No purification of the resultant ^{99m}Tc-Dx-Fe_3O_4 (dual tracer)

was required prior to use.

3.2.4 Impurity controls

To distinguish activity from the dual tracer from formulation impurities ($^{99m}TcO_4^-$, $^{99m}TcO_2$, and ^{99m}Tc-dextran fragments), a control batch of each impurity type was prepared and QC tests performed using ITLC-SG paper. The $^{99m}TcO_2$, and ^{99m}Tc-dextran controls were prepared by substituting the magnetic tracer in the original formulation with either deoxygenated 0.9% saline or deoxygenated dextran solution (15–20 kDa dextran from leuconostoc spp; 5.0 mg/mL in 0.9% saline), respectively. Undiluted sodium ^{99m}Tc-pertechnetate from the ^{99}Mo / ^{99m}Tc generator was used as a $^{99m}TcO_4^-$ control.

3.2.5 Bio-distribution of dual tracer in a small-animal model

Bio-distribution of the dual tracer was investigated across 6 inbred female Sprague-Dawley rats (150–180 g). These studies were performed in accordance with local and national regulations regarding the ethical conduct of animal experiments. For European Pharmacopeia standard bio-distribution studies, 3 rats received a 0.2 mL (4.8 MBq) dose of dual tracer (diluted to 10% of original concentration) 60 minutes after formulation, which was injected intravenously at a point halfway down the length of the tail. For lymphoscintigraphy and subdermal bio-distribution studies, 3 rats received a 0.1 mL (22.8 MBq) dose of dual tracer 40 minutes after formulation, which was injected subdermally at a point halfway down the length of the tail.

All animals were sacrificed 20 minutes after mean injection time (via isoflurane vapour for intravenous injection and via CO_2 for sub-dermal injection. Note: changes in method of sacrifice differ due to change in local regulations at the time of experiments). During intravenous bio-distribution studies, the tail, liver, lungs, spleen, and kidneys were

removed from the carcass. The activity of each organ (counts / 10 seconds) relative to the whole carcass (excluding tail) was measured using a large volume gamma counter. For subdermal bio-distribution, full-body static lymphoscintigraphy was acquired for 15 minutes before the liver, lungs, spleen, and kidneys were removed from the carcass. Using the large volume counter, the activity of each organ (counts / 10 seconds) was then compared to the activity of a standard sample of the dual tracer (counts / 10 seconds) to determine relative uptake (%ID) in each organ. The standard sample consisted of 0.1 mL of dual tracer prepared for bio-distribution studies, hence for this study:

$$\%\text{ID} = \frac{Activity\ (organ)}{Activity\ (standard)} \times 100\%$$

3.3   RESULTS

3.3.1   Quality control of dual tracer formulation

A simple 3-part formulation was optimised for the chelation of radioactive ^{99m}Tc atoms to dextran coatings on colloidal magnetic nanoparticles. Through optimisation of the formulation, a ratio of 1.0 mL magnetic tracer (35 mg/mL), 0.5 mL stannous solution (2 mg/mL), and 0.2 mL sodium ^{99m}Tc-pertechnetate (356 ± 100 MBq (s.d.) was found to produce the highest quality dual tracer, with labelling efficiencies exceeding 99%.

Labelling efficiency was determined based on the level of residual ^{99m}TcO$_4^-$ in the dual tracer formulation. From studying the retention factors of the three controls (^{99m}TcO$_4^-$, ^{99m}TcO$_2$, and ^{99m}Tc-dextran), it was found that ^{99m}TcO$_4^-$ from the generator would migrate with the solvent front when a 70:30 mixture of methanol to sterile water for injection was

used to develop the ITLC-SG paper (Fig. 3-1). Conversely, the dual tracer bolus would

remain at the origin when ITLC-SG paper was developed using the methanol solution,

making this an ideal QC test for determining the labelling efficiency (Fig. 3-2).
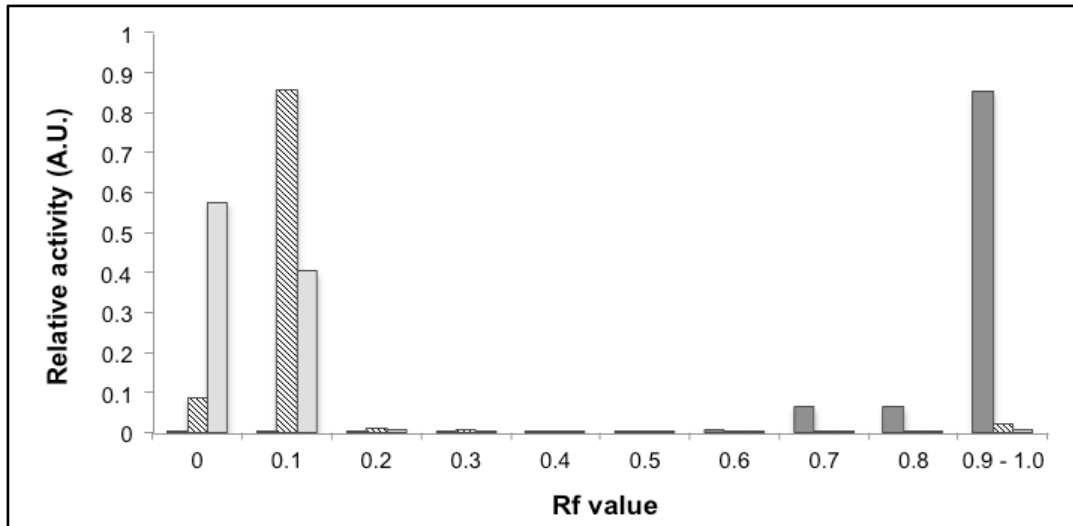
Figure 3-1   Retention factors of impurities

Notes: Shown are the relative activities achieved using thin layer chromatography for formulation impurities $^{99m}TcO_4^-$ (solid, dark grey), $^{99m}TcO_2$ (solid, light grey), and ^{99m}Tc-dextran (striped)
Note the large separation between $^{99m}TcO_4^-$, which is not present between $^{99m}TcO_2$ and ^{99m}Tc-dextran, making quantitative distinction between the latter two impurities difficult
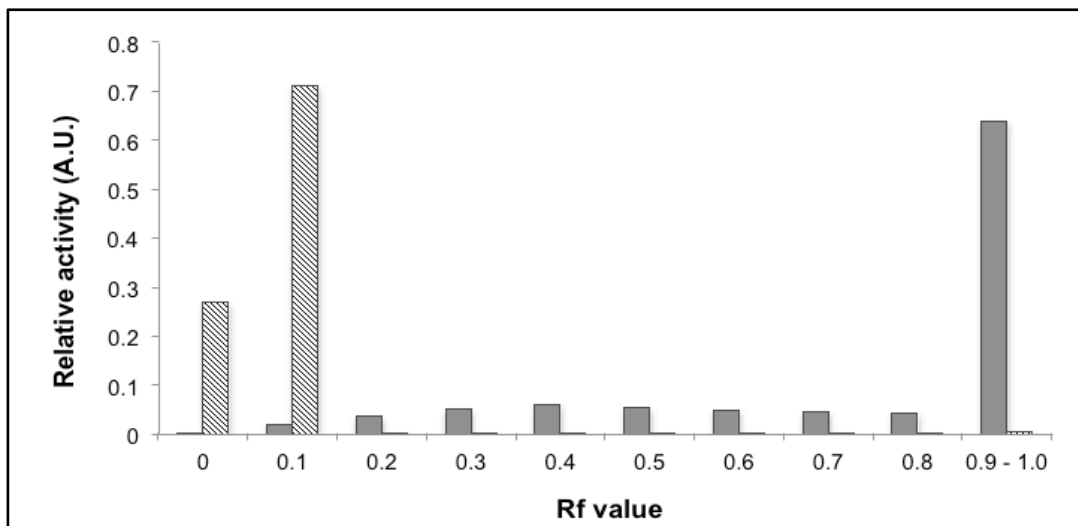
Figure 3-2   Retention factors in saline and organic solvents

Notes: Thin layer chromatography retention factors of the dual tracer formulation when developed with a 70% methanol-water solution (striped) compared to saline (solid, dark grey)
Note the gradient of residual activity along the length of the strip when saline is used. While the bulk of the

dual tracer particles migrate with the solvent front, a portion remains at the origin, making it difficult to separate the tracer particles from $^{99m}TcO_2$ and ^{99m}Tc-dextran impurities

All 17 dual tracer samples were produced using stannous solutions diluted from the same primary stock. This primary stock was stored and repeatedly used to make stannous solutions for 9 months without adversely affecting the quality of the dual tracer formulation. However, towards the end of the primary stock's use it was observed that the time (t) between thawing stannous solutions and adding ^{99m}Tc-pertechnetate began to have an increasing influence on labelling efficiency (e.g. 98.4% when t = 0.75 minutes, compared to 88.1% when t = 20 minutes using identical stannous solutions). As a result, while the long storage time and numerous thaw/refreeze cycles indicate a long shelf life for high concentration, low pH stocks, the timing of the radiolabelling process becomes an important factor to ensure a reproducible, high quality dual tracer.

Repeatability of the QC tests was studied on one occasion by comparing three identical batches with a narrow range of measured labelling efficiencies (98.5% to 98.8%).

When non-organic solvents (e.g. saline solution, water for injection) were used, the bolus of the dual tracer largely migrated with the solvent front, but a portion of the dual tracer particles remained at the origin and along the length of the strip, contributing to colouration of the ITLC-SG paper (due to the dark-brown colour of the magnetic tracer) and non-localised activity (Fig. 3-2). Given the retention of $^{99m}TcO_2$ and ^{99m}Tc-dextran impurities at the origin when either (organic or inorganic) solvent was used (Fig. 3-1), it was difficult to separate these impurities from the radiolabelled magnetic particles using the ITLC-SG technique.

Dynamic light scattering was used to compare the mean particle size and size distribution of magnetic tracer before, and approximately 30 hours after radiolabelling. Both samples were diluted in 0.9% saline, and 3 separate measurement sequences were averaged. The mean hydrodynamic diameter (33 nm) and polydispersity (30 nm) remained unchanged between the two samples, demonstrating high colloidal stability and low aggregation of the tracer nanoparticles after radiolabelling (Fig. 3-3).
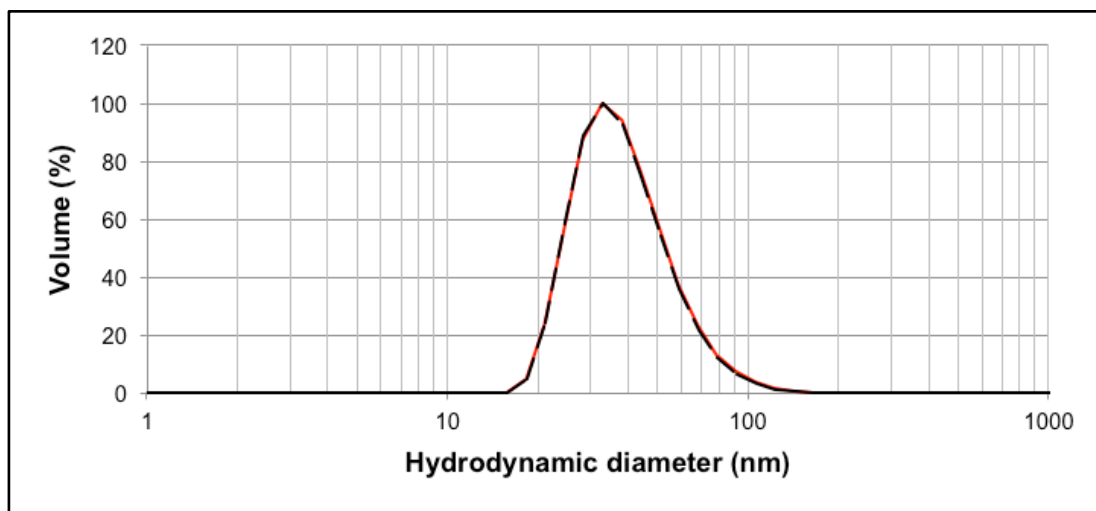
Figure 3-3   Particle sizing of labelled and unlabelled nanoparticles

Notes: Dynamic light scattering particle size distribution of magnetite nanoparticles (FluidMag-DX) before (red line) and after radiolabelling (back, broken line). Mean particle size can be determined by the peak position (33 nm), and polydispersity from the full-width at half maximum (30 nm) and does not appear to be significantly affected by the radiolabelling process

3.3.2   Bio-distribution in animal model

Following a timed 20-minute delay after intravenous injection of the dual tracer, the animals were sacrificed and the activity of select organs was compared to the activity of the complete carcass (minus tail, which included the injection site). The highest mean activity was measured in the liver (66.6%) followed by the kidneys (8.9%), spleen (6.8%) and lungs (0.2%) (Table 3-1). After removal of these organs, the activity of the carcass (e.g. from blood, bone, urine, etc.) was 17.5%.

Table 3-1 Dual tracer bio-distribution following intravenous injection

Organ	Relative Activity (% carcass, no tail)			
	Rat 1	Rat 2	Rat 3	Average
Carcass	17.1	18.0	17.4	17.5
Kidneys	9.1	8.9	8.6	8.9
Lungs	0.2	0.2	0.3	0.2
Liver	66.8	65.0	68.0	66.6
Spleen	6.8	7.8	5.8	6.8

Notes: While uptake of the iron-based tracer is expected to be present in the liver and spleen, activity in the kidneys is likely an artefact of low-molecular weight impurities. Activity for each organ is relative to whole carcass activity after tail removal

To determine the efficacy of the dual tracer as a lymphotropic contrast agent, subdermally injected rats were sacrificed after 20 minutes, and the activity of select organs was measured. By comparing the relative activities (%ID), the highest mean activity was measured in the liver (3.2%), followed by the kidneys (2.0%), spleen (0.3%), and the lungs (0.1%) (Table 3-2).

Before removing the organs of subdermally injected animals, lymphoscintigraphy was used to observe lymphatic uptake of tracer and qualify the efficacy of the dual tracer as a lymphotropic contrast agent (Fig. 3-4). Drainage of the tracer into lymphatic vessels provided excellent exogenous contrast for the first (e.g. popliteal), second (sciatic), and third tier (sacral) nodes. Whilst activity was observed in the kidneys and liver, the level of uptake was much less than that of the nodes, and hence did not greatly impact on the quality of imaging.

Table 3-2   Dual tracer bio-distribution following subdermal injection

Organ	Relative Activity (%ID)			
	Rat 4	Rat 5	Rat 6	Average
Kidney	2.1	2.2	1.8	2.0
Lungs	0.1	0.1	0.1	0.1
Liver	3.3	0.6	5.7	3.2
Spleen	0.4	0.1	0.6	0.3

Notes: As with intravenous delivery of the dual tracer, uptake in the kidneys is indicative of low-molecular weight impurities, compared to the uptake in the liver (which is typical for iron-based contrast agents). Activity for each organ is relative to the injected dose
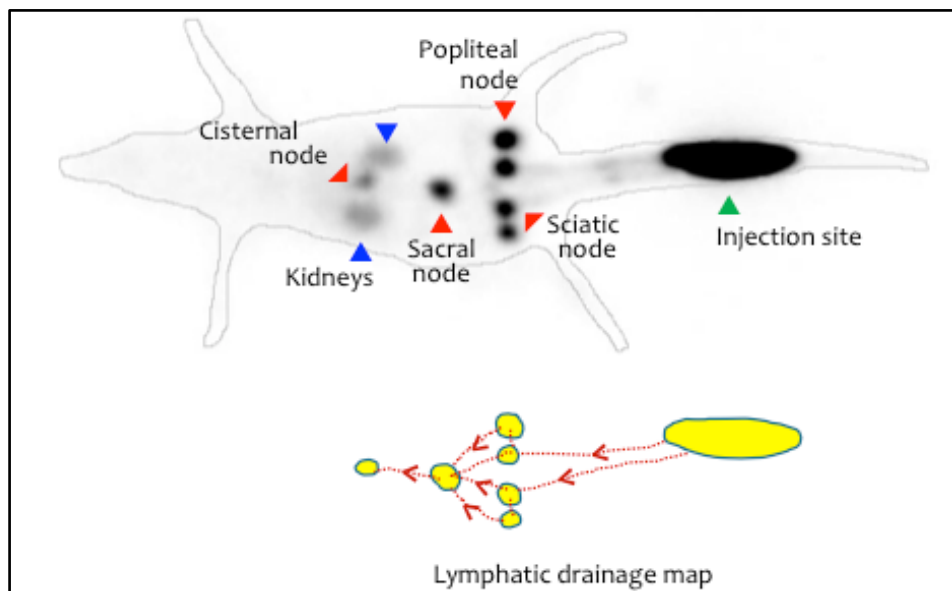
Figure 3-4   Lymphoscintigraphy in rats using dual tracer

Notes: Coloured circles represent draining nodes: first (red), second (orange), third (yellow), and fourth (blue) tiers. Dotted black lines represent kidneys. Note the clarity of the first and second tier nodes, and good visualisation of lymphatic vessels leaving the tail. While uptake in the kidneys (average of 2.0% ID) is evident, the signal in these organs is much lower than that of the lymph nodes

3.4   DISCUSSION

Overall, the formulation showed high reproducibility, with a mean labelling efficiency of 97.6 ± 1.6% (s.d.) (n = 17) after 10 minutes incubation time. Beyond reproducibility, this result demonstrates an ability for the dual tracer to be made on-demand without requiring long incubation or synthesis times. Similarly, the results suggest ease of uptake

of this method by clinical settings given the QC tests reported follow industry-standard techniques currently used for assessing radiocolloids.(14)

Iron oxide nanoparticles are known to accumulate in the liver and spleen via uptake of the particles by Kupffer cells after intravenous injection.(111, 112) This effect has also been demonstrated in radiolabeled iron oxide; (110, 111) hence activity from intravenous dual tracer is to be expected in these organs. After intravenous injection, free radiolabelled dextran will be taken up into the urinary system, pass through the kidneys and become excreted into the urine.(105, 113) From this, the measured dual tracer activity in the kidneys (8.9%) potentially indicates the presence of radiolabelled dextran fragments in the formulation.

Low levels of activity measured in the lungs (0.2%) after intravenous injection indicates that there is minimal aggregation of the dual tracer once administered, and is well below the 5% upper limit detailed in the industry standard European Pharmacopoeia.(114) Such 'biostability' is important in SLN mapping, as large / aggregated particles will have slow clearance from the injection site into the lymphatic system, and may bypass first or second tier sentinel nodes, particularly if they harbour metastatic tumour cells.

As with the intravenous injection bio-distribution, activity in the kidneys after subdermal injection of the dual tracer suggests the presence of radioactive dextran fragments. In early studies of ^{99m}Tc-labelling of dextrans, (115) it was found that fragments less than ~ 40 kDa penetrate into the vasculature following subdermal injection and are filtered by the kidneys. Inconsistency in the level of liver uptake between rats after subdermal

injection may be indicative of the difficulty in reproducing the injection in each animal.

Due to the size of the rats, and the small blood vessels present in the tail of these

animals, it is possible that an uncontrollable percentage of the subdermally injected

tracer entered the venous system. However, it should be noted that even in larger

animals, some uptake of ^{99m}Tc-dextran into the liver after subdermal injection has been

demonstrated previously.(113, 116)

Due to differences in molecular weight and hydrodynamic diameter between iron oxide

nanoparticles and free dextran, migration rates through the lymphatics for impurities are

expected to be much faster than that of the dual tracer. As a result, the radioactive signal

observed in the fourth tier cisternal node (Fig. 3-4) may be skewed by a greater

percentage of radiolabelled impurities compared to the first or second tier. Likewise, the

activity in nodes farther from the injection site may not accurately represent the

magnitude of the magnetic signal (e.g. as MRI contrast) associated with the presence of

iron oxide tracers. Considering the small quantity of residual impurities in the dual tracer

formulation, this effect is expected to be of low impact, although further investigation is

required to determine the impact of this effect in large animal / clinical studies.

Whilst the above limitations need to be considered, depending on the intended

application of the dual tracer, they may be of low impact. For example, following injection

of radiolabelled ^{99m}Tc-magnetite nanoparticles, a patient with a gastrointestinal cancer

could be imaged with MRI to locate the SLN(s), followed by gamma probe detection *in*

vivo. In such an application, the presence of radiolabelled impurities would be

inconsequential to preoperative lymphatic mapping (which is dependent only on

magnetic signal). Furthermore, given the rapid migration of radiolabelled dextrans,(105) at the time of surgery these low molecular weight impurities would have been largely cleared from the lymphatics, reducing the likelihood of false-positive gamma detection *in vivo*. In this regard, a combined magnetic / radioactive tracer could be used to actually increase the accuracy of preoperative lymphatic road mapping in oesophageal and other gastrointestinal cancers.(117)

3.5   CONCLUSION

A high quality radioactive / magnetic dual tracer for lymphatic mapping was formulated using an efficient 1-step, 3-part mixture. The shelf life of magnetic particles is approximately 2 years (according to the manufacturer), and the stannous reductant had a > 9 month lifetime when stored at −15 ˚C in concentrated stock form. Overall, the labelling efficiency of the dual tracer was 97.6%, demonstrating high reproducibility of the optimised formulation. An industry-standard thin paper chromatography QC test was employed to determine radiolabelling efficiency, however it was difficult to precisely quantify the level of impurities using this approach. After formulation, the mean particle size and size distribution of the tracer was unaffected when compared to unlabelled magnetic tracer, and the dual tracer showed excellent colloidal stability at room temperature. Results from intravenous injection show minimal aggregation, and primary uptake of the iron-based dual tracer in the liver and spleen. After subdermal injection the dual tracer shows high uptake and retention in the draining lymph nodes, with some radioactivity present in the liver and kidneys (3% and 2% of the ID, respectively).

Following on from these results, of interest is the performance of the dual tracer in a large-animal model. While small-animal studies are useful for preliminary testing of the dual trace formulation quality, large-animal studies allow use of clinically relevant techniques, such as preoperative MRI, and intraoperative gamma and magnetometer probe detection of draining nodes. As such, application of the dual tracer in large animals will help determine the efficacy of the dual tracer in clinical trials proposed for the future, where relative performance of the gamma and magnetometer probes can be compared.

CHAPTER 4:   NOVEL HAND-HELD MAGNETOMETER PROBE BASED ON MAGNETIC TUNNELLING JUNCTION SENSORS FOR INTRAOPERATIVE SENTINEL LYMPH NODE IDENTIFICATION

Cousins A*, Balalis GL, Thompson SK, Forero Morales D, Mohtar A, Wedding BA, Thierry B

*Ian Wark Research Institute, University of South Australia, South Australia

Statement of Authorship

Title of Paper	Novel Handheld Magnetometer Probe Based on Magnetic Tunnelling Junction Sensors for Intraoperative Sentinel Lymph Node Identification
Publication Status	☑ Published ☐ Accepted for Publication ☐ Submitted for Publication ☐ Publication Style
Publication Details	Cousins A, Balalis GL, Thompson SK, Forero Morales D, Mohtar A, Wedding AB, Thierry B. Novel Handheld Magnetometer Probe Based on Magnetic Tunnelling Junction Sensors for Intraoperative Sentinel Lymph Node Identification. *Sci. Rep. 5, 10842; doi: 10.1038/srep10842* (2015).

Co-Author

Name of Candidate (Second author)	George Balalis		
Contribution to the Paper	Assisted with all experiments on animals, including with the handheld magnetometer probe. Assisted with data collection and editing of paper.		
Overall percentage (%)	30%		
Signature		Date	1/9/15

Principal Author

Name of Co-Author	Aidan Cousins		
Contribution to the Paper	Was main author responsible for project, whose PhD project was the development and validation of the magnetoprobe. Assisted with development of experiments, the execution of experiments and writing of manuscript.		
Signature		Date	1/9/15

Co-Author Contributions

By signing the Statement of Authorship, each author certifies that:

  i.   the candidate's stated contribution to the publication is accurate (as detailed above);
  ii. permission is granted for the candidate in include the publication in the thesis; and
  iii. the sum of all co-author contributions is equal to 100% less the candidate's stated contribution.

Name of Co-Author	Sarah Thompson		
Contribution to the Paper	Assisted with development of experiments, and writing of manuscript		
Signature		Date	1/9/15

Name of Co-Author	Daniel Forero Morales
Contribution to the Paper	Assisted with all experiments, and manuscript. Assisted with bioavailability process
Signature		Date	1/9/15

Name of Co-Author	Aaron Mohtar
Contribution to the Paper	Supervised development of work and assisted in editing manuscript
Signature		Date	1/9/15

Name of Co-Author	Bruce Wedding
Contribution to the Paper	Supervised development of MRI protocol and reviewed MRI images
Signature		Date	1/9/15

Name of Co-Author	Benjamin Thierry
Contribution to the Paper	Supervised development of bioavailability work and assisted in editing manuscript
Signature		Date	1/9/15

4.1 ABSTRACT

Using MTJ sensors, a novel magnetometer probe for the identification of the SLN using magnetic tracers was developed. Probe performance was characterised *in vitro* and validated in a preclinical swine model. Compared to conventional gamma probes, the magnetometer probe showed excellent spatial resolution of 4.0 mm, and the potential to detect as few as 5 μg of magnetic tracer. Due to the high sensitivity of the magnetometer, all first-tier nodes were identified in the preclinical experiments, and there were no instances of false positive or false negative detection. Furthermore, these preliminary data encourage the application of the magnetometer probe for use in more complex lymphatic environments, such as in gastrointestinal cancers, where the sentinel node is often in close proximity to other non-sentinel nodes, and high spatial resolution detection is required.

4.2 INTRODUCTION

In the TNM classification system, the lymphatic system plays a central role in the standard of care for breast cancer and melanoma. Of most prognostic significance is the SLN: the first-tier lymph node to receive drainage from a primary tumour. The presence of metastasis in the SLN has a strong prognostic value in a number of solid cancers.(118-120) If the SLN can be accurately identified and distinguished from surrounding or lower-tier nodes, then a much more targeted approach to cancer staging and treatment is achievable. In order to identify the SLN, lymphotropic contrast agents must be used, as the 'sentinel' status cannot be determined based on anatomical features or location

alone. Currently the gold standard lymphotropic contrast agents for breast cancer and melanoma are low soluble blue dyes and radioactive colloids (usually ^{99m}Tc-based). The role of the dyes is to visually guide the surgery by staining the lymphatic vessels leading from the tumour site and subsequently, stain the SLN. Radioactive tracers have the advantage that gamma camera or SPECT (single-photon emission computed tomography) imaging can be performed preoperatively to provide the surgical team with a lymphatic 'roadmap'. During the surgery, the location of the SLN can then be confirmed with a handheld gamma-detecting probe. Both contrast agents may be used independently, but greater accuracy can be achieved if they are used simultaneously.(121) Whilst these gold standard contrast agents have well-established efficacy in breast cancer and melanoma SLN identification, they have limited application in cancer types with more complex lymphatic draining routes, due to radiation shine-through affecting spatial resolution and accuracy.

In order to overcome the challenges associated with applying the SLN concept beyond breast cancer and melanoma, alternative approaches are currently being investigated.(121) Due to the high quality magnetic signal and validated use in clinical trials, iron oxide nanoparticle-based magnetic tracers show great promise as a real-world alternative to conventional lymphotropic contrast agents.(122-124) One particular advantage to using magnetic tracers is that the SLN detection protocol remains analogous to the protocol currently performed using radioactive tracers (preoperative roadmap imaging and detection with a handheld probe). Furthermore, magnetic tracers eliminate the need for ionising radiation sources and therefore reduce the logistical issues currently associated with the manufacturing, handling, and licensing required to administer

radioactive tracers. In the magnetic tracer alternative, MRI can be readily used instead of gamma cameras for preoperative localisation of the SLN, providing high-resolution imaging and consequently better anatomically detailed images compared to gamma cameras.

To enable intraoperative detection of the SLN, handheld magnetometer probes are required in place of gamma probes. A number of magnetometer probe technologies have been proposed using a range of sensing technologies – from Hall effect sensors(125, 126) and SQUID sensors, to the current embodiment of a commercially available instrument, the SentiMag probe, which uses precisely constructed induction coil sensors.(127) The SentiMag probe provides a notable example of the application of magnetic tracers and magnetometer detection of sentinel nodes, and has been demonstrated in a large clinical breast cancer trial(6) and recently, in a clinical prostate cancer trial.(124) A common compromise that exists with conventional magnetometer technology (Hall effect, giant magnetoresistor, fluxgate, induction coil, or SQUID-based sensors) is that cost and sensitivity are often inversely related. For example, whilst some commercial Hall effect sensors can be bought for less than \$1, their sensitivity is often limited to the millitesla range. Alternatively, the cost for SQUID magnetometers can extend into hundreds of thousands of dollars, which is a reflection of their superior (femtotesla) sensitivity.

MTJ-sensing technology is as an ideal compromise between cost and sensitivity. Limited by the nanofabrication techniques required to produce them, MTJ sensors were not developed until the early 1990s, with commercial products available in limited supply

from the early 2000s. MTJ sensors utilise the spin tunnel magnetoresistance

phenomenon, with passive electrical characteristics dependent on the net magnetic flux

parallel to the sensor's sensing axis. Like Hall effect and giant magnetoresistor sensors,

they can be integrated into surface-mounted packages for electronics, or as bare die can

be used to make magnetometers with a sensing area only tens of microns wide.(128) In

the last 15 years, development of MTJ technology has been rapid, with room temperature

tunnelling magnetoresistance (an indicator of MTJ sensitivity) increasing from

approximately 40%(129) to over 600%.(130) Currently available commercial MTJ sensors,

such as the STJ-240 (MicroMagnetics, Massachusetts, USA) can be bought off-the-shelf

with room temperature magnetoresistance as high as 200% and capable of measuring

nanotesla (nT) fields, yet (at the time of writing) only cost US$50. With such

developments, magnetometers developed using MTJ technology have the potential to

create an economically competitive alternative to conventional induction coil and, in

particular, fluxgate magnetometers.

Importantly, MTJ technology also has the potential to offer higher spatial resolution in

the detection of small accumulations of magnetic tracers. In order to distinguish

individual lymph nodes in tightly packed clusters, the overall spatial resolution of

handheld probes must be less than the average distance between nodes (often taken as

<25 mm for gamma probes used in breast cancer and melanoma procedures(131)).

Overall spatial resolution (i.e. for gamma probes) is measured as the full width half

maximum (FWHM) of a device's response curve when scanned laterally over a point

source. Due to the radiant nature of gamma tracer signals and the size of detectors used

in gamma probes, spatial resolution of commercial probes may vary from 13 to 20 mm

depending on the manufacturer.(132) While satisfactory for detecting the SLN in breast cancer and melanoma, spatial resolutions of this order become problematic in complex lymphatic environments such as oesophageal cancer, where approximately 90% of the SLNs are within 30 mm of the primary tumour(46) and are often clustered in close proximity to other non-sentinel nodes.

Taking these limitations into account, a novel magnetometer probe designed using advanced MTJ sensors has been developed to enable the accurate and reliable detection of small quantities of magnetic tracers in the SLN. More specifically, the characteristic features of MTJ sensors are used here to create a sensitive, high spatial resolution, and a cost-effective alternative to other magnetometer designs aimed at replacing gamma probe technology.

4.3   METHODS

4.3.1   Magnetometer probe

Highly sensitive (2 nT/Hz$^{0.5}$ at 100 Hz) single-axis MgO-based MTJ sensors were purchased from MicroMagnetics (STJ-201, Massachusetts, USA). Ultrasonic wedge bonding of aluminium wire between the contact pads of the MTJ sensors and contact pads on the sensor PCB was required due to the small size of each device. Conventional soldering was used for all other electronic components. Electromagnet for the probe tip was machined out of mild steel into a cylindrical bobbin shape 25 mm long, and with a hollow, central aperture 4.0 mm in diameter for the sensor PCB to sit within. Output signals from the probe were acquired via DAQ6009 hardware (National Instruments, Texas, USA) into a

custom LabVIEW executable. Detected signals from the magnetic tracer were graphed in real time to provide user feedback during use of the probe. All data were saved to a data file for computational analysis.

4.3.2   Measuring magnetic particles

Iron oxide nanoparticles with a dextran coating were purchased from Chemicell (*FluidMag-DX*, Berlin, Germany) for use in magnetic phantoms during *in vitro* characterisation, and as a lymphotropic tracer in large-animal experiments. The hydrodynamic diameter of the tracer was measured using dynamic light scattering to be 28 nm with a distribution width of 20 nm. Changes in tracer size distribution were measured over a wide range of pH levels (1.5 to 11), as well as in a saline and phosphate buffer solution, with no significant changes to stability evident. Two types of dried magnetic phantom were constructed for use with the magnetometer probe: nonpoint-source (NPS) and PS phantoms. NPS phantoms were used for sensitivity measurements, and were constructed by cementing glass coverslips to the face of 4.0 mm thick polyoxymethylene discs with a 5.0 mm central aperture, creating a small well. Controlled volumes of magnetic tracer were dried in the wells, creating a thin, uniform layer of magnetic particles at the bottom of the well. PS phantoms were used for *in vitro* spatial resolution measurements and were constructed by creating a 3.0 mm diameter aperture in a 1.5 mm thick polycarbonate disk, and laminating it to another equally sized disk without an aperture, creating a smaller volume well. Similarly, quantities of magnetic tracer were dried in the well, but due to the small aperture size and viscosity of the tracer, the result was a volume of dried particles of similar dimensions to the well, rather than a thin layer at the bottom. In order to determine the quantity of tracer in each

phantom, 0.1 mL of the stock was dissolved in 36% HCl solution, which was added to an

aqueous solution of $K_4[Fe(CN)_6]$. After 3 minutes, the UV-Vis absorption spectrum of the

solution was measured from 500–800 nm, and the intensity of the spectrum was

compared to a calibration curve from known concentrations of $FeCl_3$ solution to

determine the iron content. For all measurements, the uncertainty in a signal was taken

as the ±1 s.d. of variation in the measured background signal, and the noise level as ±3

s.d. The noise level calculated in this manner was used to find the SNR.

4.3.3   Large-animal experiments

Pre-clinical large-animal experiments using swine were carried out in accordance with the

National Health and Medical Research Council's Australian code of practice for the care

and use of animals for scientific purposes. All experimental protocols using animals were

approved by both Adelaide University and National Imaging Facility animal ethics. In total,

three female Large White swine (31–35 kg) were used across two preclinical studies. For

all the swine studies, the magnetic tracer was prepared to a 20 mg/mL concentration in

0.9% saline, and injected without further purification. Patent Blue V dye was prepared

according to manufacturer's instructions and used to visually identify the lymphatic

vessels leading to draining lymph nodes. T1 sequences were acquired using the following

parameters: TR/TE 1530 ms/4.08 ms, flip angle 15°, field-of-view (FOV) phase 75%, 5 mm

slice thickness (axial and coronal). T2* sequences were acquired using: TR/TE of 155

ms/10 ms, flip angle of 90°, FOV phase of 75%, 5 mm slice thickness (axial and coronal).

Excised nodes were stored in a 10% formalin solution with any surrounding adventitia or

adipose tissue left intact, unless sectioned for Prussian blue staining. If used for staining,

nodes <5 mm in size were halved, and nodes >5 mm were sliced into 3–5 mm sections

and embedded in paraffin wax blocks. Two slices of 4 μm thickness were taken from each

embedded node section for haematoxylin and eosin (H&E) and Prussian blue staining,

respectively.

4.4   RESULTS

4.4.1   Constructing the magnetometer probe

A custom double-sided printed circuit board (PCB) was designed to make the probe's

sensor, and to fit securely inside the hollow core of a bobbin-shaped electromagnet. For

the construction of the magnetometer probe sensor, 4 single-axis MTJ sensors (two

sensors per side of the circuit board) were arranged into a full-bridge Wheatstone

configuration on one end of the PCB. The sensor bridge had a total resistance of 1.5 kΩ in

zero field) with an input current of 3.3 mA. The sensor PCB was mounted inside a 90-turn

cylindrical electromagnet with ferrous core, which formed the tip of the probe (Fig. 4-1

[a]). From finite element analysis of the electromagnet's hollow-core bobbin design, the

magnetic flux density peaks in magnitude approximately 2.5 mm from the tip of the

probe, before decaying in a manner more comparable to solid-core electromagnets (Fig.

4-1 [b]).
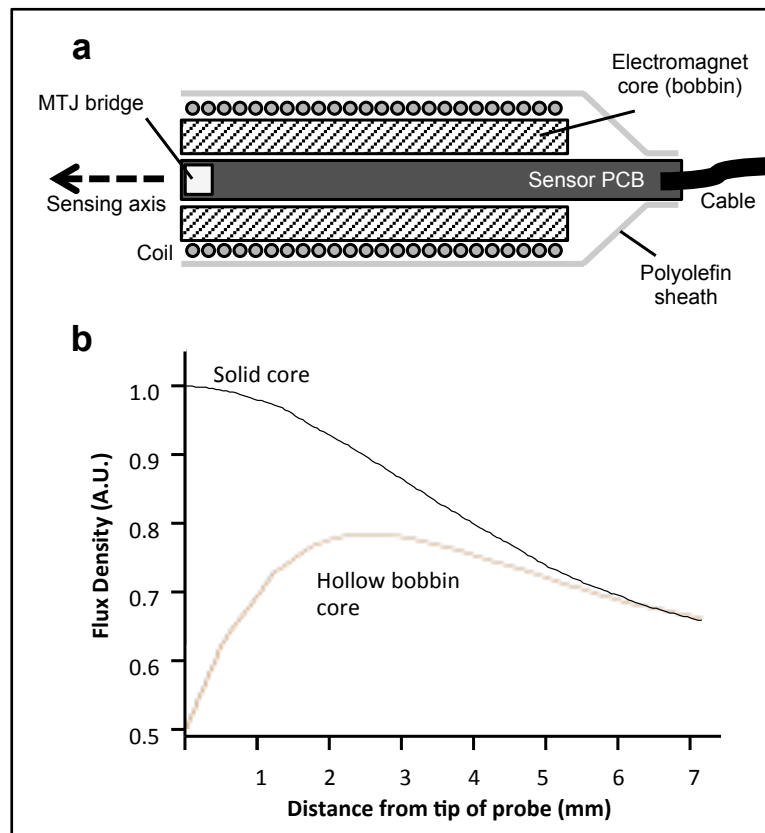
Figure 4-1   Magnetic tunnelling junction magnetometer probe schematic diagram

Figure 4-1 (a): The MTJ sensor bridge is mounted on the end of a small double-sided PCB, and positioned inside a cylindrical electromagnet's aperture, forming the probe tip. The electromagnet consisted of a 90-turn coil wound onto a ferrous core and was used to excite magnetic nanoparticles in either parallel or antiparallel magnetisation with respect to the sensing axis of the probe.

Figure 4-1 (b): Due to the hollow core of the bobbin-shaped electromagnet, from finite element analysis, the magnetic signal can be seen to peak at approximately 2.5 mm from the probe tip, before decaying in a manner similar to that of solid-core electromagnets.

The electromagnet at the tip of the magnetometer probe was used to excite the magnetic

tracer with an alternating parallel / antiparallel magnetic field (square wave alternating

current, 180 Hz, 50% duty cycle). This approach was chosen such that the magnetisation

signal from the magnetic tracer (in phase with the electromagnet) could be distinguished

from background signals such as the baseline magnetic signal from the electromagnet,

50 Hz mains power noise, and Earth's background magnetic field, which are often orders

of magnitude greater than the magnetic tracer signal. By processing the Wheatstone

bridge signal using high gain, high Q active filters, any signals not in phase with the

switching electromagnet (i.e. the noise) could be strongly attenuated. Finally, the filtered

signal was converted to a DC signal proportionate to the magnitude of the signal from the

magnetic tracers; hence changes in the magnetometer probe output could indicate both

the presence and quantity of magnetic tracer in the vicinity of the probe tip.

4.4.2 Measuring the magnetometer probe detection limit

In order to measure the detection limit, a series of magnetic phantoms were made by

drying various quantities of a magnetic tracer stock.

The detection threshold was defined as the quantity of magnetic tracer detected by the

probe with a signal to noise ratio (SNR) of 2.0. Detection threshold measurements for the

sensor bridge were performed using three phantoms of varying magnetic tracer quantity

(0.3 mg, 0.7 mg, and 1.3 mg). A custom rotating stage was used to measure multiple

phantoms in sequence and control the distance between the probe and phantoms

between measurements. The probe was mounted vertically above the sample stage, and

positioned such that the sensor bridge was 4.0 mm from the dried particles of each

passing phantom. This distance value was chosen as a practical probe-to-node distance due to the likely presence of adipose tissue or adventitia surrounding SLNs. Based on the magnitude and noise level of signal for the three measured phantoms, a 50 µg detection threshold at 4.0 mm distance was calculated (Fig. 4-2).

4.4.3   Longitudinal range measurement

Longitudinal sensitivity of a device is the ability to resolve the presence of a signal at distance, and hence is a measurement of the signal from a source as it is moved further away from the tip of the probe. The MTJ magnetometer probe longitudinal sensitivity was measured using a concentrated 10 mg phantom (to improve SNR), which consisted of 0.1 mL of colloidal tracer in a 1.5 mL microcentrifuge tube. A liquid phantom was selected as it better represented the volume of a small lymph node, compared to the thin film of tracer in dried phantoms used in detection limit measurements. The probe was mounted horizontally, and displacement (0.0 mm to 7.5 mm from the probe tip) was controlled via a 2-inch translational stage driven by a DC motor. The phantom was then mounted horizontally on one end of a 30 cm rigid plastic strip with the other end attached to the stage, to act as a spacer and attenuate any magnetic interference from the stage / motor that may be measured by the probe. From the measured data (Fig. 4-3), it can be seen that the magnetic signal from the phantom has a short range, with the signal decaying to 50% at a distance of just 1.0 mm, and below an SNR of 2.0 at approximately 5.1 mm.

Sentinel lymph nodes in oesophageal cancer
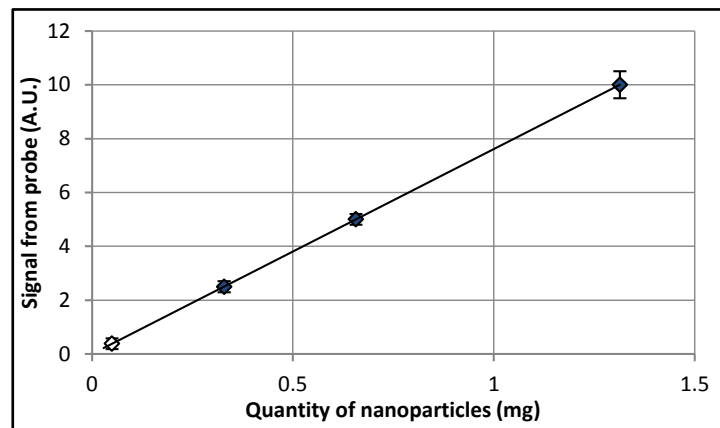
Figure 4-2   Probe link of detection

Figure 4-2: By measuring a range of magnetic tracer quantities at a fixed distance of 4.0 mm from the signal source, a 50µg limit of detection (SNR = 2.0) was calculated. Due to the short-range nature of magnetic fields, this value can be significantly improved if the probe is moved closer to the signal source. ◆ = Measured data; ◇ = Calculated datum.
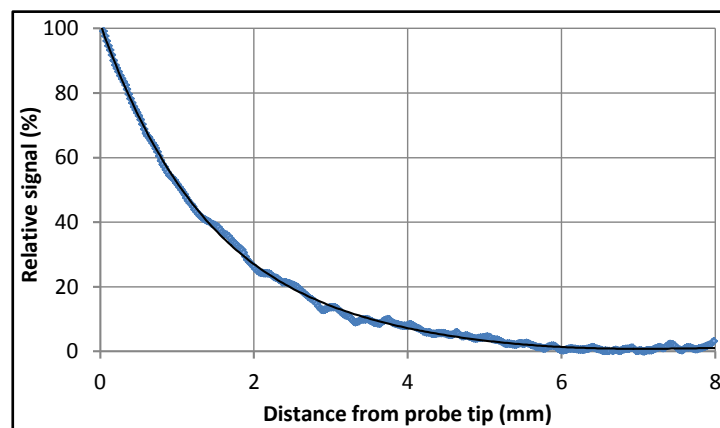
Figure 4-3   Range of magnetic signal

Figure 4-3: The magnetic signal from a simulated lymph node approximately 6 mm in diameter decays at a lower rate than predicted by theoretical inverse-cubed law for magnetic dipoles due predominantly to the finite volume of the phantom.

4.4.4 Lateral response curve measurement

For conventional gamma probes, the spatial resolution is a measure of the lateral response of the probe, that is, the FWHM of the signal obtained by scanning a small point source phantom past the probe at a fixed distance. Likewise, the spatial resolution of the magnetometer probe was quantified by measuring the response curve resulting from scanning a small 1.0 mg dried-tracer phantom. The translational stage was again used to provide controlled displacement of the phantom. The probe was mounted vertically during measurements such that phantom displacement was perpendicular to the sensing axis of the sensor bridge. Due to the high attenuation of magnetic signals with distance, the phantom-probe distance was reduced to 1.0 mm (longitudinal distance), and scanned ±6.0 mm (lateral distance) from the centre of the probe (x = 0). From the resultant lateral response curve (Fig. 4-4), a spatial resolution of 4.0 mm for the magnetometer probe was measured.
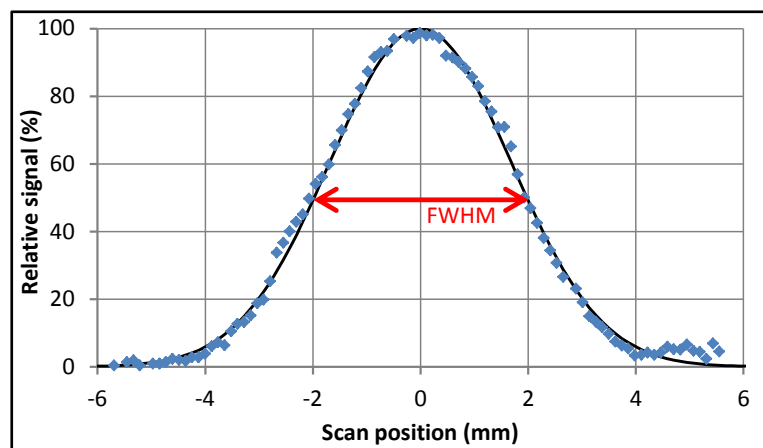
Figure 4-4   Spatial resolution of probe

Figure 4-4: Normalised response curve of a point-source (PS) phantom (centred at x=0) scanned at a height of 1.0 mm. A probe spatial resolution of 4.0 mm can be determined from the response curve's FWHM, which is considerably less than that of a coil magnetometer or gamma probe.

4.4.5   *Ex vivo* measurement of swine lymph nodes

Evaluation of the magnetometer probe *in vivo* was determined using large animal (swine) preclinical studies. To begin with, a 10 mg quantity (20 mg/mL) of magnetic tracer was injected intradermally at a pre-marked site on the dorsal surface above each hind hoof of a single swine. T1 and T2* MRI sequences of the hind leg and groin region were acquired pre-injection as a control. Post-injection, the MRI sequences were repeated at t = 0, 30, and 60 minutes to monitor the uptake of magnetic tracer into the first- and second-tier draining lymph nodes. Once the nodes had been identified on the MRI scans, the swine was moved to an operating theatre. Before surgery, 0.5 mL of blue dye was intradermally injected in the same marked location as the magnetic tracer. During surgery a total of 2 first-tier draining nodes (one from each hind leg) were surgically removed. Both were identified in 30 and 60 minutes post-injection MRI as being deep popliteal nodes (Fig. 4-5 [a]). The blue dye was used to visualise the lymphatic vessels (Fig. 4-5 [b]). In one limb, the first-tier node was visibly identifiable due to the blue staining from the dye, as well as brown staining from the magnetic tracer. Conversely, the first-tier node from the other limb was only identifiable from brown staining, with no apparent uptake of the blue dye (Fig. 4-5 [c]). The maximum magnetic signal from each node was found by measuring the node at various positions. Due to variations in the level of noise between measurements,

SNR was favoured over outright DC signal as a cross-measurement indicator of signal strength and quality. Although both *ex vivo* nodes (N1 and N2) were of comparable size, the SNR from N1 (7.8) was smaller than that of N2 (12.4, see Fig. 4-6 [a]).
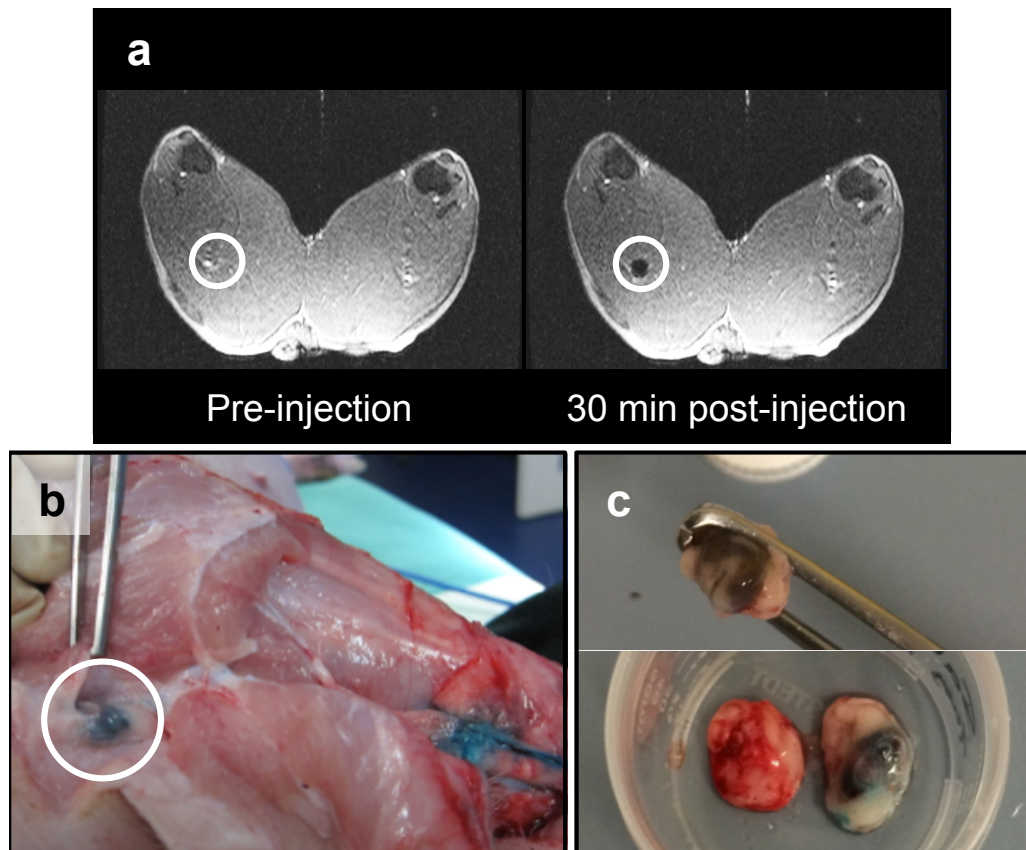
Figure 4-5   'Sentinel' node identification *in vivo*

Figure 4-5 (a): Pre-injection and post-injection coronal MRI scans of a swine's hind legs showing the negative contrast in 1 first-tier node (circled) resulting from the uptake of the magnetic tracer. Post-injection scans were used preoperatively to identify the location and number of first-tier nodes in both limbs for each animal.

Figure 4-5 (b): After the anatomical location of the nodes had been determined with MRI, Patent Blue V dye was used to guide the surgery, and the identification of first-tier nodes (circled).

Figure 4-5 (c): Some nodes were only visualised due to the dark brown staining from magnetic tracer accumulation (top). Compared to a control lymph node (bottom left), either blue dye (bottom right) or magnetic tracer uptake was sufficient to distinguish the nodes from surrounding tissue.

In this study, resected nodes were also used to measure the spatial resolution of the MTJ probe in a simulated close-packed node scenario. To do this, a one-dimensional array of lymph nodes (each of approximately 10–15 mm in largest dimension with adipose tissue and adventitia intact) was made using N1 and N2, and one negatively measured 'control' node (from the groin of the animal). As before, the probe was mounted vertically and the translational stage was used to control node displacement. As the uptake of tracer was non-uniform throughout the node samples (most concentrated where the primary afferent vessel entered the node), N1 and N2 were orientated such that the region of highest tracer accumulation was facing the probe. All nodes were positioned such that their top surface was 1.0 mm from the probe tip. Scanning the node array with the magnetometer probe showed excellent distinction between the simulated 'sentinel' and 'non-sentinel' nodes (Fig. 4-6 [b]). The level measured from N1 and N2 remained above the threshold level (SNR of 5.3 and 7.3, respectively), yet the signal from the control node remained below the threshold level.

4.4.6 *In vivo* measurement of swine lymph nodes

Intraoperative measurements of first-tier draining nodes were performed across two swine. The work was all completed while the animal was anaesthetised, and on completion of the experiments, the animals were euthanised. As described above, a 10 mg dose of magnetic tracer was intradermally administered and MRI was used to localise the SLN(s) before surgery. Blue dye was then used to visualise the lymphatics and map the draining from the injection site. After visual identification of the nodes during surgery, the magnetometer probe was used to measure the signal of each node from a range of positions. When the maximum strength signal was identified, the node was measured 3 times at that location and the signal from the node referenced to the surrounding, non-lymphatic tissue. As before, a node was considered positive if the average maximum signal from the node was greater than the probe threshold level (i.e. SNR = 2.0). After excision, the signal from all nodes was measured once more *ex vivo* by comparing the node signal to the local background.

A total of 6 first-tier (also identified as deep popliteal; n = 2 + 4) and 2 second-tier (identified as superficial inguinal; n = 1 + 1) draining nodes were identified with preoperative MRI due to the uptake of the magnetic tracer. During surgery, all first-tier nodes were visually identifiable from the dark brown staining of the magnetic tracer, yet only 4 of these were also identifiable with the blue dye. All first-tier nodes that showed a presence of magnetic tracer on the MRI scans were measured above the probe threshold (Fig. 4-6a), and confirmed with *ex vivo* measurement. First-tier nodes (N3 and N4) were removed from the hind legs of the first animal, and first-tier nodes (N5a, N5b, N6a, and

N6b) were removed from the hind legs of the second animal. The SNRs for N3–N6b were
6.7, 2.8, 5.2, 8.2, 8.3, and 2.8, respectively. Both of the second-tier nodes identified with
MRI were measured with the probe and were above the threshold level (SNR of 3.5 and
4.5, respectively). During surgery, drainage of the blue dye to an additional second-tier
node was observed in each animal. These additional nodes did not register a signal when
measured with the magnetometer probe, which is supported by the absence of strong
negative contrast of these nodes in post-injection MRI scans.
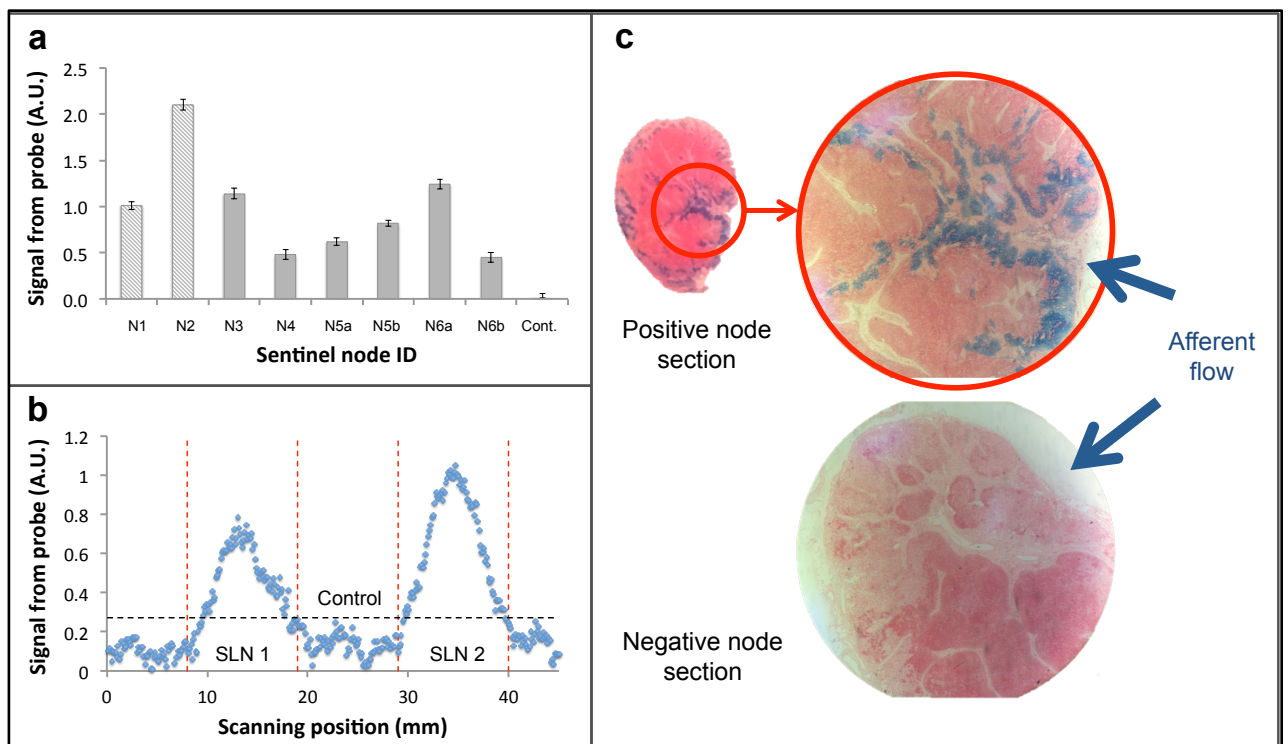
Figure 4-6 Swine lymph node measurements

Figure 4-6 (a): MTJ magnetometer probe measurement of first-tier nodes from three
animals. N1, N2, and control were measured *ex vivo*, and N3–N6b were measured *in vivo*.

Error bars indicate the uncertainty in measurement due to background signal fluctuations (electronic noise).

Figure 4-6 (b): Distinguishing nodes in close proximity in *ex vivo* array of lymph nodes. The boundary of each node is indicated with the vertical dotted lines and the threshold level is indicated with the horizontal dotted line.

Figure 4-6 (c): Prussian blue staining of two separate node sections. The presence of magnetic tracer in afferent trabecula and subcapsular sinuses is evident in positive first- and second-tier nodes (e.g. top), but absent in negative nodes (e.g. bottom).

Through Prussian blue staining of node sections, it was found that in all positively measured nodes from the *in vivo* experiment, significant blue staining in afferent trabecular and subcapsular sinuses was observed (Fig. 4-6[c]). Likewise, Prussian blue staining of negatively measured nodes (2 second-tier, 5 control nodes) revealed little to no presence of magnetic tracer.

4.5 DISCUSSION

A handheld magnetometer probe based on MTJ technology has been developed. Based on the specific requirement of intraoperative detection of SLNs, the main design criteria were high sensitivity and high spatial resolution. An advanced prototype has been fabricated and validated in a preclinical study using swine as a large animal model. The observed detection limit of 50 µg of magnetic tracer equates to 0.25% of an ID for a clinically relevant 20 mg dose of magnetic tracer. Accumulation of lymphotropic magnetic

tracers in SLNs is highly dependent on a number of factors, including the type of cancer, administration route, and the physicochemical properties of the tracers (mostly the hydrodynamic diameter).(91) For a relatively standard 18 MBq dose of filtered 99m-Tc sulfur colloid administered intradermally in breast cancer patients, average SLN accumulation is around 2.5 ± 4.9 (s.d.)%.(133)

Based on the magnetometer probe's longitudinal sensitivity characteristics, the detection limit can be significantly increased if the probe-to-node distance is reduced. Unlike the standard inverse-cubed decay of fields from magnetic dipoles, the decay of the magnetic signal is largely dependent on three factors: the finite volume of the magnetic source, finite size of the sensing volume of the magnetometer probe, and the architecture of the magnetic flux density from the excitation coil. As the sensing volume and magnetic flux density remain constant for the magnetometer probe, then changes to the range will be largely affected by the size / shape of the signal sources (i.e. accumulation in the sentinel node). From the measured data, the magnetic signal decay for a small (6 mm diameter), homogenous concentration of tracer can be modelled with a cubic polynomial function (true for 0 mm < x < 7.5 mm). As a result, and with reference to Figure 4-3, the signal measured for this sample at a distance of 4.0 mm is approximately 10% of the signal at 0.0 mm. This indicates the magnetometer probe would be most effective when measuring nodes with tracer uptake concentrated close to the node surface; where it can be measured at very close range and the limit of detection would approach 5 µg of magnetic tracer, or 0.03% of a 20 mg ID.

During preclinical large-animal studies using swine, uptake of the magnetic tracer in lymph nodes resulted in significant negative contrast on the postinjection MRI scans, providing an anatomically detailed roadmap to assist surgical removal of draining nodes. Across magnetometer probe measurements of first-tier nodes, there was significant variation in the magnetic signal strength, which is likely the result of a combination of factors.

Primarily, variation in lymph node uptake is expected to occur between animals, and even between limbs in the same animal. This is demonstrated by the significant variation in size of the 8 first-tier nodes (ranging from 4 mm to 15 mm in largest dimension). Variation in size can have a number of effects, such as variation in the uptake between nodes, and variation in the concentration of the tracer within the node. Another factor affecting the magnetometer probe's signal magnitude was the varying level of adventitia and adipose tissue surrounding *in vivo* first-tier nodes. This can limit the distance of the probe to the node, and in some cases, the adipose tissue surrounding the node had to be partially or fully resected during surgery to sufficiently expose the node and register a signal with the magnetometer probe.

The presence of tissue in the vicinity of the probe tip introduces a secondary effect: reduction in the magnetic signal *in vivo* due to the negative susceptibility (and hence diamagnetic nature) of surrounding tissue. Using a simple mathematical approximation, more than 0.4 μg of iron oxide nanoparticles would be required per 1.0 cm^3 of tissue to counteract this diamagnetic effect and be measured by a coil or induction-based

magnetometer.(134) However, the impact of diamagnetic tissue on overall signal strength

is expected to be low for the MTJ magnetometer probe, given the large dependence of

signal strength on distance from the probe tip. Using the measured range (Fig. 4-3) and

spatial resolution (Fig. 4-4) of the MTJ magnetometer probe, the sensing volume can be

approximated with that of a cone (i.e. ~ 0.03 cm^3). Based on the above calculation, it is

approximated that the limit of iron oxide detection due to diamagnetic interference

would be 0.01 µg of tracer – a value much lower than the previously calculated 5 µg of

tracer required for detection using the MTJ magnetometer probe.

Although the factors above must be considered for the application of the magnetometer

probe in the intraoperative setting, variation in signal between nodes *in vivo* was not

found to be of consequence. This is because only binary, qualitative (positive/negative)

detection is required to locate the SLN; and this can be adequately achieved as long as

the signal is above the predetermined threshold value.

By analysing the Prussian blue stained node sections under an optical microscope, the

presence of the magnetic tracers in positively measured nodes could be confirmed.

Furthermore, while the two negatively measured second-tier nodes could be seen to

contain a small level of magnetic tracer, there was a clear distinction in the quantity of

magnetic tracer when compared to positively measured first-tier and second-tier nodes.

Besides sensitivity, the spatial resolution of the magnetometer probe is of high

importance, especially for malignancies with complex lymphatic drainage such as

gastrointestinal and oesophageal cancer. Compared to the spatial resolution of gamma

probes and competing magnetometer probes such as the SentiMag (spatial resolution of

~ 20 mm(135)), the MTJ magnetometer probe demonstrates excellent spatial resolution at just 4.0 mm. From the spatial resolution, the magnetometer probe's ability to differentiate a SLN signal from an injection site's background signal can also be determined. For gamma probes, an SLN must be a minimum distance equal to 3 s.d. of the response curve from an injection site to minimise erroneous readings due to gamma shine-through.(136) For a probe with a spatial resolution of 20 mm, this distance equates to >25 mm, but for the MTJ magnetometer probe, only a distance of >5 mm would be required. Resolution of this order may offer a significant advantage in complex, close-packed lymphatic environments, as further demonstrated in the *ex vivo* spatial resolution measurements presented in Figure 4-6 [b].

In a simulated close-packed array of lymph nodes, the probe demonstrated the ability to accurately distinguish positive (sentinel) nodes from control nodes with near-pinpoint precision. These experiments demonstrate the potential for the MTJ magnetometer probe to be applied beyond breast cancer and melanoma to more complex cancer types such as oesophageal, and other deep tissue cancers of the abdomen.

CHAPTER 5:   A MULTIMODALITY ^{99m}Tc-LABELLED IRON OXIDE NANOTRACER TO IMPROVE SENTINEL NODE IDENTIFICATION IN EARLY OESOPHAGEAL CANCER

Balalis GL[*], Cousins A, Tsopelas C, Devitt PG, Madigan D, Bartholomeusz D, Thierry B, Thompson SK
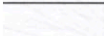
[*]Discipline of Surgery, University of Adelaide, Adelaide, SA 5000, Australia

(In submission)

Statement of Authorship

Title of Paper	A multimodality ^{99m}Tc-labelled iron oxide nanotracer to improve sentinel node identification in early oesophageal cancer
Publication Status	☐ Published ☐ Accepted for Publication ☑ Submitted for Publication ☐ Publication Style
Publication Details	Balalis GL, Cousins A, Tsopelas C, Devitt P, Madigan D, Bartholomeusz D, Thierry B, Thompson SK. A multimodality ^{99m}Tc-labelled iron oxide nanotracer to improve sentinel node identification in early oesophageal cancer. *Currently in review.*

Principal Author

Name of Principal Author (Candidate)	George Balalis
Contribution to the Paper	Development of surgical protocol for experiments. Personally carried out all surgical experiments, including endoscopically injecting tracer, laparotomy and nodal harvest. Was also main author of manuscript.
Overall percentage (%)	60%
Signature	Date 1/9/15

Co-Author Contributions

By signing the Statement of Authorship, each author certifies that:

i. the candidate's stated contribution to the publication is accurate (as detailed above);

ii. permission is granted for the candidate in include the publication in the thesis; and

iii. the sum of all co-author contributions is equal to 100% less the candidate's stated contribution.

Name of Co-Author	Aidan Cousins
Contribution to the Paper	Assisted with all experiments, and manuscript. Assisted with bioavailability process.
Signature	Date 1/9/15

Name of Co-Author	Chris Tsopelas
Contribution to the Paper	Assisted with all experiments, and manuscript. Assisted with bioavailability process.
Signature	Date 1/9/15

Name of Co-Author	Peter Devitt
Contribution to the Paper	Supervised development of work and assisted in editing manuscript
Signature	Date 1/9/15

Name of Co-Author	Dan Madigan
Contribution to the Paper	Supervised development of MRI protocol and reviewed MRI images
Signature	Date 1/9/15

Name of Co-Author	Dylan Bartholomeusz
Contribution to the Paper	Supervised development of bioavailability work and assisted in editing manuscript
Signature	Date 1/9/15

Name of Co-Author	Benjamin Thierry
Contribution to the Paper	Supervised development of bioavailability work and assisted in editing manuscript
Signature	Date 1/9/15

Name of Co-Author	Sarah Thompson
Contribution to the Paper	Supervised development of work and assisted in editing manuscript
Signature	Date 1/9/15

5.1 ABSTRACT

Purpose: Early oesophageal cancer can now be treated with endoscopic resection, however accurate methods of staging lymph nodes pre-operatively remain elusive. To improve detection of SLNs, ^{99m}Tc labelled SPIONs were evaluated in a swine model.

Methodology: An initial study was undertaken on 9 swine, with injection of either 30 nm SPION or ^{99m}Tc-SPION into the hind limbs, followed by assessment with MRI. In the second study, 4 swine were injected with ^{99m}Tc-SPION into the oesophagus, and pre- and post-injection MRI images were acquired. Sentinel nodes were identified using a gamma probe. Finally, bio-distribution of the tracer was evaluated with injection of ^{99m}Tc-ATC and ^{99m}Tc-SPIONs, respectively. Lymph nodes and reticuloendothelial organs were harvested, and counted to determine the percentage of ID.

Results: In the hind-limb study, clear uptake of SPIONs and ^{99m}Tc-SPIONs were seen in sentinel nodes (deep popliteal nodes), and continuation to the superficial inguinal nodes on MRI imaging. In the SPION alone group, uptake was confirmed in all blue lymph nodes, confirming a consistent lymphatic pathway. In the ^{99m}Tc-SPION group, uptake of the tracer was confirmed on surgical exploration, with the gamma probe detecting all nodes seen on MRI imaging. Radiolabelling efficiency was >98%. In the oesophageal study, MRI images confirmed uptake of SPIONs to the celiac lymph nodes. ^{99m}Tc-ATC and ^{99m}Tc-SPIONs were taken up by swine liver and lungs with similar percentage ID values, and there was 7% ID of ^{99m}Tc-SPIONs by the kidneys, compared to <1% ID of ^{99m}Tc-ATC in the same organs.

Conclusion: A multimodality tracer comprised of ^{99m}Tc-SPIONs was prepared and validated using both MRI imaging and gamma probe. This new tracer could allow thoracoscopic evaluation of SLNs in patients with early oesophageal cancer, and guide treatment decisions.

5.2 INTRODUCTION

The increasing use of endoscopic approaches for the management of early oesophageal cancer now means that some patients can forego an oesophagectomy for a far less radical endoscopic procedure(137). Patients with an intramucosal tumour (pT1a) and, in some instances, a submucosal tumour (pT1b) are those suitable for either EMR or endoscopic submucosal dissection (ESD)(138). However, there is still a risk of nodal metastases in this patient population; less than 5% for pT1a tumours and up to 22% for pT1b lesions.(139, 140) Due to the higher risk of positive nodes in the latter group of patients, most of these individuals are counselled to undergo an oesophagectomy, unless contraindicated, as this provides the best treatment outcome.(76, 141-144) However, up to 78% of patients would benefit from an endoscopic treatment alone, if one could be certain that the nodes were all negative. It is this challenge that has led us to pursue SLN assessment in oesophageal cancer.(117)

Preoperative staging is important in the stratification of patients with oesophageal cancer, but the assessment of lymph node status has its limitations. PET is unable to assess lymph nodes close to the primary tumour with great accuracy (145), due to the shine-through effect, 'where a strong radioactive signal from the primary tumour hinders the SLN detection with radiocolloid'.(10) CT positive lymph nodes are based upon size criteria, where a node greater than 10 mm in diameter is assumed to be involved in the malignant process (146). However, smaller lymph nodes may also contain metastatic cancer cells.(147) PET is more sensitive than CT for differentiating benign and malignant

lymph nodes, but it lacks resolution, and nodes are required to be at least 6–8 mm in size for diagnosis.(148) PET scans also have false-positive findings in lymph nodes, rising from inflammatory lesions, infections or strictures.(149) EUS is currently the most effective test to assess loco-regional nodal disease and combined with FNA has a higher sensitivity and specificity, from 85 to 96% (150, 151). In a retrospective analysis of 149 patients, only 1 out of 18 patients with a cT2N0 cancer was staged accurately as a pT2N0 cancer.(152)

In breast cancer and melanoma, SLN biopsy is the gold standard for preoperative nodal assessment.(61, 62) We have previously shown that in patients with oesophageal cancer intraoperative detection of SLNs can be performed with excellent accuracy using ^{99m}Tc antimony and an intraoperative gamma probe. (153) This technique has obvious limitations in oesophageal cancer, due to the logistical difficulty of accessing the chest cavity, and the shine-through effect (92) of PET. To improve staging accuracy in patients with oesophageal cancer, a more sensitive method of assessing lymphatic status (both preoperatively and intraoperatively) is required.

The current study was designed to assess the role of MRI as a novel imaging tool in the detection of SLNs in the oesophagus. Swine was chosen as the large-animal model in our study due to their monogastric anatomy mimicking human anatomy. MRI was chosen as the imaging modality due to its superior resolution of tissue planes, and lack of radiation, and SPIONs used as the contrast agent.(154-156) The aim of this study was to develop and evaluate a multimodal contrast agent, comprised of ^{99m}Tc labelled SPIONs for imaging and detection with MRI and gamma probe. Such an agent would combine the advantages

of high quality pre-operative imaging afforded by MRI with the high intraoperative reliability of gamma tracers.

5.3 METHODS

5.3.1 Tracer preparation

Non-radioactive cold kits containing SPION and stannous chloride reductant were prepared and QC tested according to a technique reported elsewhere (Chapter 3). The agents used were: SPION (Chemicell, Germany), sodium ^{99m}Tc-pertechnetate [obtained from the daily elution of a ^{99}Mo/^{99}Tc generator (Gentech: Australian Radioisotopes, Sydney, Australia)], and ^{99m}Tc-ATC(157). Radiochemical purity was determined by instant thin-layer chromatography as described previously, in saline (^{99m}Tc-pertechnetate at R_f = 1.0). ^{99m}Tc-ATC or ^{99m}Tc-SPIONs with radiochemical purity >95% was used in the study. All results are reported as mean ± s.d.

5.3.2 Magnetic resonance imaging

For all experiments, T1 and T2* images were acquired before and after a radiotracer injection using a 1.5T Siemens MRI scanner. Post-injection T1 and T2* MRI images were taken at specific time intervals: 0 minutes, 60 minutes and 120 minutes. Images were subsequently assessed for lymphatic uptake by an experienced radiologist.

In the lower limb experiments, MRI scans ranged from the hind hoof to the inguinal canal. The parameters for the T1 images were as follows: TR/TE 1530 ms/4.08 ms, flip angle 15°, FOV phase 75%, and a slice thickness of 5 mm in axial and coronal. The T2* images had a

TR/TE of 155 ms/10 ms, flip angle of 90°, FOV phase of 75%, and a slice thickness of 5 mm in axial and coronal.

For the oesophageal experiments, the scan ranged from the tracheal bifurcation to the inguinal canal. The T1 image parameters were: TR/TE of 145 ms/4.76 ms, flip angle of 70°, FOV phase 75%, and a slice thickness of 5 mm in axial. The T2* images had a TR/TE of 155ms/10ms, flip angle of 90°, FOV phase of 75%, and a slice thickness of 5 mm in axial.

5.3.3   Swine studies

Experiments performed with the pigs complied with the Australian Code of Practice for the Care and Use of Animals for Scientific Purposes (National Health and Medical Research Council) and according to a protocol approved by the Animal Ethics Committee of the Institute of Medical and Veterinary Science, Adelaide, South Australia.

5.3.4   Operative protocol

A total of 14 female domestic pigs (40–45kg) were used in the study, and each animal was pre-medicated by intravenous injection of thiopentone sodium (12 mg/kg) via the jugular vein. Each pig was placed in the supine position, and secured by adhesive tape to the operating table. Anaesthesia was maintained by intubation and delivery of halothane in air (2.5 L/min) plus oxygen (4 L/min) throughout the entire procedure. In all swine, at a selected time point, lymph node chains or basins (two or more nodes) were harvested simultaneously, and individual node samples were stored separately in neutral buffered formalin (4% w/v) before analysis. Upon completion, swine were euthanised by intravenous injection of pentobarbitone (325 mg/mL; 23 mL).

5.3.5   Hind-limb injections

For each animal in the hind-limb injection group, a single dose of contrast agent (0.5 mL) was injected into the subcutaneous space of the anterior hoof region, 5 cm above the hoof. This was either: (i) SPION (10 mg) in 4 animals; or (ii) multimodal ^{99m}Tc-SPION (394.0 +/- 5.5 MBq) in 5 animals. The bleb at the injection site was massaged for 2 minutes to facilitate migration. In the SPION alone group, just prior to operative exposure, the lymphatic stain Patent Blue V (CAS 3536-49-0; 25 mg/mL; 0.5 mL) was injected subcutaneously. After 5 minutes the lymphatic networks leading from the injection site to draining nodes were exposed and discoloured lymph nodes identified. Lymph nodes were observed for brown (SPIONs) or blue (Patent Blue V). Sentinel nodes identified on the MRI images were compared and matched to those identified by the dye method.

In the ^{99m}Tc-SPION swine, a short vertical incision was made in the skin of the popliteal fossa, inguinal or upper abdominal area, approximately 90 minutes after injection of ^{99m}Tc-SPION tracer, and the discoloured lymphatic channels were identified. A gamma probe (SRP Mk II; Gammasonics, NSW, Australia) was used to assist in localising the SLN(s).

5.3.6   Oesophageal injections

In 4 swine, a single dose (0.5 mL) of ^{99m}Tc-SPION was injected into the submucosa of the distal oesophagus using endoscopy and a small injection needle (sclerotherapy needle; 23 gauge; TeleMed Systems; Hudson, Massachusetts, USA). An experienced endoscopist achieved all injections with minimal spillage into the oesophageal lumen.

5.3.7   Bio-distribution comparison

Distribution of ^{99m}Tc-SPION was compared to the gold standard ^{99m}Tc-ATC tracer systems in the hind limbs of 2 swine (1 swine each). Harvested lymph nodes were carefully processed to remove gross adipose tissue and assessed for colour. The lungs, liver, spleen and kidneys were harvested as organ samples. Each sample was then counted in a large-volume gamma counter (AEI-EKCO, Biosentry; Australia) linked to a multichannel analyser (Gammasonics; Victoria, Australia) over a ^{99m}Tc window (70-210 KeV). Results were calculated on the basis of a representative ^{99m}Tc dose standard (0.1 mL) and reported as the percentage of the ID. All counted samples were background corrected.

5.3.8   Pathologic handling of sentinel nodes

Lymph nodes were submitted for pathologic examination, and examined by an experienced pathologist. Fresh lymph nodes were sent to the laboratory where sections were fixed in 10% buffered formalin, then stained with H&E and/or Prussian blue prior to histological analysis.

5.4   RESULTS

5.4.1   Hind limb injections

In the SPION swine (n = 4), sentinel nodes were identified in the post-injection MRI (at all 3 time points) in the deep popliteal nodes. Blue dye was then injected in the same location to provide an effective visual signal for resection of the SLNs in the deep popliteal regions. Prussian blue staining of the excised tissue confirmed iron deposition in the resected blue nodes (Fig. 5-1). There was a consistent lymphatic drainage in all 4 swine to the deep popliteal lymph nodes, and subsequently to the superficial inguinal

nodes. The sentinel node (deep popliteal) was consistent in all swine, and was located

with the blue dye injections. In all of the resected nodes, Prussian blue staining confirmed

iron oxide deposition.
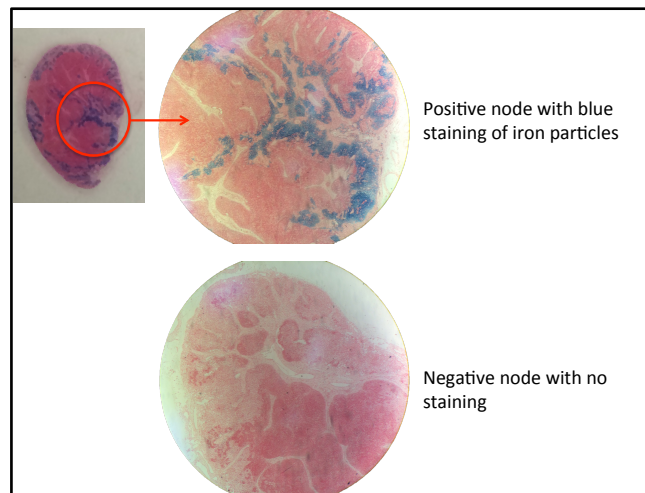
Figure 5-1   Prussian Blue staining of a lymph node demonstrating uptake of iron oxide particles

In the ^{99m}Tc-SPION swine (n = 5), MRI images visualised the deep popliteal node (Fig. 5-2)

as the SLN in 4 of the 5 swine. The superficial inguinal nodes were demonstrated as the

second tier nodes in 4 of 5 swine (Table 5-1). In one swine, the superficial inguinal node

was the sentinel node, with drainage bypassing the deep popliteal nodal station. Nodes

containing the ^{99m}Tc-SPIONs appeared darker than normal nodes in T2* imaging, because

of the shortening of the T2 relaxation time. The gamma probe effectively detected

(qualitative audible noise) the SLN and second tier nodes in all swine.
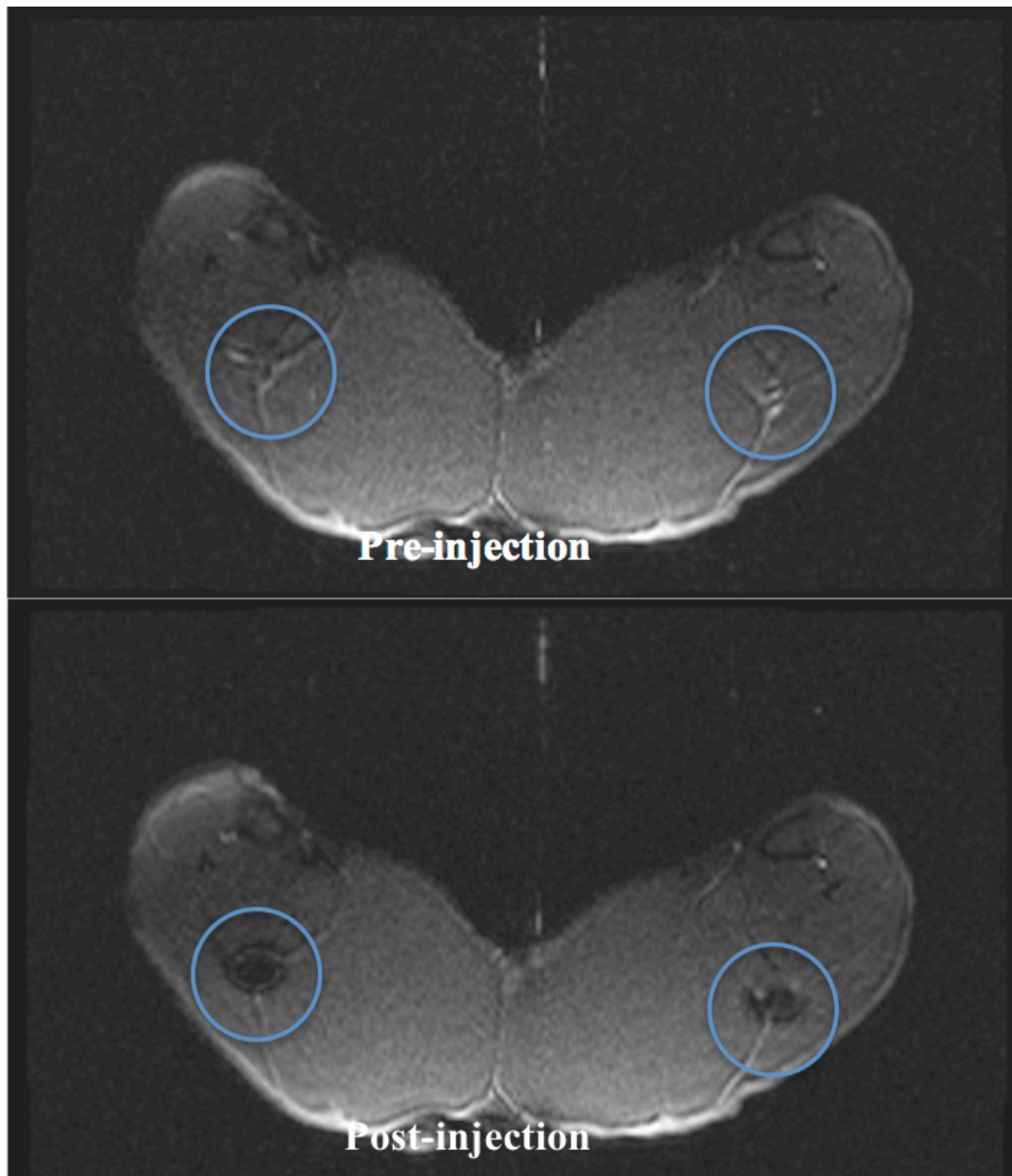
Figure 5-2 Magnetic resonance images of the lower limbs of a swine model pre- and post-injection, following uptake of ^{99m}Tc-supraparamagnetic iron oxide nanoparticles into the deep popliteal nodes

Table 5-1 Physiological distribution of ^{99m}Tc-SPIONs in swine (n = 5) after injection of the lower limbs at 93 minutes post-injection

% ID 99m Tc-SPION Limbs			
Organ	**Mean**	**SD**	**n**
Popliteal R	1.5	0.7	3
Popliteal L	1.5	0.94	4
Iliac R	1.89	1.02	2
Iliac L	1.46	1.71	5
Superficial Inguinal R	8.4	4.1	4
Superficial Inguinal L	6.6	3.4	5

5.4.1.2 Oesophageal injections

Endoscopic injection into the submucosal layer of the oesophagus (n = 4) resulted in loss of signal in regional lymph nodes, due to SPION incorporation into the nodes. The dose of 0.5 mL of 20 mg/mL iron oxide was adequate to provide a loss of signal on T2*-weighted coronal MRI scan, compared to pre-injection MRI scan. However, the radiologist noted difficulty in his ability to consistently distinguish SPION uptake in sentinel nodes (in the celiac axis or paracardial tissue) from background artefact (gas in bowel loops). The MRI scans did not clearly identify lymph nodes to a point that was considered reproducible throughout the mediastinum. The celiac and left gastric nodes were the dominant basins following endoscopic injection, and were found in all swine (Table 5-2). The low percentage ID is likely related to the submucosal injection of the oesophagus, as there was a significant amount of the dose still at the original injection site. The gamma probe was accurate in its identification of the nodal basins. In 2 swine, para-oesophageal nodes were identified, however the percentage ID was minimal.

Table 5-2   Physiological distribution of ^{99m}Tc-SPIONs in swine (n = 4) after injection of the distal oesophagus at 93 minutes post

% ID 99m Tc-SPION Oesophagus			
Nodes	Mean	SD	n
L Paraoesophageal	0.025	0	1
R Paraoesophageal	0.027	0	1
L Gastric	1.747	0.723	4
Celiac	1.599	1.2	4

5.4.2   Bio-distribution comparison

Gamma counter readings confirmed that ^{99m}Tc-antimony and ^{99m}Tc-SPIONs went to the lungs, liver and spleen in similar percentage ID. The kidneys received 7% of the ID in the ^{99m}Tc-SPIONs swine, compared to <1% in the ^{99m}Tc-antimony swine (Table 5-3).

Table 5-3   Physiological distribution of ^{99m}Tc-ATC (n=1) vs. ^{99m}Tc-SPIONs (n=1) in swine reticuloendothelial organs after injection in the lower limbs at 93 minutes post

% ID 99m Tc-SPION						
Organ	Mean		SD		n	
	ATC	SPION	ATC	SPION	ATC	SPION
Lungs	0.8	0.5	0	0	1	1
Liver	1	1.2	0	0	1	1
Spleen	0	0.1	0	0	1	1
Kidneys	0.9	7	0	0	1	1

5.5   DISCUSSION

Using blue dye as a control tracer, we have shown that SPIONs provide a feasible method of identifying lymph nodes preoperatively. MRI may allow more accurate identification of metastatic lymph nodes, using this type of contrast material. However, discerning lymph nodes based on T1, T2 and T2* relaxation sequences was difficult due to the overlap

between normal, metastatic, hyperplastic, and reactive lymph nodes. In this study, we demonstrated that an injection of a SPION tracer generated a negative signal evident on T2* imaging (i.e. they were dark on T2* sequencing).

In our study, we used a 1.5T MRI and this provided adequate spatial resolution. Improved 3.0T MRI machines are becoming more commonplace and these will provide even greater spatial resolution and improved nodal detection.(158) In the present study, motion artefact was more noticeable in the thoracic injection rather than the limb injection, even with breath hold and anesthetic. With the compliance of real patients, the amount of artefact should decrease with shorter periods of complete breath holds, allowing better spatial resolution. In support of this, *Nishimura et al*. found that SPIONs alone were 100% sensitive, 95% specific and 96% accurate for diagnosis of metastatic nodes in the chest cavity.(56) *Motoyama et al.* also injected SPIONs into 23 patients with oesophageal cancer, and found the technique showed promise in mapping lymphatic drainage preoperatively.(159)

The distribution of lymphatic drainage following injection of ^{99m}Tc-SPIONs in the lower limbs was consistent in 4 of the 5 swine. In those 4, the tracer drained initially into the deep popliteal nodes, followed by the superficial inguinal nodes. In the single swine with drainage variability, the deep popliteal nodes were bypassed, and the superficial inguinal nodes were the first drainage sites. This mirrors the variability seen in other animals and in the human population.

The percentage of ID in the popliteal (1.5, 1.5) and iliac nodes (1.89, 1.46) was far less than the superficial inguinal nodes (8.4, 6.6). The superficial inguinal nodes are a major drainage basin for the lower limbs, reflected in the number of swine who had positive superficial inguinal nodes.

In the swine that underwent oesophageal injections, the left gastric and celiac nodes were the most consistent sentinel node basins, with percentage ID of 1.747 and 1.599, respectively. These basins correlate with the expected lymphatic drainage in a patient with a lower oesophageal tumour, and suggest that the sentinel nodes can be found effectively with this technique.

We have shown that a multimodal tracer, ^{99m}Tc-SPIONs, showed very consistent drainage to the first and second tier sentinel nodes in all swine. ^{99m}Tc-SPIONs provide good spatial visualisation via MRI, and the gamma probe was used effectively for intraoperative assessment. If these results are consistent and can be applied in patients, such technology will go a long way towards the application of the SLN concept in the staging of oesophageal cancer.

Several other different imaging modalities have been used to identify SLNs draining the oesophagus. Whilst other investigators have reported similar modality tracer composition, not all have done so using MRI. *Madru et al.* reports injection of ^{99m}Tc-SPIONs into 2 rats followed by imaging with SPECT/CT and MRI, confirming accumulation of ^{99m}Tc-SPIONs in the lymphatics (110) This was a preliminary small-animal study, and demonstrated that both imaging techniques were able to detect SLN in rats. A recent paper by *Tsai et al.* (160) assessed SPECT/CT imaging of sentinel nodes in oesophageal

cancer. Eight patients were injected with ^{99m}Tc-nanocoll (GE Healthcare Srl., Milan, Italy), and in 7 of the 8 patients, SLNs were identified preoperatively. SPECT/CT hybrid imaging had adequate resolution to assess lymph node stations, with accurate correlation using the intraoperative gamma probe. However, in one patient a positive SLN on SPECT/CT could not be located intraoperatively using the gamma probe. These authors noted that the 'shine-through' effect caused difficulty with 2 patients showing no uptake in the adjacent SLNs on SPECT/CT, but present intraoperatively using the gamma probe.

There are other imaging modalities, which may improve the detection of SLNs. Ultrasound, with the aid of microbubbles, has been trialled by *Choi et al*, in the footpad of rabbits. Microbubbles are particles that, after subcutaneous injection, enter the lymphatic vessels through gaps between endothelial cells or by end- or exocytosis.(161) Microbubbles are visible with ultrasound, but it is user-dependent and has poor spatial resolution. The technique is not suitable for upper gastrointestinal cancers, as the chest cavity and/or abdomen are relatively inaccessible. For more superficial cancers, such as breast cancer and melanoma, there may be merit in microbubbles.(162)

Another modality that is currently being investigated for lymph node assessment is optical imaging. This is light detection in the NIR spectrum, which is imaged with operating theatre equipment. Quantum dots are a type of optical fluorophore that has been investigated. They emit very bright light, and the wavelength of this light can be changed depending on the size and shape of the dots. There have been significant issues with quantum dots to date.(163) They often have difficulty visualising tissues deeper than

1–2 cm, and the toxicity is of concern.(164-166) A further NIR agent is FDA-approved ICG, which is readily taken up into the lymphatic system. It has been used with success in identifying SLN in breast cancer and melanoma. It has also been confirmed as part of a multimodality tracer, for use alongside radioactive methods.(167-169) There are limitations to ICG, with depth penetration and difficulty with conjugation of moieties or other contrast agents. It is still being investigated for use in superficial cancers.

An emerging platform is PET/MRI bimodality scanners, which enable advantages over current PET/CT scanners. There is a significant improvement in spatial resolution, with enhancement of soft-tissue contrast, and the ability to use nanotracers in MRI for greater detection of positive lymph nodes. In a study by *Lee et al.*, although not statistically significant, the nodal assessment of PET/MRI was superior to other modalities.(170) *Madru et al.* created a tri-modality PET/MRI/Cherenkov Gd-labelled SPION for assessment of sentinel nodes. This aimed at detection via a single injection, and was used in Wistar rats.(171)

There are still some unknowns to be addressed. These include the implication of long-term deposition of the iron component of the contrast agent and the effect – if any – of injecting contrast into the oesophagus. The physiological profile of our multimodal tracer was similar to ^{99m}Tc-antimony colloid, with the exception of increased uptake in the kidneys. This may be due to ^{99m}Tc-dextran that has dissociated from the iron oxide particle, with subsequent deposition in the kidney.(172) (173). Dextran-coated iron oxide nanoparticles are biodegradable and therefore should not have any long-term side

effects; however, this is unclear. As well, it is possible that slight variability in the location of oesophageal injection points may identify different SLNs. This needs further evaluation.

In summary, a novel multimodality tracer (^{99m}Tc-SPIONs) was effective in identifying SLNs in a large-animal model. We believe that multimodal tracers may allow more accurate staging of patients with early oesophageal cancer and obviate the need for invasive oesophagectomy in some patients with an early oesophageal cancer.

5.6   ACKNOWLEDGMENTS

5.7   DISCLOSURES

None.

CHAPTER 6:   CONCLUSIONS AND FUTURE DIRECTIONS

6.1 AIM 1

To critically evaluate current literature of the SLN concept in less superficial cancers (i.e. oesophageal cancer)

There are several problems that currently limit the use of SLN assessment in oesophageal cancer.

First, I have identified that the type of radiocolloid legislated for use differs in each continent. This limits the use of an internationally acceptable colloid, with uniform size characteristics. There is a balance that exists between a smaller colloid's faster transit through the nodes, and a larger colloid's retention time in the SLNs.

Second, it is more difficult to inject the colloid in non-superficial cancers. This is more invasive than the superficial skin injection that is conducted in breast and melanoma patients. Therefore blue dye is not a good option as it is difficult to gain access to the chest cavity in the short transit time inherent to blue dye injections.

Third, in oesophageal cancer, the majority of SLNs are within 3 cm of the primary tumour. This means that PET/CT scanners may find it difficult to distinguish hot/positive sentinel nodes from the primary tumour (i.e. the shine-through effect). Another limitation in the widespread application of SLN assessment in oesophageal cancer is the lack of a clear pre-operative anatomical roadmap.

6.2   AIM 2

To create a multimodal ^{99m}Tc labelled SPIONs tracer, and to assess its stability in a small-animal model

The dual assessment ability of ^{99m}Tc-colloid and SPIONs, through preoperative MRI and intraoperative gamma probe, is an enticing prospect for oesophageal cancer. It could provide a method of sentinel node detection, with more sensitivity than current blue DT/RCTs.

We created a novel multimodality tracer in the lab and then tested its chemical qualities with thin paper chromatography. The tracer was acceptable in its impurities and its radiolabelling efficiency of around 98%. The tracer was assessed in Sprague-Dawley rats, with lymphoscintigraphy used to delineate lymphatic drainage. The reticuloendothelial organs were resected from four rats and counted in a large gamma counter. This showed that the multimodality tracer had distributed effectively into the lymph nodes.

These experiments provided confirmation that the tracer was reliable, efficient and ready for use in a large-animal model.

6.3   AIM 3

To use the ^{99m}Tc labelled SPIONs tracer in a large-animal model to assess its accuracy and bio-distribution

In a large animal, the multimodal tracer was first injected into the hind limbs, to capitalise on their more predictable and linear lymphatic drainage pathways. It also provided an ability to compare the multimodal ^{99m}Tc-SPIONs to the SPIONs, with different tracers

injected into each leg. The limb model showed consistent lymphatic drainage for the SPIONs in all 4 swine, from the deep popliteal nodes to the superficial inguinal nodes. For the ^{99m}Tc-SPIONs, the drainage pathway was confirmed in 4 out of 5 swine. In one swine, the superficial inguinal node was the sentinel node, rather than the deep popliteal station. This was confirmed on MRI imaging. The gamma probe was effective in identifying all hot nodes in the swine.

The magnetoprobe was developed alongside our planned experiments. The magnetoprobe is a device that was developed by Aidan Cousins and Benjamin Thierry, as part of a PhD project. It is another way to detect iron oxide nanoparticles, and has been shown to be useful in breast cancer.(135) Their device focused on a different method of detection (MTJ), which was more economical than other similar commercialised devices, whilst still providing sensitivity. The new magnetoprobe, however, was not found to be as sensitive as the gamma probe (in detecting radiocolloid) in our experiments, showing there is still some room for improvement. The obvious advantage of pursuing this technology is that a sensitive, specific and accurate magnetic detection device would obviate the need to include a radiocolloid into the tracer.

The second phase of the experiments in swine was to inject the novel multimodal tracer into the oesophagus. This was performed effectively with minimal spillage. The radiologist found that the MRI images were difficult to assess for lymph node uptake of tracer. This was because of the background artefact of the swine's small bowel which is more than double the length of human small intestine and consequently interfered with

the detection of SLNs in the coeliac or paracardial (paraoesophageal in Table 5-2) stations. More work is required on the MRI imaging aspect of lymph node detection to ensure that the sequences, as well as the timing of acquisition, are optimised. Human patients, with less small bowel, may have superior anatomical qualities and therefore may provide more detailed and accurate images.

The third phase of the experiments was to assess bio-distribution. This was conducted in 2 swine, with injections into the hind limbs. One swine was injected with ^{99m}Tc-ATC and the other with ^{99m}Tc-SPIONs. The swine lymph nodes, lungs, liver, spleen and kidneys were harvested and then counted in a large-volume gamma counter. These results were calculated, relative to a standard ^{99m}Tc (0.1 mL) dose. The lymph nodes removed were the same nodal stations, as those in the original hind limb experiments (deep popliteal and superficial inguinal).

The percentage ID, that is, the amount of tracer in the particular tissue compared to the total tracer injected, was comparable for the two tracers, in all organs apart from the kidneys. This may be due to the dextran coating of iron oxide nanoparticles, which detaches, and then accumulates in the kidneys. This is a known phenomenon and is one aspect of dextran-coated nanoparticles that still requires more thorough assessment, prior to routine human use. There are no reports that the dextran coating creates renal injury, however, there has not been enough work into the long-term effects of this coating.

6.4   FUTURE DIRECTIONS

There remain several unanswered questions from the research I have undertaken. The optimal size of radiocolloid is still an issue that requires further research. Further work is also required to assess what modality of lymph node assessment is most effective. There are many emerging technologies, each with their own benefits, limitations, and logistical factors.

Lymph node assessment is extremely important in an age of improving and more conservative therapies. The impetus of such therapies is merely one factor that should drive clinicians to strive to improve the SLN concept in oesophageal cancer.

Further studies are required to assess the SLN concept with a thoracoscopic gamma probe, as part of a minimally invasive oesophagectomy. If possible, this could allow better staging pre-operatively, and/or facilitate endoscopic resection of early oesophageal cancers along with thoracoscopic removal of SLNs.

REFERENCES

1.   Cabanas RM. An approach for the treatment of penile carcinoma. Cancer. 1977 Feb;39(2):456-66. PubMed PMID: 837331. Epub 1977/02/01. eng.

2.   Morton DL, Wen DR, Wong JH, Economou JS, Cagle LA, Storm FK, et al. Technical details of intraoperative lymphatic mapping for early stage melanoma. Arch Surg. 1992 Apr;127(4):392-9. PubMed PMID: 1558490. Epub 1992/04/01. eng.

3.   Giuliano AE, Kirgan DM, Guenther JM, Morton DL. Lymphatic mapping and sentinel lymphadenectomy for breast cancer. Annals of surgery. 1994 Sep;220(3):391-8; discussion 8-401. PubMed PMID: 8092905. Pubmed Central PMCID: 1234400. Epub 1994/09/01. eng.

4.   Veronesi U, Paganelli G, Viale G, Luini A, Zurrida S, Galimberti V, et al. A randomized comparison of sentinel-node biopsy with routine axillary dissection in breast cancer. The New England journal of medicine. 2003 Aug 7;349(6):546-53. PubMed PMID: 12904519.

5.   Lens MB, Dawes M, Newton-Bishop JA, Goodacre T. Tumour thickness as a predictor of occult lymph node metastases in patients with stage I and II melanoma undergoing sentinel lymph node biopsy. The British journal of surgery. 2002 Oct;89(10):1223-7. PubMed PMID: 12296887.

6.   Ang CH, Tan MY, Teo C, Seah DW, Chen JC, Chan MY, et al. Blue dye is sufficient for sentinel lymph node biopsy in breast cancer. The British journal of surgery. 2014 Mar;101(4):383-9; discussion 9. PubMed PMID: 24492989.

7.   Radovanovic Z, Golubovic A, Plzak A, Stojiljkovic B, Radovanovic D. Blue dye versus combined blue dye-radioactive tracer technique in detection of sentinel lymph node in breast cancer. European journal of surgical oncology : the journal of the European Society of Surgical Oncology and the British Association of Surgical Oncology. 2004 Nov;30(9):913-7. PubMed PMID: 15498633.

8.   Valsecchi ME, Silbermins D, de Rosa N, Wong SL, Lyman GH. Lymphatic mapping and sentinel lymph node biopsy in patients with melanoma: a meta-analysis. Journal of clinical oncology : official journal of the American Society of Clinical Oncology. 2011 Apr 10;29(11):1479-87. PubMed PMID: 21383281.

9.   Hung WK, Chan CM, Ying M, Chong SF, Mak KL, Yip AW. Randomized clinical trial comparing blue dye with combined dye and isotope for sentinel lymph node biopsy in breast cancer. The British journal of surgery. 2005 Dec;92(12):1494-7. PubMed PMID: 16308853.

10.   Gretschel S, Bembenek A, Hunerbein M, Dresel S, Schneider W, Schlag PM. Efficacy of different technical procedures for sentinel lymph node biopsy in gastric cancer staging. Annals of surgical oncology. 2007 Jul;14(7):2028-35. PubMed PMID: 17453300. Epub 2007/04/25. eng.

11.   Thompson SK, Bartholomeusz D, Jamieson GG. Sentinel lymph node biopsy in esophageal cancer: should it be standard of care? Journal of gastrointestinal surgery : official journal of the Society for Surgery of the Alimentary Tract. 2011 Oct;15(10):1762-8. PubMed PMID: 21809166.

12.   Hirche C, Mohr Z, Kneif S, Doniga S, Murawa D, Strik M, et al. Ultrastaging of colon cancer by sentinel node biopsy using fluorescence navigation with indocyanine green. International journal of colorectal disease. 2012 Mar;27(3):319-24. PubMed PMID: 21912878.

13.   Bredell MG. Sentinel lymph node mapping by indocyanin green fluorescence imaging in oropharyngeal cancer - preliminary experience. Head Neck Oncol. 2010;2:31. PubMed PMID: 21034503. Pubmed Central PMCID: 2984381.

14.   Murawa D, Hirche C, Dresel S, Hunerbein M. Sentinel lymph node biopsy in breast cancer guided by indocyanine green fluorescence. The British journal of surgery. 2009 Nov;96(11):1289-94. PubMed PMID: 19847873.

15.   Noura S, Ohue M, Seki Y, Tanaka K, Motoori M, Kishi K, et al. Feasibility of a lateral region sentinel node biopsy of lower rectal cancer guided by indocyanine green using a near-infrared camera system. Annals of surgical oncology. 2010 Jan;17(1):144-51. PubMed PMID: 19774415.

16.   Kobayashi H, Koyama Y, Barrett T, Hama Y, Regino CA, Shin IS, et al. Multimodal nanoprobes for radionuclide and five-color near-infrared optical lymphatic imaging. ACS nano. 2007 Nov;1(4):258-64. PubMed PMID: 19079788. Pubmed Central PMCID: 2600721.

17.   Lovric J, Cho SJ, Winnik FM, Maysinger D. Unmodified cadmium telluride quantum dots induce reactive oxygen species formation leading to multiple organelle damage and cell death. Chemistry & biology. 2005 Nov;12(11):1227-34. PubMed PMID: 16298302.

18.   Jemal A, Bray F, Center MM, Ferlay J, Ward E, Forman D. Global cancer statistics. CA: a cancer journal for clinicians. 2011 Mar-Apr;61(2):69-90. PubMed PMID: 21296855. Epub 2011/02/08. eng.

19.   Australian Institute of Health and Welfare. Australia's health ... in brief. Canberra: Australian Institute of Health and Welfare. p. v.

20.   Welfare AIoHa. Oesophageal Cancer 2011. Available from: http://www.aihw.gov.au/acim-books.

21.   Stavrou EP, McElroy HJ, Baker DF, Smith G, Bishop JF. Adenocarcinoma of the oesophagus: incidence and survival rates in New South Wales, 1972-2005. The Medical journal of Australia. 2009 Sep 21;191(6):310-4. PubMed PMID: 19769552.

22.   Spechler SJ, Fitzgerald RC, Prasad GA, Wang KK. History, molecular mechanisms, and endoscopic treatment of Barrett's esophagus. Gastroenterology. 2010 Mar;138(3):854-69. PubMed PMID: 20080098. Pubmed Central PMCID: 2853870. Epub 2010/01/19. eng.

23.   Kamangar F, Chow WH, Abnet CC, Dawsey SM. Environmental causes of esophageal cancer. Gastroenterology clinics of North America. 2009 Mar;38(1):27-57, vii. PubMed PMID: 19327566. Pubmed Central PMCID: 2685172. Epub 2009/03/31. eng.

24.   Leeuwenburgh I, Scholten P, Alderliesten J, Tilanus HW, Looman CWN, Steijerberg EW, et al. Long-Term Esophageal Cancer Risk in Patients With Primary Achalasia: A Prospective Study.

25.   Allaix ME, Patti MG. Endoscopic Dilatation, Heller Myotomy, and Peroral Endoscopic Myotomy: Treatment Modalities for Achalasia. The Surgical clinics of North America. 2015 Jun;95(3):567-78. PubMed PMID: 25965130.

26.   Dent J. Endoscopic grading of reflux oesophagitis: the past, present and future. Best practice & research Clinical gastroenterology. 2008;22(4):585-99. PubMed PMID: 18656818.

27.   Lundell LR, Dent J, Bennett JR, Blum AL, Armstrong D, Galmiche JP, et al. Endoscopic assessment of oesophagitis: clinical and functional correlates and further validation of the Los Angeles classification. Gut. 1999 Aug;45(2):172-80. PubMed PMID: 10403727. Pubmed Central PMCID: 1727604.

28.   Spechler SJ. Barrett esophagus and risk of esophageal cancer: a clinical review. JAMA : the journal of the American Medical Association. 2013 Aug 14;310(6):627-36. PubMed PMID: 23942681.

29.   Burke ZD, Tosh D. Barrett's metaplasia as a paradigm for understanding the development of cancer. Curr Opin Genet Dev. 2012 Oct;22(5):494-9. PubMed PMID: 22981230.

30.   Whiteman DC, Appleyard M, Bahin FF, Bobryshev YV, Bourke MJ, Brown I, et al. Australian clinical practice guidelines for the diagnosis and management of Barrett's esophagus and early esophageal adenocarcinoma. Journal of gastroenterology and hepatology. 2015 May;30(5):804-20. PubMed PMID: 25612140.

31.   Spechler SJ, Sharma P, Souza RF, Inadomi JM, Shaheen NJ, American Gastroenterological A. American Gastroenterological Association technical review on the management of Barrett's esophagus. Gastroenterology. 2011 Mar;140(3):e18-52; quiz e13. PubMed PMID: 21376939. Pubmed Central PMCID: 3258495.

32.   Fitzgerald RC, di Pietro M, Ragunath K, Ang Y, Kang JY, Watson P, et al. British Society of Gastroenterology guidelines on the diagnosis and management of Barrett's oesophagus. Gut. 2014 Jan;63(1):7-42. PubMed PMID: 24165758.

33.   Wani S, Falk G, Hall M, Gaddam S, Wang A, Gupta N, et al. Patients with nondysplastic Barrett's esophagus have low risks for developing dysplasia or esophageal adenocarcinoma. Clinical gastroenterology and hepatology : the official clinical practice journal of the American Gastroenterological Association. 2011 Mar;9(3):220-7; quiz e26. PubMed PMID: 21115133. Epub 2010/12/01. eng.

34.   Cameron AJ, Lomboy CT, Pera M, Carpenter HA. Adenocarcinoma of the esophagogastric junction and Barrett's esophagus. Gastroenterology. 1995 Nov;109(5):1541-6. PubMed PMID: 7557137. Epub 1995/11/01. eng.

35.   Reid BJ, Li X, Galipeau PC, Vaughan TL. Barrett's oesophagus and oesophageal adenocarcinoma: time for a new synthesis. Nature reviews Cancer. 2010 Feb;10(2):87-101. PubMed PMID: 20094044. Pubmed Central PMCID: 2879265. Epub 2010/01/23. eng.

36.   Shaheen NJ, Crosby MA, Bozymski EM, Sandler RS. Is there publication bias in the reporting of cancer risk in Barrett's esophagus? Gastroenterology. 2000 Aug;119(2):333-8. PubMed PMID: 10930368. Epub 2000/08/10. eng.

37.   Pohl H, Pech O, Arash H, Stolte M, Manner H, May A, et al. Length of Barrett's oesophagus and cancer risk: implications from a large sample of patients with early oesophageal adenocarcinoma. Gut. 2015 Jun 25. PubMed PMID: 26113177.

38.   Rastogi A, Puli S, El-Serag HB, Bansal A, Wani S, Sharma P. Incidence of esophageal adenocarcinoma in patients with Barrett's esophagus and high-grade dysplasia: a meta-analysis. Gastrointestinal endoscopy. 2008 Mar;67(3):394-8. PubMed PMID: 18045592. Epub 2007/11/30. eng.

39.   Griffin SM, Raimes, S.A. Oesophagogastric Surgery. 4th ed: Elsevier; 2009.

40.   Kakeji Y, Yamamoto M, Ito S, Sugiyama M, Egashira A, Saeki H, et al. Lymph node metastasis from cancer of the esophagogastric junction, and determination of the appropriate nodal dissection. Surgery today. 2012 Apr;42(4):351-8. PubMed PMID: 22245924. Epub 2012/01/17. eng.

41.   Schroder W, Monig SP, Baldus SE, Gutschow C, Schneider PM, Holscher AH. Frequency of nodal metastases to the upper mediastinum in Barrett's cancer. Annals of surgical oncology. 2002 Oct;9(8):807-11. PubMed PMID: 12374665. Epub 2002/10/11. eng.

42.   Rudiger Siewert J, Feith M, Werner M, Stein HJ. Adenocarcinoma of the esophagogastric junction: results of surgical therapy based on anatomical/topographic classification in 1,002 consecutive patients. Annals of surgery. 2000 Sep;232(3):353-61. PubMed PMID: 10973385. Pubmed Central PMCID: 1421149. Epub 2000/09/06. eng.

43.   Siewert JR, Stein HJ, Feith M. Adenocarcinoma of the esophago-gastric junction. Scandinavian journal of surgery : SJS : official organ for the Finnish Surgical Society and the Scandinavian Surgical Society. 2006;95(4):260-9. PubMed PMID: 17249275. Epub 2007/01/26. eng.

44.   Akiyama H, Tsurumaru M, Udagawa H, Kajiyama Y. Radical lymph node dissection for cancer of the thoracic esophagus. Annals of surgery. 1994 Sep;220(3):364-72; discussion 72-3. PubMed PMID: 8092902. Pubmed Central PMCID: 1234394. Epub 1994/09/01. eng.

45.   Omloo JM, Lagarde SM, Hulscher JB, Reitsma JB, Fockens P, van Dekken H, et al. Extended transthoracic resection compared with limited transhiatal resection for adenocarcinoma of the mid/distal esophagus: five-year survival of a randomized clinical trial. Annals of surgery. 2007 Dec;246(6):992-1000; discussion -1. PubMed PMID: 18043101. Epub 2007/11/29. eng.

46.   van de Ven C, De Leyn P, Coosemans W, Van Raemdonck D, Lerut T. Three-field lymphadenectomy and pattern of lymph node spread in T3 adenocarcinoma of the distal esophagus and the gastro-esophageal junction. European journal of cardio-thoracic surgery : official journal of the European Association for Cardio-thoracic Surgery. 1999 Jun;15(6):769-73. PubMed PMID: 10431857. Epub 1999/08/04. eng.

47.   Thompson SK, Ruszkiewicz AR, Jamieson GG, Sullivan TR, Devitt PG. Isolated tumor cells in esophageal cancer: implications for the surgeon and the pathologist. Annals of surgery. 2010 Aug;252(2):299-306. PubMed PMID: 20622664. Epub 2010/07/14. eng.

48.   Nagaraja V, Eslick GD, Cox MR. Sentinel lymph node in oesophageal cancer-a systematic review and meta-analysis. J Gastrointest Oncol. 2014 Apr;5(2):127-41. PubMed PMID: 24772341. Pubmed Central PMCID: 3999634.

49.   Grotenhuis BA, Wijnhoven BP, van Marion R, van Dekken H, Hop WC, Tilanus HW, et al. The sentinel node concept in adenocarcinomas of the distal esophagus and gastroesophageal junction. The Journal of thoracic and cardiovascular surgery. 2009 Sep;138(3):608-12. PubMed PMID: 19698844. Epub 2009/08/25. eng.

50.   Yasuda S, Shimada H, Chino O, Tanaka H, Kenmochi T, Takechi M, et al. Sentinel lymph node detection with Tc-99m tin colloids in patients with esophagogastric cancer. Japanese journal of clinical oncology. 2003 Feb;33(2):68-72. PubMed PMID: 12629056. Epub 2003/03/12. eng.

51.   Kato H, Miyazaki T, Nakajima M, Takita J, Sohda M, Fukai Y, et al. Sentinel lymph nodes with technetium-99m colloidal rhenium sulfide in patients with esophageal carcinoma. Cancer. 2003 Sep 1;98(5):932-9. PubMed PMID: 12942559. Epub 2003/08/28. eng.

52.   Takeuchi H, Fujii H, Ando N, Ozawa S, Saikawa Y, Suda K, et al. Validation study of radio-guided sentinel lymph node navigation in esophageal cancer. Annals of surgery. 2009 May;249(5):757-63. PubMed PMID: 19387329. Epub 2009/04/24. eng.

53.   Kim HK, Kim S, Park JJ, Jeong JM, Mok YJ, Choi YH. Sentinel node identification using technetium-99m neomannosyl human serum albumin in esophageal cancer. The Annals of thoracic surgery. 2011 May;91(5):1517-22. PubMed PMID: 21377648. Epub 2011/03/08. eng.

54.   Kubota K, Yoshida M, Kuroda J, Okada A, Ohta K, Kitajima M. Application of the HyperEye Medical System for esophageal cancer surgery: a preliminary report. Surgery today. 2013 Feb;43(2):215-20. PubMed PMID: 22782594.

55.   Ferrari M. Cancer nanotechnology: opportunities and challenges. Nature reviews Cancer. 2005 Mar;5(3):161-71. PubMed PMID: 15738981. Epub 2005/03/02. eng.

56.   Nishimura H, Tanigawa N, Hiramatsu M, Tatsumi Y, Matsuki M, Narabayashi I. Preoperative esophageal cancer staging: magnetic resonance imaging of lymph node with ferumoxtran-10, an ultrasmall superparamagnetic iron oxide. Journal of the American College of Surgeons. 2006 Apr;202(4):604-11. PubMed PMID: 16571430.

57.   UK CR. Cancer Research UK Statistical Information Team 2007. Available from: http://www.cancerresearchuk.org/cancer-info/cancerstats/types/oesophagus/incidence/uk-oesophageal-cancer-incidence-statistics.

58.   Urschel JD, Vasan H, Blewett CJ. A meta-analysis of randomized controlled trials that compared neoadjuvant chemotherapy and surgery to surgery alone for resectable esophageal cancer. American journal of surgery. 2002 Mar;183(3):274-9. PubMed PMID: 11943125. Epub 2002/04/12. eng.

59.   Burmeister BH, Smithers BM, Gebski V, Fitzgerald L, Simes RJ, Devitt P, et al. Surgery alone versus chemoradiotherapy followed by surgery for resectable cancer of the oesophagus: a randomised controlled phase III trial. The lancet oncology. 2005 Sep;6(9):659-68. PubMed PMID: 16129366. Epub 2005/09/01. eng.

60.   Akutsu Y, Matsubara H. The significance of lymph node status as a prognostic factor for esophageal cancer. Surgery today. 2011 Sep;41(9):1190-5. PubMed PMID: 21874413. Epub 2011/08/30. eng.

61.   Leong SP. Sentinel lymph node mapping and selective lymphadenectomy: the standard of care for melanoma. Current treatment options in oncology. 2004 Jun;5(3):185-94. PubMed PMID: 15115647. Epub 2004/04/30. eng.

62.   Vidal-Sicart S, Valdes Olmos R. Sentinel node mapping for breast cancer: current situation. Journal of oncology. 2012;2012:361341. PubMed PMID: 22927845. Pubmed Central PMCID: 3426254. Epub 2012/08/29. eng.

63.   Gershenwald JE, Mansfield PF, Lee JE, Ross MI. Role for lymphatic mapping and sentinel lymph node biopsy in patients with thick (> or = 4 mm) primary melanoma. Annals of surgical oncology. 2000 Mar;7(2):160-5. PubMed PMID: 10761797. Epub 2000/04/13. eng.

64.   Gajdos C, Griffith KA, Wong SL, Johnson TM, Chang AE, Cimmino VM, et al. Is there a benefit to sentinel lymph node biopsy in patients with T4 melanoma? Cancer. 2009 Dec 15;115(24):5752-60. PubMed PMID: 19827151. Epub 2009/10/15. eng.

65.   Russell-Jones R. When will selective lymphadenectomy become standard of care in melanoma? International journal of clinical practice. 2012 Jul;66(7):671-4. PubMed PMID: 22329440. Epub 2012/02/15. eng.

66.   Mansel RE, Fallowfield L, Kissin M, Goyal A, Newcombe RG, Dixon JM, et al. Randomized multicenter trial of sentinel node biopsy versus standard axillary treatment in operable breast cancer: the ALMANAC Trial. Journal of the National Cancer Institute. 2006 May 3;98(9):599-609. PubMed PMID: 16670385. Epub 2006/05/04. eng.

67.   Kim T, Giuliano AE, Lyman GH. Lymphatic mapping and sentinel lymph node biopsy in early-stage breast carcinoma: a metaanalysis. Cancer. 2006 Jan 1;106(1):4-16. PubMed PMID: 16329134. Epub 2005/12/06. eng.

68.   Leong SP. The role of sentinel lymph nodes in malignant melanoma. The Surgical clinics of North America. 2000 Dec;80(6):1741-57. PubMed PMID: 11140870. Epub 2001/01/05. eng.

69.   Morton DL, Hoon DS, Cochran AJ, Turner RR, Essner R, Takeuchi H, et al. Lymphatic mapping and sentinel lymphadenectomy for early-stage melanoma: therapeutic utility and implications of nodal microanatomy and molecular staging for improving the accuracy of detection of nodal micrometastases. Annals of surgery. 2003 Oct;238(4):538-49; discussion 49-50. PubMed PMID: 14530725. Pubmed Central PMCID: 1360112. Epub 2003/10/08. eng.

70.   Gershenwald JE, Thompson W, Mansfield PF, Lee JE, Colome MI, Tseng CH, et al. Multi-institutional melanoma lymphatic mapping experience: the prognostic value of sentinel lymph node status in 612 stage I or II melanoma patients. Journal of clinical oncology : official journal of the American Society of Clinical Oncology. 1999 Mar;17(3):976-83. PubMed PMID: 10071292. Epub 1999/03/10. eng.

71.   Shahbaz Sarwar CM, Luketich JD, Landreneau RJ, Abbas G. Esophageal cancer: an update. Int J Surg. 2010;8(6):417-22. PubMed PMID: 20601255. Epub 2010/07/06. eng.

72.   Hermansson M, DeMeester SR. Management of stage 1 esophageal cancer. The Surgical clinics of North America. 2012 Oct;92(5):1155-67. PubMed PMID: 23026275. Epub 2012/10/03. eng.

73.   Ancona E, Rampado S, Cassaro M, Battaglia G, Ruol A, Castoro C, et al. Prediction of lymph node status in superficial esophageal carcinoma. Annals of surgical oncology. 2008 Nov;15(11):3278-88. PubMed PMID: 18726651. Epub 2008/08/30.

74.   Akutsu Y, Uesato M, Shuto K, Kono T, Hoshino I, Horibe D, et al. The overall prevalence of metastasis in T1 esophageal squamous cell carcinoma: a retrospective

analysis of 295 patients. Annals of surgery. 2013 Jun;257(6):1032-8. PubMed PMID: 23108117. Epub 2012/10/31.

75.   Manner H, Pech O, Heldmann Y, May A, Pohl J, Behrens A, et al. Efficacy, safety, and long-term results of endoscopic treatment for early stage adenocarcinoma of the esophagus with low-risk sm1 invasion. Clinical gastroenterology and hepatology : the official clinical practice journal of the American Gastroenterological Association. 2013 Jun;11(6):630-5; quiz e45. PubMed PMID: 23357492. Epub 2013/01/30.

76.   Sepesi B, Watson TJ, Zhou D, Polomsky M, Litle VR, Jones CE, et al. Are endoscopic therapies appropriate for superficial submucosal esophageal adenocarcinoma? An analysis of esophagectomy specimens. Journal of the American College of Surgeons. 2010 Apr;210(4):418-27. PubMed PMID: 20347733. Epub 2010/03/30. eng.

77.   Pech O, Bollschweiler E, Manner H, Leers J, Ell C, Holscher AH. Comparison between endoscopic and surgical resection of mucosal esophageal adenocarcinoma in Barrett's esophagus at two high-volume centers. Annals of surgery. 2011 Jul;254(1):67-72. PubMed PMID: 21532466. Epub 2011/05/03.

78.   Das A, Singh V, Fleischer DE, Sharma VK. A comparison of endoscopic treatment and surgery in early esophageal cancer: an analysis of surveillance epidemiology and end results data. The American journal of gastroenterology. 2008 Jun;103(6):1340-5. PubMed PMID: 18510606. Epub 2008/05/31.

79.   Schembre DB, Huang JL, Lin OS, Cantone N, Low DE. Treatment of Barrett's esophagus with early neoplasia: a comparison of endoscopic therapy and esophagectomy. Gastrointestinal endoscopy. 2008 Apr;67(4):595-601. PubMed PMID: 18279860. Epub 2008/02/19.

80.   Fovos A, Jarral O, Panagiotopoulos N, Podas T, Mikhail S, Zacharakis E. Does endoscopic treatment for early oesophageal cancers give equivalent oncological outcomes as compared with oesophagectomy? Best evidence topic (BET). Int J Surg. 2012;10(9):415-20. PubMed PMID: 22771501. Epub 2012/07/10.

81.   Edge SB, Compton CC. The American Joint Committee on Cancer: the 7th edition of the AJCC cancer staging manual and the future of TNM. Annals of surgical oncology. 2010 Jun;17(6):1471-4. PubMed PMID: 20180029. Epub 2010/02/25. eng.

82.   de Boer M, van Deurzen CH, van Dijck JA, Borm GF, van Diest PJ, Adang EM, et al. Micrometastases or isolated tumor cells and the outcome of breast cancer. The New England journal of medicine. 2009 Aug 13;361(7):653-63. PubMed PMID: 19675329. Epub 2009/08/14. eng.

83.   Prenzel KL, Holscher AH, Drebber U, Agavonova M, Gutschow CA, Bollschweiler E. Prognostic impact of nodal micrometastasis in early esophageal cancer. European journal of surgical oncology : the journal of the European Society of Surgical Oncology and the British Association of Surgical Oncology. 2012 Apr;38(4):314-8. PubMed PMID: 22277724. Epub 2012/01/27. eng.

84.   Cao L, Hu X, Zhang Y, Huang G. Adverse prognosis of clustered-cell versus single-cell micrometastases in pN0 early gastric cancer. Journal of surgical oncology. 2011 Jan 1;103(1):53-6. PubMed PMID: 21031429. Epub 2010/10/30. eng.

85.   Koenig AM, Prenzel KL, Bogoevski D, Yekebas EF, Bubenheim M, Faithova L, et al. Strong impact of micrometastatic tumor cell load in patients with esophageal carcinoma. Annals of surgical oncology. 2009 Feb;16(2):454-62. PubMed PMID: 19015923. Epub 2008/11/19. eng.

86.	Izbicki JR, Hosch SB, Pichlmeier U, Rehders A, Busch C, Niendorf A, et al. Prognostic value of immunohistochemically identifiable tumor cells in lymph nodes of patients with completely resected esophageal cancer. The New England journal of medicine. 1997 Oct 23;337(17):1188-94. PubMed PMID: 9337377. Epub 1997/10/23. eng.

87.	Liu XY, Chen G, Wang Z, Liu FY. Clinical significance of detecting mucin 1 mRNA in diagnosing occult lymph node micrometastasis in esophageal cancer patients. Ai zheng = Aizheng = Chinese journal of cancer. 2007 Feb;26(2):194-9. PubMed PMID: 17298752. Epub 2007/02/15. eng.

88.	de Boer M, van Deurzen CHM, van Dijck JAAM, Borm GF, van Diest PJ, Adang EMM, et al. Micrometastases or Isolated Tumor Cells and the Outcome of Breast Cancer. New England Journal of Medicine. 2009;361(7):653-63.

89.	Yonemura Y, Endo Y, Hayashi I, Kawamura T, Yun HY, Bandou E. Proliferative activity of micrometastases in the lymph nodes of patients with gastric cancer. The British journal of surgery. 2007 Jun;94(6):731-6. PubMed PMID: 17377930. Epub 2007/03/23. eng.

90.	Cheng G, Kurita S, Torigian DA, Alavi A. Current status of sentinel lymph-node biopsy in patients with breast cancer. European journal of nuclear medicine and molecular imaging. 2011 Mar;38(3):562-75. PubMed PMID: 20700739. Epub 2010/08/12. eng.

91.	Mariani G, Moresco L, Viale G, Villa G, Bagnasco M, Canavese G, et al. Radioguided sentinel lymph node biopsy in breast cancer surgery. Journal of nuclear medicine : official publication, Society of Nuclear Medicine. 2001 Aug;42(8):1198-215. PubMed PMID: 11483681. Epub 2001/08/03. eng.

92.	Gretschel S, Bembenek A, Huenerbein M, Dresel S, Schneider W, Schlag PM. Efficacy of different technical procedures for sentinel lymph node biopsy in gastric cancer staging. Annals of surgical oncology. 2007 Jul;14(7):2028-35. PubMed PMID: WOS:000247467000008.

93.	Thompson SK, Bartholomeusz D, Jamieson GG. Sentinel Lymph Node Biopsy in Esophageal Cancer: Should It Be Standard of Care? Journal of Gastrointestinal Surgery. 2011 Oct;15(10):1762-8. PubMed PMID: WOS:000295177600017.

94.	Leidenius MH, Leppanen EA, Krogerus LA, Smitten KA. The impact of radiopharmaceutical particle size on the visualization and identification of sentinel nodes in breast cancer. Nuclear medicine communications. 2004 Mar;25(3):233-8. PubMed PMID: 15094440. Epub 2004/04/20. eng.

95.	Harisinghani MG, Barentsz J, Hahn PF, Deserno WM, Tabatabaei S, van de Kaa CH, et al. Noninvasive detection of clinically occult lymph-node metastases in prostate cancer. The New England journal of medicine. 2003 Jun 19;348(25):2491-9. PubMed PMID: 12815134.

96.	Kern KA. Concordance and validation study of sentinel lymph node biopsy for breast cancer using subareolar injection of blue dye and technetium 99m sulfur colloid. Journal of the American College of Surgeons. 2002 Oct;195(4):467-75. PubMed PMID: 12375751. Epub 2002/10/12.

97.	Argon AM, Duygun U, Acar E, Daglioz G, Yenjay L, Zekioglu O, et al. The use of periareolar intradermal Tc-99m tin colloid and peritumoral intraparenchymal isosulfan

blue dye injections for determination of the sentinel lymph node. Clinical nuclear medicine. 2006 Dec;31(12):795-800. PubMed PMID: 17117076. Epub 2006/11/23.

98.	Lee JH, Ryu KW, Kim CG, Kim SK, Lee JS, Kook MC, et al. Sentinel node biopsy using dye and isotope double tracers in early gastric cancer. Annals of surgical oncology. 2006 Sep;13(9):1168-74. PubMed PMID: 16924376. Epub 2006/08/23.

99.	Borgstein PJ, Pijpers R, Comans EF, van Diest PJ, Boom RP, Meijer S. Sentinel lymph node biopsy in breast cancer: guidelines and pitfalls of lymphoscintigraphy and gamma probe detection. Journal of the American College of Surgeons. 1998 Mar;186(3):275-83. PubMed PMID: 9510258.

100.	Valdes Olmos RA, Hoefnagel CA, Nieweg OE, Jansen L, Rutgers EJ, Borger J, et al. Lymphoscintigraphy in oncology: a rediscovered challenge. European journal of nuclear medicine. 1999 Apr;26(4 Suppl):S2-S10. PubMed PMID: 10199926.

101.	Aarsvold JN, Alazraki NP. Update on detection of sentinel lymph nodes in patients with breast cancer. Seminars in nuclear medicine. 2005 Apr;35(2):116-28. PubMed PMID: 15765374.

102.	Albertini JJ, Lyman GH, Cox C, Yeatman T, Balducci L, Ku N, et al. Lymphatic mapping and sentinel node biopsy in the patient with breast cancer. JAMA : the journal of the American Medical Association. 1996 Dec 11;276(22):1818-22. PubMed PMID: 8946902.

103.	Landi G, Polverelli M, Moscatelli G, Morelli R, Landi C, Fiscelli O, et al. Sentinel lymph node biopsy in patients with primary cutaneous melanoma: study of 455 cases. J Eur Acad Dermatol Venereol. 2000 Jan;14(1):35-45. PubMed PMID: 10877250.

104.	Tsopelas C, Bevington E, Kollias J, Shibli S, Farshid G, Coventry B, et al. 99mTc-Evans blue dye for mapping contiguous lymph node sequences and discriminating the sentinel lymph node in an ovine model. Annals of surgical oncology. 2006 May;13(5):692-700. PubMed PMID: 16523365.

105.	Henze E, Robinson GD, Kuhl DE, Schelbert HR. Tc-99m dextran: a new blood-pool-labeling agent for radionuclide angiocardiography. Journal of nuclear medicine : official publication, Society of Nuclear Medicine. 1982 Apr;23(4):348-53. PubMed PMID: 6175736.

106.	Bouziotis P, Psimadas D, Tsotakos T, Stamopoulos D, Tsoukalas C. Radiolabeled iron oxide nanoparticles as dual-modality SPECT/MRI and PET/MRI agents. Curr Top Med Chem. 2012;12(23):2694-702. PubMed PMID: 23339765.

107.	Ferro-Flores G, Ocampo-Garcia BE, Santos-Cuevas CL, Morales-Avila E, Azorin-Vega E. Multifunctional radiolabeled nanoparticles for targeted therapy. Curr Med Chem. 2014;21(1):124-38. PubMed PMID: 23992338.

108.	Fu X, Nishimura S, Porter TE. Evidence that lactotrophs do not differentiate directly from somatotrophs during chick embryonic development. The Journal of endocrinology. 2004 Nov;183(2):417-25. PubMed PMID: 15531729.

109.	Glaus C, Rossin R, Welch MJ, Bao G. In vivo evaluation of (64)Cu-labeled magnetic nanoparticles as a dual-modality PET/MR imaging agent. Bioconjugate chemistry. 2010 Apr 21;21(4):715-22. PubMed PMID: 20353170. Pubmed Central PMCID: 2865436.

110.	Madru R, Kjellman P, Olsson F, Wingardh K, Ingvar C, Stahlberg F, et al. 99mTc-labeled superparamagnetic iron oxide nanoparticles for multimodality SPECT/MRI of sentinel lymph nodes. Journal of nuclear medicine : official publication, Society of Nuclear Medicine. 2012 Mar;53(3):459-63. PubMed PMID: 22323777.

111.	Wang A-Y, Kuo C-L, Lin J-L, Fu C-M, Wang Y-F. Study of magnetic ferrite nanoparticles labeled with 99mTc-pertechnetate. Journal of radioanalytical and nuclear chemistry. 2010;284(2):405-13.

112.	Bellin MF, Beigelman C, Precetti-Morel S. Iron oxide-enhanced MR lymphography: initial experience. European journal of radiology. 2000 Jun;34(3):257-64. PubMed PMID: 10927166.

113.	Matsunaga K, Hara K, Imamura T, Fujioka T, Takata J, Karube Y. Technetium labeling of dextran incorporating cysteamine as a ligand. Nuclear medicine and biology. 2005 Apr;32(3):279-85. PubMed PMID: 15820763.

114.	d'Europa C. Technetium (99mTc) colloidal sulphur injection2004.

115.	Henze E, Schelbert HR, Collins JD, Najafi A, Barrio JR, Bennett LR. Lymphoscintigraphy with Tc-99m-labeled dextran. Journal of nuclear medicine : official publication, Society of Nuclear Medicine. 1982 Oct;23(10):923-9. PubMed PMID: 6181235.

116.	Ercan MT, Schneidereit M, Senekowitsch R, Kriegel H. Evaluation of 99mTc-dextran as a lymphoscintigraphic agent in rabbits. European journal of nuclear medicine. 1985;11(2-3):80-4. PubMed PMID: 2412822.

117.	Balalis GL, Thompson SK. Sentinel lymph node biopsy in esophageal cancer: an essential step towards individualized care. Annals of surgical innovation and research. 2014;8:2. PubMed PMID: 24829610. Pubmed Central PMCID: 4019891.

118.	Carter CL, Allen C, Henson DE. Relation of tumor size, lymph node status, and survival in 24,740 breast cancer cases. Cancer. 1989 Jan 1;63(1):181-7. PubMed PMID: 2910416.

119.	Ferrone CR, Panageas KS, Busam K, Brady MS, Coit DG. Multivariate prognostic model for patients with thick cutaneous melanoma: importance of sentinel lymph node status. Annals of surgical oncology. 2002 Aug;9(7):637-45. PubMed PMID: 12167577.

120.	Statius Muller MG, van Leeuwen PA, de Lange-De Klerk ES, van Diest PJ, Pijpers R, Ferwerda CC, et al. The sentinel lymph node status is an important factor for predicting clinical outcome in patients with Stage I or II cutaneous melanoma. Cancer. 2001 Jun 15;91(12):2401-8. PubMed PMID: 11413531.

121.	Cousins A, Thompson SK, Wedding AB, Thierry B. Clinical relevance of novel imaging technologies for sentinel lymph node identification and staging. Biotechnology advances. 2014 Mar-Apr;32(2):269-79. PubMed PMID: 24189095.

122.	Anzai Y, Piccoli CW, Outwater EK, Stanford W, Bluemke DA, Nurenberg P, et al. Evaluation of neck and body metastases to nodes with ferumoxtran 10-enhanced MR imaging: phase III safety and efficacy study. Radiology. 2003 Sep;228(3):777-88. PubMed PMID: 12954896.

123.	Douek M, Klaase J, Monypenny I, Kothari A, Zechmeister K, Brown D, et al. Sentinel node biopsy using a magnetic tracer versus standard technique: the SentiMAG Multicentre Trial. Annals of surgical oncology. 2014 Apr;21(4):1237-45. PubMed PMID: 24322530.

124.	Winter A, Woenkhaus J, Wawroschek F. A novel method for intraoperative sentinel lymph node detection in prostate cancer patients using superparamagnetic iron oxide nanoparticles and a handheld magnetometer: the initial clinical experience. Annals

of surgical oncology. 2014 Dec;21(13):4390-6. PubMed PMID: 25190119. Pubmed Central PMCID: 4218978.

125.   Ogawa J MY, Katayose Y, Saito R, Kamada S, Ueda T inventorMagnetic fluid detection method and magnetic fluid detection apparatus.2010.

126.   Ookubo T, Inoue Y, Kim D, Ohsaki H, Mashiko Y, Kusakabe M, et al. Characteristics of magnetic probes for identifying sentinel lymph nodes. Conference proceedings : Annual International Conference of the IEEE Engineering in Medicine and Biology Society IEEE Engineering in Medicine and Biology Society Conference. 2013;2013:5485-8. PubMed PMID: 24110978.

127.   Hattersley S PQ, inventorMagnetic probe apparatus2011.

128.   Shen W.F LXY, Mazumdar D, Xiao G. In situ detection of singlie micron-sized magnetic beads using magnetic tunnel junction sensors. Applied Physics Letters. 2005 (86).

129.   al PSSPe. Exchange-biased magnetic tunnel junctions and application to nonvolatile magnetic random access memory. Journal of applied physics. 1999 (85):5828-33.

130.   Ikeda Sea. Tunnel magnetoresistance of 604% at 300 K by suppression of Ta diffusion in CoFeb/MgO.CoFeB pseudo-spin-valves annealed at high temperature. Applied Physics Letters. 2008 (93).

131.   Wengenmair H KJ, Sciuk J. Quality Criteria of Gamma Probes: Requirements and Future Developments. In: Schauer A BW, Reiser M, Possinger K, editor. The Sentinel Lymph Node Concept. Germany: Springer; 2005. p. 113--25.

132.   Zanzonico P, Heller S. The intraoperative gamma probe: basic principles and choices available. Seminars in nuclear medicine. 2000 Jan;30(1):33-48. PubMed PMID: 10656242.

133.   Wallace AM, Hoh CK, Ellner SJ, Darrah DD, Schulteis G, Vera DR. Lymphoseek: a molecular imaging agent for melanoma sentinel lymph node mapping. Annals of surgical oncology. 2007 Feb;14(2):913-21. PubMed PMID: 17146742.

134.   Visscher M WS, Pouw J, ten Haken B. Depth limitations for in vivo magnetic nanoparticle detection with a compact handheld device. Journal of Magnetism and Magnetic Materials. 2015 (380):246-50.

135.   Coufal O, Fait V, Lzicarova E, Chrenko V, Zaloudik J. [SentiMag - the magnetic detection system of sentinel lymph nodes in breast cancer]. Rozhledy v chirurgii : mesicnik Ceskoslovenske chirurgicke spolecnosti. 2015 Jul;94(7):283-8. PubMed PMID: 26305347. Magneticka detekce sentinelovych uzlin u karcinomu prsu metodou SentiMag.

136.   Britten AJ. A method to evaluate intra-operative gamma probes for sentinel lymph node localisation. European journal of nuclear medicine. 1999 Feb;26(2):76-83. PubMed PMID: 9933340.

137.   Merkow RP, Bilimoria KY, Keswani RN, Chung J, Sherman KL, Knab LM, et al. Treatment trends, risk of lymph node metastasis, and outcomes for localized esophageal cancer. Journal of the National Cancer Institute. 2014 Jul;106(7). PubMed PMID: 25031273.

138.   Yoshii T, Ohkawa S, Tamai S, Kameda Y. Clinical outcome of endoscopic mucosal resection for esophageal squamous cell cancer invading muscularis mucosa and submucosal layer. Diseases of the esophagus : official journal of the International Society for Diseases of the Esophagus / ISDE. 2013 Jul;26(5):496-502. PubMed PMID: 22676622.

139.   Lee L, Ronellenfitsch U, Hofstetter WL, Darling G, Gaiser T, Lippert C, et al. Predicting lymph node metastases in early esophageal adenocarcinoma using a simple scoring system. Journal of the American College of Surgeons. 2013 Aug;217(2):191-9. PubMed PMID: 23659947.

140.   Nentwich MF, von Loga K, Reeh M, Uzunoglu FG, Marx A, Izbicki JR, et al. Depth of submucosal tumor infiltration and its relevance in lymphatic metastasis formation for T1b squamous cell and adenocarcinomas of the esophagus. Journal of gastrointestinal surgery : official journal of the Society for Surgery of the Alimentary Tract. 2014 Feb;18(2):242-9; discussion 9. PubMed PMID: 24091912.

141.   Holscher AH, Bollschweiler E, Schroder W, Metzger R, Gutschow C, Drebber U. Prognostic impact of upper, middle, and lower third mucosal or submucosal infiltration in early esophageal cancer. Annals of surgery. 2011 Nov;254(5):802-7; discussion 7-8. PubMed PMID: 22042472. Epub 2011/11/02. eng.

142.   Griffin SM, Burt AD, Jennings NA. Lymph node metastasis in early esophageal adenocarcinoma. Annals of surgery. 2011 Nov;254(5):731-6; discussion 6-7. PubMed PMID: 21997815.

143.   Barbour AP, Jones M, Brown I, Gotley DC, Martin I, Thomas J, et al. Risk stratification for early esophageal adenocarcinoma: analysis of lymphatic spread and prognostic factors. Annals of surgical oncology. 2010 Sep;17(9):2494-502. PubMed PMID: 20349213.

144.   Leers JM, DeMeester SR, Oezcelik A, Klipfel N, Ayazi S, Abate E, et al. The prevalence of lymph node metastases in patients with T1 esophageal adenocarcinoma a retrospective review of esophagectomy specimens. Annals of surgery. 2011 Feb;253(2):271-8. PubMed PMID: 21119508.

145.   Lehr L, Rupp N, Siewert JR. Assessment of resectability of esophageal cancer by computed tomography and magnetic resonance imaging. Surgery. 1988 Mar;103(3):344-50. PubMed PMID: 3344487. Epub 1988/03/01. eng.

146.   Dooms GC, Hricak H, Crooks LE, Higgins CB. Magnetic resonance imaging of the lymph nodes: comparison with CT. Radiology. 1984 Dec;153(3):719-28. PubMed PMID: 6093190.

147.   Kajiyama Y, Tsurumaru M, Iwanuma Y, Tomita N, Amano T, Ouchi K, et al. [Controversies in esophageal cancer surgery]. Gan to kagaku ryoho Cancer & chemotherapy. 2003 Sep;30(9):1225-9. PubMed PMID: 14518399.

148.   Kato H, Kuwano H, Nakajima M, Miyazaki T, Yoshikawa M, Ojima H, et al. Comparison between positron emission tomography and computed tomography in the use of the assessment of esophageal carcinoma. Cancer. 2002 Feb 15;94(4):921-8. PubMed PMID: 11920459. Epub 2002/03/29.

149.   Kato H, Miyazaki T, Nakajima M, Takita J, Kimura H, Faried A, et al. The incremental effect of positron emission tomography on diagnostic accuracy in the initial staging of esophageal carcinoma. Cancer. 2005 Jan 1;103(1):148-56. PubMed PMID: 15558794.

150.   Puli SR, Reddy JB, Bechtold ML, Antillon D, Ibdah JA, Antillon MR. Staging accuracy of esophageal cancer by endoscopic ultrasound: a meta-analysis and systematic review.

World journal of gastroenterology : WJG. 2008 Mar 14;14(10):1479-90. PubMed PMID: 18330935. Pubmed Central PMCID: 2693739. Epub 2008/03/12. eng.

151.   Pfau PR, Perlman SB, Stanko P, Frick TJ, Gopal DV, Said A, et al. The role and clinical value of EUS in a multimodality esophageal carcinoma staging program with CT and positron emission tomography. Gastrointestinal endoscopy. 2007 Mar;65(3):377-84. PubMed PMID: 17321235.

152.   Crabtree TD, Yacoub WN, Puri V, Azar R, Zoole JB, Patterson GA, et al. Endoscopic ultrasound for early stage esophageal adenocarcinoma: implications for staging and survival. The Annals of thoracic surgery. 2011 May;91(5):1509-15; discussion 15-6. PubMed PMID: 21435632.

153.   Thompson SK, Bartholomeusz D, Devitt PG, Lamb PJ, Ruszkiewicz AR, Jamieson GG. Feasibility study of sentinel lymph node biopsy in esophageal cancer with conservative lymphadenectomy. Surgical endoscopy. 2011 Mar;25(3):817-25. PubMed PMID: 20725748. Epub 2010/08/21. eng.

154.   Weissleder R, Elizondo G, Wittenberg J, Rabito CA, Bengele HH, Josephson L. Ultrasmall superparamagnetic iron oxide: characterization of a new class of contrast agents for MR imaging. Radiology. 1990 May;175(2):489-93. PubMed PMID: 2326474. Epub 1990/05/01.

155.   Lee AS, Weissleder R, Brady TJ, Wittenberg J. Lymph nodes: microstructural anatomy at MR imaging. Radiology. 1991 Feb;178(2):519-22. PubMed PMID: 1987619. Epub 1991/02/01.

156.   Guimaraes R, Clement O, Bittoun J, Carnot F, Frija G. MR lymphography with superparamagnetic iron nanoparticles in rats: pathologic basis for contrast enhancement. AJR American journal of roentgenology. 1994 Jan;162(1):201-7. PubMed PMID: 8273666. Epub 1994/01/01.

157.   Tsopelas C. Particle size analysis of (99m)Tc-labeled and unlabeled antimony trisulfide and rhenium sulfide colloids intended for lymphoscintigraphic application. Journal of nuclear medicine : official publication, Society of Nuclear Medicine. 2001 Mar;42(3):460-6. PubMed PMID: 11337524. Epub 2001/05/05.

158.   Heesakkers RA, Futterer JJ, Hovels AM, van den Bosch HC, Scheenen TW, Hoogeveen YL, et al. Prostate cancer evaluated with ferumoxtran-10-enhanced T2*-weighted MR Imaging at 1.5 and 3.0 T: early experience. Radiology. 2006 May;239(2):481-7. PubMed PMID: 16641354.

159.   Motoyama S, Ishiyama K, Maruyama K, Okuyama M, Sato Y, Hayashi K, et al. Preoperative mapping of lymphatic drainage from the tumor using ferumoxide-enhanced magnetic resonance imaging in clinical submucosal thoracic squamous cell esophageal cancer. Surgery. 2007 Jun;141(6):736-47. PubMed PMID: 17560250.

160.   Tsai JA, Celebioglu F, Lindblad M, Lorinc E, Nilsson M, Olsson A, et al. Hybrid SPECT/CT imaging of sentinel nodes in esophageal cancer: first results. Acta radiologica. 2013 May;54(4):369-73. PubMed PMID: 23507936.

161.   Choi SH, Kono Y, Corbeil J, Lucidarme O, Mattrey RF. Model to quantify lymph node enhancement on indirect sonographic lymphography. AJR American journal of roentgenology. 2004 Aug;183(2):513-7. PubMed PMID: 15269049.

162.   Yang WT, Goldberg BB. Microbubble contrast-enhanced ultrasound for sentinel lymph node detection: ready for prime time? AJR American journal of roentgenology. 2011 Feb;196(2):249-50. PubMed PMID: 21257872.

163. Winnik FM, Maysinger D. Quantum dot cytotoxicity and ways to reduce it. Accounts of chemical research. 2013 Mar 19;46(3):672-80. PubMed PMID: 22775328.
164. Vahrmeijer AL, Frangioni JV. Seeing the invisible during surgery. The British journal of surgery. 2011 Jun;98(6):749-50. PubMed PMID: 21484776. Pubmed Central PMCID: 3083469.
165. Bhunia SK, Saha A, Maity AR, Ray SC, Jana NR. Carbon nanoparticle-based fluorescent bioimaging probes. Scientific reports. 2013;3:1473. PubMed PMID: 23502324. Pubmed Central PMCID: 3600594.
166. Sun X, Liu Z, Welsher K, Robinson JT, Goodwin A, Zaric S, et al. Nano-Graphene Oxide for Cellular Imaging and Drug Delivery. Nano research. 2008;1(3):203-12. PubMed PMID: 20216934. Pubmed Central PMCID: 2834318.
167. Samorani D, Fogacci T, Panzini I, Frisoni G, Accardi FG, Ricci M, et al. The use of indocyanine green to detect sentinel nodes in breast cancer: A prospective study. European journal of surgical oncology : the journal of the European Society of Surgical Oncology and the British Association of Surgical Oncology. 2015 Jan;41(1):64-70. PubMed PMID: 25468752.
168. Guo W, Zhang L, Ji J, Gao W, Liu J, Tong M. Breast cancer sentinel lymph node mapping using near-infrared guided indocyanine green in comparison with blue dye. Tumour biology : the journal of the International Society for Oncodevelopmental Biology and Medicine. 2014 Apr;35(4):3073-8. PubMed PMID: 24307620.
169. van den Berg NS, Brouwer OR, Schaafsma BE, Matheron HM, Klop WM, Balm AJ, et al. Multimodal Surgical Guidance during Sentinel Node Biopsy for Melanoma: Combined Gamma Tracing and Fluorescence Imaging of the Sentinel Node through Use of the Hybrid Tracer Indocyanine Green-Tc-Nanocolloid. Radiology. 2014 Dec 17:140322. PubMed PMID: 25521776.
170. Lee G, I H, Kim SJ, Jeong YJ, Kim IJ, Pak K, et al. Clinical Implication of PET/MR Imaging in Preoperative Esophageal Cancer Staging: Comparison with PET/CT, Endoscopic Ultrasonography, and CT. Journal of nuclear medicine : official publication, Society of Nuclear Medicine. 2014 May 27;55(8):1242-7. PubMed PMID: 24868109.
171. Madru R, Tran TA, Axelsson J, Ingvar C, Bibic A, Stahlberg F, et al. (68)Ga-labeled superparamagnetic iron oxide nanoparticles (SPIONs) for multi-modality PET/MR/Cherenkov luminescence imaging of sentinel lymph nodes. American journal of nuclear medicine and molecular imaging. 2013;4(1):60-9. PubMed PMID: 24380046. Pubmed Central PMCID: 3867730.
172. Lodhia J, Mandarano G, Ferris N, Eu P, Cowell S. Development and use of iron oxide nanoparticles (Part 1): Synthesis of iron oxide nanoparticles for MRI. Biomedical imaging and intervention journal. 2010 Apr-Jun;6(2):e12. PubMed PMID: 21611034. Pubmed Central PMCID: 3097763.
173. Corot C, Robert P, Idee JM, Port M. Recent advances in iron oxide nanocrystal technology for medical imaging. Advanced drug delivery reviews. 2006 Dec 1;58(14):1471-504. PubMed PMID: 17116343.